UNIVERSITY OF CALIFORNIA, MERCED

INVESTIGATION OF THE MECHANISM OF GRIFFITHSIN (GRFT): A POTENT HIV ENTRY INHIBITOR

A dissertation submitted in partial satisfaction of the
requirements for the degree of
Doctor of Philosophy

in

Quantitative and Systems Biology

by

Jie Xue

Committee in charge:

Professor Andy LiWang, Chair
Professor David Ojcius
Professor Jinah Choi
Professor Patricia J. LiWang, Supervisor

2014

The dissertation of Jie Xue, titled Investigation of the Mechanism of Griffithsin (GRFT), a Potent HIV entry inhibitor, is approved, and it is acceptable in quality and form for publication on microfilm and electronically:

_____ Date _____

Professor David Ojcius

_____ Date _____

Professor Jinah Choi

Supervisor _____ Date _____

Professor Patricia LiWang

Chair _____ Date _____

Professor Andy LiWang

University of California, Merced

2014

To My Family,

Thank you for all of your love, support, and sacrifice throughout my life.

Table of Contents

Abstract

INVESTIGATION OF THE MECHANISM OF GRIFFITHSIN (GRFT): A POTENT HIV ENTRY INHIBITOR

Jie Xue

Doctor of Philosophy

University of California, Merced

2014

Supervisor: Prof Patricia LiWang

Griffithsin (GRFT) is a potent protein lectin that has been shown to inhibit HIV infection by binding to high mannose glycans on the surface of gp120. However, important biochemical details on the antiviral mechanism of GRFT action remain unexplored.

In chapter 2, we investigate the role of individual carbohydrate binding sites in the function of GRFT. Individual point mutants of GRFT showed a small loss of binding to gp120, but a significant loss of activity to inhibit viral infection. The disparity between HIV-1 gp120 binding ability and HIV inhibitory potency for these GRFT variants indicates that gp120 binding and virus neutralization do not necessarily correlate, and suggests a mechanism that is not based on simple gp120 binding.

In chapter 3 we investigated the role of the dimer in GRFT's anti-HIV activity. An obligate dimer of GRFT was designed, as well as a "one-armed" obligate dimer which has one carbohydrate binding arm mutated while the other subunit remained intact. While GRFT only needs one functional arm to tightly bind to gp120, it needs both arms to potently inhibit HIV entry. Furthermore, our experiments showed that GRFT needs both arms to alter the structure of gp120 by exposing the CD4 binding site as well as to cross-link two separate gp120 subunits. Evidence is provided that the dimer form of Grft is critical to the function of this protein in HIV inhibition.

In chapter 4 we studied a chemokine analog vMIP-II (viral macrophage inflammatory protein-II) that inhibits multiple HIV strains by binding to both CCR5 and CXCR4 co-receptors. We

have made a vMIP-II variant, “5P12-vMIP-II” in which the N-terminus of vMIP-II has been replaced by the N-terminus of 5P12-RANTES that have been shown to greatly enhance the anti-HIV potency of the chemokine RANTES for R5 HIV strains. Both vMIP-II and 5P12-vMIP-II showed the ability to inhibit multiple strains of HIV. While the 5P12 N-terminus did not improve the potency of the protein, our results provide evidence about the interaction of vMIP-II with CCR5, indicating that vMIP-II does not bind CCR5 in the same way as human chemokines.

List of Figures

List of Tables

List of Abbreviations

HIV-1: human immunodeficiency virus type 1;

GRFT: griffithsin;

HHA: hippeastrum hybrid agglutinin;

UDA: urtica dioica agglutinin;

PRMS: pradimicin S;

GAG: glycosaminoglycan;

CBS: carbohydrate binding site;

SPR: surface plasmon resonance;

ELISA: enzyme-linked immunosorbent assay;

RU: resonance unit;

IPTG: Isopropyl β-D-1-thiogalactopyranoside;

CPRG: chlorophenol red-D-galactopyranoside;

DSS: 2,2-dimethyl-2-silapentane-5-sulfonic acid;

SDS-PAGE: sodium dodecyl sulfate polyacrylamide gel electrophoresis;

AUC: analytical ultracentrifugation;

NMR: nuclear magnetic resonance;

HSQC: heteronuclear single quantum coherence;

FBS: fetal bovine serum;

DMEM: dulbecco's modified eagle's medium;

PBMC: peripheral blood mononuclear cell;

sCD4: soluble CD4;

HRP: horseradish peroxidase;

HHV-8: human herpesvirus 8;

vMIP-II: viral macrophage inflammatory protein-II;

MCP-1: monocyte chemoattractant protein-1;

MIP-1α: macrophage inflammatory protein-1 alpha;

MIP-1β: macrophage inflammatory protein-1 beta;

RANTES: regulated on activation normal T cell expressed and secreted.

Acknowledgements

I would like to thank my advisor Prof. Patricia J. LiWang for the support and the opportunity to work with her. I thank Prof. Andy LiWang for the support and serving as chair of my committee. I thank Prof. David Ojcius and Prof. Jinah Choi for serving as members of my committee. I thank the members of both Prof. Andy and Patricia LiWang groups.

I thank Prof. Jan Balzarini and Dr. Bart Hoorelbeke for designing and performing the surface plasmon resonance experiments at Regan Institute for Medical Research, KU Leuven, Belgium. I thank Dr. Yonggang Gao for performing NMR assignment. I thank Prof. Borries Demeler for designing and performing the sedimentation velocity experiments at the Center for Analytical Ultracentrifugation of Macromolecular Assemblies at the University of Texas Health Science Center at San Antonio. I thank Dr. Naiwei Kuo for designing and purifying 5P12-vMIP-II for single-round infection assays. I thank Dr. Ioannis Kagiampakis and Dr. Bo Zhao for suggestions and technical assistance in the lab.

My work was supported by NIH (R21 AI079777), 1P20MD005049-01 from the National Center on Minority Health and Health Disparities, U.S. Army grantW911NF-11-1-0139, NCI P30 CA054174, and grants from the KU Leuven (PF 10/018, GOA 10/14, G-0528-12N). Computations were performed at the Texas Advanced Computing Center of the University of Texas, Austin, on Lonestar and Ranger with support from NSF TeraGrid allocation TG-MCB070039 (B.D.).

The text of this thesis/dissertation is a reprint of the material as it appears in ***Molecular Pharmaceutics****,* ***Antimicrobial Agents and Chemotherapy****, and* ***Biochemistry and Physiology****. The co-authors listed in this publication directed and supervised research which form the basis for the thesis/dissertation.*

Chapter 1

Introduction

1.1 HIV pandemic around the world

1.1.1 History and pandemic of HIV

AIDS (Acquired Immune Deficient Syndrome) is a severe pandemic disease around the world, being the most prevalent in Sub-Saharan Africa. The syndrome is exhibited through progressive failure of parts of the immune system, including several important antigen-presenting cells and cells regulating antibody generation, which leads to life-threatening opportunistic infections and various cancers.

The virus that causes AIDS is called HIV (Human Immunodeficiency Virus). It is a type of lentinvirus, a family of retroviruses that uses RNA instead of DNA as its genetic material, and is characterized by slow replication and disease causation. This virus was so named because one major feature for this syndrome is immune deficiency due to severe depletion of $CD4^+$ T lymphocytes, which are responsible for the adaptive immune response. Due to deficiency of immune cells, people infected with HIV develop life-threatening opportunistic infections. With the failure of the adaptive immune response, AIDS patients gradually lose response to pathogens from the environment that do not infect people with healthy immune systems, or else their immune system fails to clear out mutated cells, which then results in cancer. Because the syndrome is not specific and the time window (also known as the latent period or incubation time) is relatively long (usually 5-10 years), 20% of people infected with HIV are not aware they are infected, so they may still be transmitting this life-threatening virus to their sex partners, children or blood product receivers. Since the virus was discovered in 1989, it has annually killed around 1.6-1.8 millions of people.

The first AIDS case was reported by the Center for Disease Control (CDC) in San Francisco in 1980, which had resulted in a rare lung infection called *Pneumocystis carinii* pneumonia (PCP) in a young adult. This opportunistic infection usually only affects elderly people but the patient was only in his 20s. Soon, there were five more PCP cases in Los Angeles, all of which affected young, gay men. Due to this pattern, this disease was initially called “Gay-Related Immune Deficiency” because the only people discovered to be infected were all homosexual males, and doctors could not pinpoint a reason for their infections. But later on, similar opportunistic infections were reported in injecting drug users who had no homosexual contact. In 1983, female patients in

hospitals who got blood transfusion but had no other risk factors like needle sharing history were reported with similar immunodeficiency syndromes, suggesting that this disease could be transmitted through hetero-sexual sex or other transmission methods. Then, children were found to develop AIDS if their mothers had previously been infected. This soon brought to light the three major transmission pathways for HIV: sexual transmission, blood transmission, and mother-to-child transmission.

Since the beginning of the epidemic, almost 70 million people have been infected with the HIV virus and about 36 million people have died of AIDS. Around 34 million people were living with HIV at the end of 2011 worldwide. An estimated 0.8% of adults aged 15-49 years worldwide are living with HIV, although the burden of the epidemic continues to vary considerably between countries and regions. Sub-Saharan Africa remains most severely affected, with nearly 1 in every 20 adults (4.9%) living with HIV and this number accounts for 69% of the people living with HIV worldwide (Figure 1-1). Currently in United States, there are 1.2 million people living with HIV/AIDS, and the number of new HIV infections in 2010 alone was 49,273 according to Center of Disease Control (Stacy C, Xiaohong H, Daxa S, et al. Diagnoses of HIV Infection in the United States and Dependent Areas, 2011, HIV Surveillance Report, Volume 23. Hyattsville, MD: National Center for Health Statistics. 2011). This disease has caused 36 million of deaths since it was discovered, and even in 2009, the number of death was still more than 18,000 in just one year. AIDS now is among the top 3 causes of death for African Americans in men aged 25-54 and women aged 35-44. African makes up to 47% of HIV/AIDS cases and African American women have a 17 times higher chance of being infected than Caucasian women. Table 1-1 lists the regional HIV/AIDS statistics and features, as reported by UNAIDS and WHO.

The estimated lifetime cost of treatment for one person with HIV is $379,668, with the average annual cost for HIV treatment being $23,000. While 50% of those diagnosed with HIV cannot get regular care, the US government is spending 27.2 billion dollars in 2011 on AIDS research and medical care, with 52% spent on AIDS treatment, 10% on housing, and assistance and 11% on research.

Table 1-1: Regional HIV/AIDS statistics and features, end of 2012

Region	Adults &children living with HIV/AIDS	Adults &children newly infected with HIV	Adults prevalence rate(*)	% of HIV positive adults who are women	Main mode(s) of transmission (#) for adults living with HIV/AIDS
Sub-Saharan Africa	25.0 million	1.6 million	4.7%	55%	Hetero
North Africa &Middle East	260,000	32,000	0.1%	40%	Hetero, IDU
South &South-East Asia	3.9 million	270,000	0.3%	35%	Hetero, IDU
East Asia &Pacific	880,000	81,000	<0.1%	20%	IDU, hetero, MSM
Latin America	1.5 million	86,000	0.4%	30%	MSM, IDU, hetero
Caribbean	250,000	12,000	1.0%	50%	Hetero, MSM
Eastern Europe &Central Asia	1.3 million	130,000	0.7%	20%	IDU
Western &Central Europe	860,000	29,000	0.2%	25%	MSM, IDU
North America	1.3 million	48,000	0.5%	20%	MSM, IDU, hetero
Oceania	51,000	2100	0.2%	10%	MSM
Total	35.3 million	2.3 million	0.8%	48%	

Source: UNAIDS and WHO (2001), AIDS Epidemic Update: December 2012 (Geneva, 2001), p. 3.

Notes:
* Hetero (heterosexual transmission), IDU (transmission through infecting drug use), and MSM (sexual transmission among men who have sex with men).

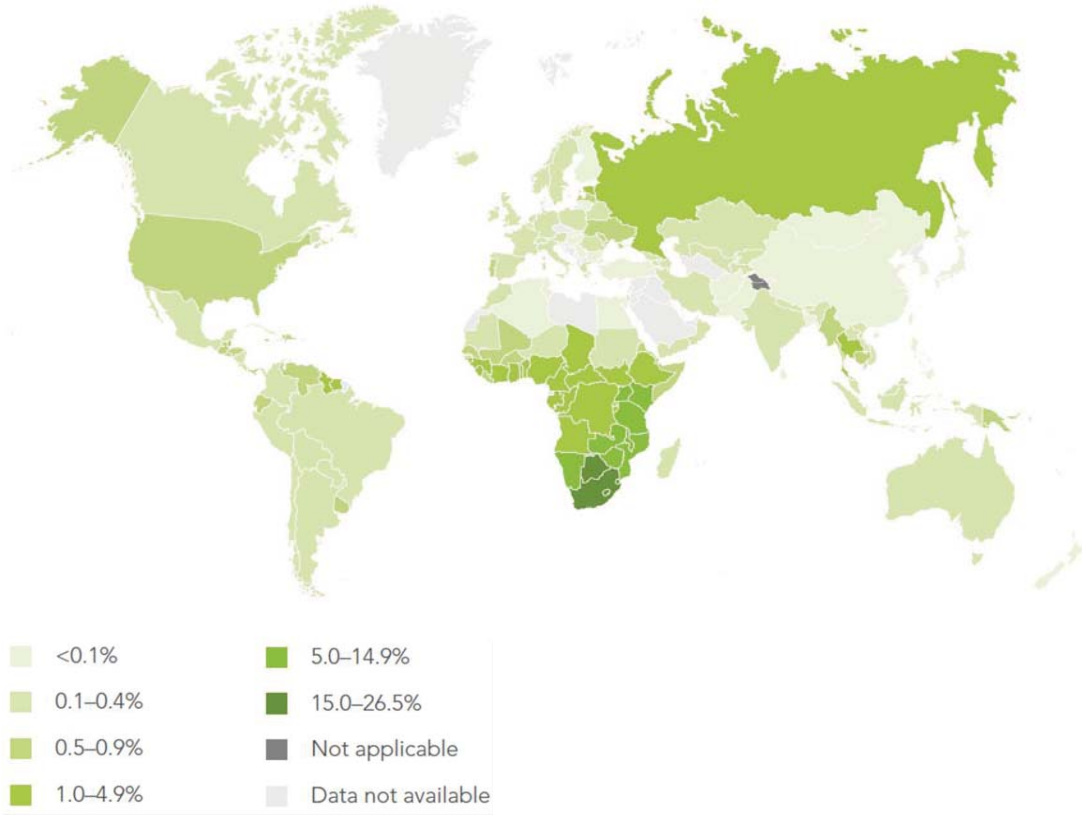

Figure 1-1: Global HIV prevalence among adults aged 15-49, 2012.

Data from: http://www.who.int/hiv/data/en/ *HIV/AIDS Global epidemiology*

1.1.2 HIV transmission

Three major venues of HIV transmission are: mother-to-child, blood-borne, and sexual contact. HIV can also be transmitted through many other pathways, but at fairly low risk. Table 1-2 lists the major transmission pathways, risks and current rate of transmission for AIDS cases by each pathway.

Different countries or regions can have cases infected by different transmission pathways. Currently, the demographics most affected by AIDS are young women and girls in southern sub-Saharan Africa who contract the virus through sexual transmission, and young men who have sex with men (MSM) in the Americas, Asia, and Africa [17]. In the United States, over 60% of new infections are homosexual males, and they get the virus from having sex with other men. This makes microbicides (which we will discuss later) a promising venue for trying to prevent the spread of HIV in the United States.

Table 1-2: Contribution of HIV invasion sites to global HIV infections [18].

HIV invasion site	Anatomical sub-location	Transmission medium	Transmission probability per exposure event	Estimated contribution to HIV cases worldwide
Female genital tract	Vagina	Semen	1 in 200 -1 in 2,000	12.6 million
	Ectocervix			
	Endocervix			
	Other			
Male genital tract	Inner foreskin	Cervicovaginal and rectal secretions and desquamations	1 in 700 – 1 in 3,000	10.2 million*
	Penile urethra			
	Other			
Intestinal tract	Rectum	Semen	1 in 20 – 1 in 300	3.9 million**
	Upper GI tract	Semen	1 in 2,500	1.5 million
Mother to child		Maternal blood, genital secretions (intrapartum)	1 in 5 – 1 in 10	960,000***
		Breast milk	1 in 5 – 1 in 10	960,000***
Placenta	Chorionic villi	Maternal blood (intrauterine)	1 in 10 – 1 in 20	480,000***
Blood stream		Blood products, sharps	95 in 100 – 1 in 150	2.6 million****

Notes:

* Includes men having sex with men (MSM), bisexual men and heterosexual men.

**Includes MSM, bisexual men and women infected via anal receptive intercourse.

***Mother-to-child transmission.

****Mostly intravenous drug use (IDU), but includes infections by transfusions and health care related accidents.

1.1.3 HIV clades (subtypes) and geographic distribution

Due to different DNA sequences, glycosylation sites, and coreceptor usages, HIV viruses can be classified into several subtypes (clades): clades A, B, C, D, E, and F. HIV-1 clades are phylogenetically linked strains of HIV-1 that are approximately the same genetic distance from one another; in some cases, subtypes are also linked geographically or epidemiologically [19]. Genetic variation within a subtype can be 15 to 20%, whereas variation between subtypes is usually 25 to 35% [20]. Clade B dominates in United States and Europe, while clade C viruses are mostly found in Africa and Asia. Recombinant clades are also found in patients, possibly because of dual infection of viruses from both strains in the same person and gene recombination occurring after such dual infection. Different clades usually have different glycosylation patterns on the viral surface, have different sensitivities to antiviral drugs, and also affect the rate of progression to AIDS [21]. The anti-HIV lectin griffithsin (GRFT), which recognizes HIV surface glycoproteins and interferes with HIV entry, behaves differently on different strains. This will be further discussed in Chapter 3.

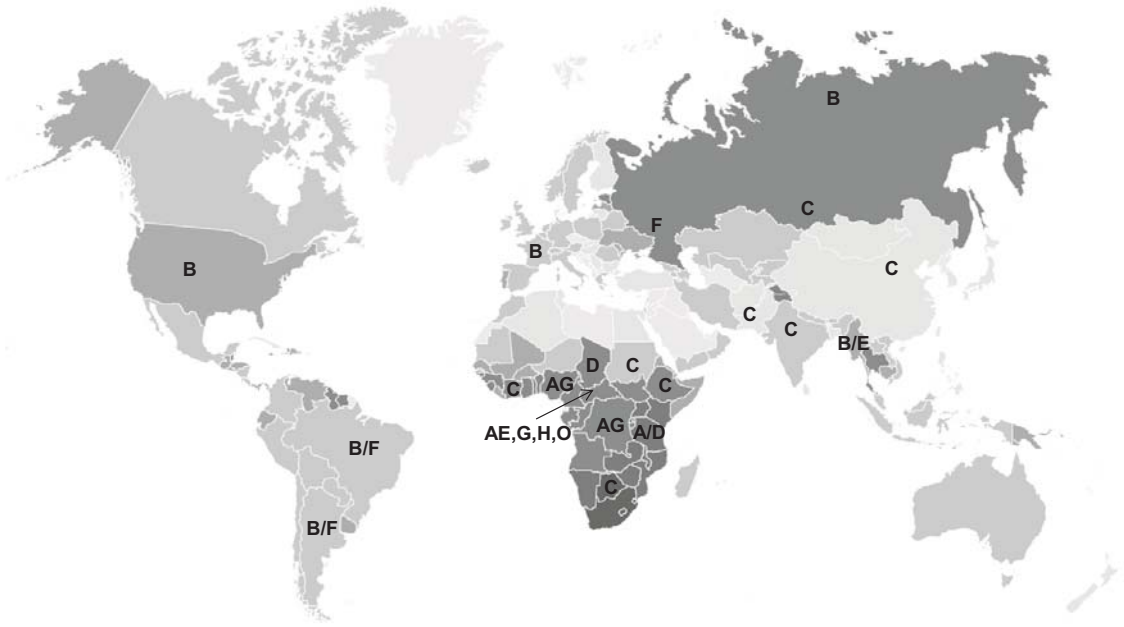

Figure 1-2: The geographical distribution of HIV-1 clades [8]**.**

Letters indicate the predominant HIV-1 clade circulating in selected countries. A/B, B/E, and B/F indicate co-circulation of two dominant clades; AE and AG indicate circulating recombinant forms.

1.2 HIV entry process

During HIV infection, the first step involves gp120 contacting its receptor, the glycoprotein CD4, and coreceptor, CCR5 or CXCR4, on the human target cell surface. Receptor and coreceptor binding causes a conformational change on the gp120, and exposes gp41. When gp41 is exposed, the N-terminus and C-terminus of gp41 from a trimeric spike fold and form a 6 helix bundle, bringing the virus close to the cell membrane while the fusion peptide on gp41 inserts into the human cell membrane and initiates viral fusion with target cell (Figure 1-3).

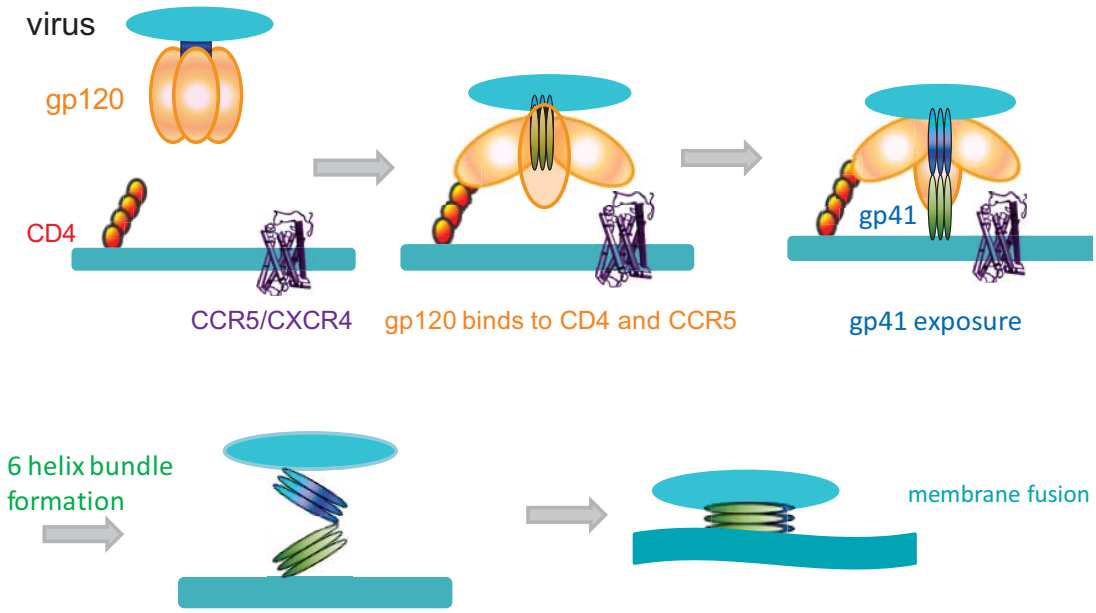

Figure 1-3: HIV entry process.

Yellow balls represent gp120 trimer, while green and blue sticks represent gp41 C heptad repeats and N heptad repeats. On the HIV surface, the envelope protein gp120 (gold) interacts with receptor CD4 (orange) and coreceptor CCR5 or CXCR4 (purple) on the host cell surface. Middle: When viral gp120 binds to the receptor CD4 and coreceptor (CCR5 or CXCR4; purple, 7-transmembrane helix), gp120 undergoes a conformational change and exposes gp41 (cyan and green). When gp41 is exposed, the N-terminus and C-terminus of gp41 form a 6-helix bundle, assisting fusion with the host cell membrane.

1.3 Trimeric envelope spikes (*env*) on the HIV surface

HIV envelope glycoprotein is the molecular machinery mediating virus entry into target cells. Together with influenza and paramyxovirus glycoproteins, the HIV glycoproteins belong to the "type I viral membrane protein" category, where the proteins share similarities in protease cleavage, sequence, and entry process [22]. Here we will discuss the structures of HIV envelope protein gp120 and gp41, and how HIV enters into target cell.

1.3.1 Env trimers form clusters on HIV surface

Using cryo-electron microscopy, Zhu et al. found that the HIV-1 virion surface usually only has 14 ± 7 env spikes per virion particle (ranging from 4 to 35). This number is much smaller compared to other viruses, such as simian immunodeficiency virus, which has almost 4-fold the amount of spikes (73 ± 25). Influenza type A virus has also been reported to have 450 spikes per virus particle, spaced at intervals ≤10 nm [23]. HIV spikes form clusters on the viral surface (red circles in Figure 1-4), and the closest distance between two spikes is 15 nm (150 Å) [4]. HIV has much fewer spikes and longer distances between spikes than do other viruses.

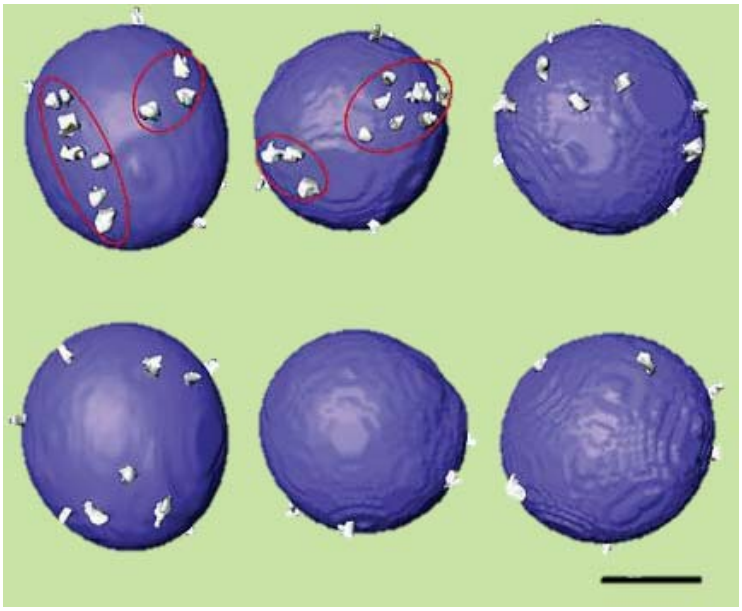

Figure 1-4: Surface-rendered models of HIV spikes.

Models of three representative HIV-1 virions with presumptive *env* spikes shown in white [4]. Ellipses encircle clusters of three or more spikes. Scale bar, 50 nm.

1.3.2 HIV envelope protein gp120 and gp41

HIV trimeric spikes are composed of envelope (*env*) glycoprotein gp120 and gp41 on the HIV surface (gp is short for glycoprotein). The precursor of the HIV env protein is gp160. The gp160 protein is glycosylated in the Golgi apparatus and cleaved into two subunits by a protease named furin. The two subunits produced are the exterior subunit, gp120, and transmembrane subunit, gp41.

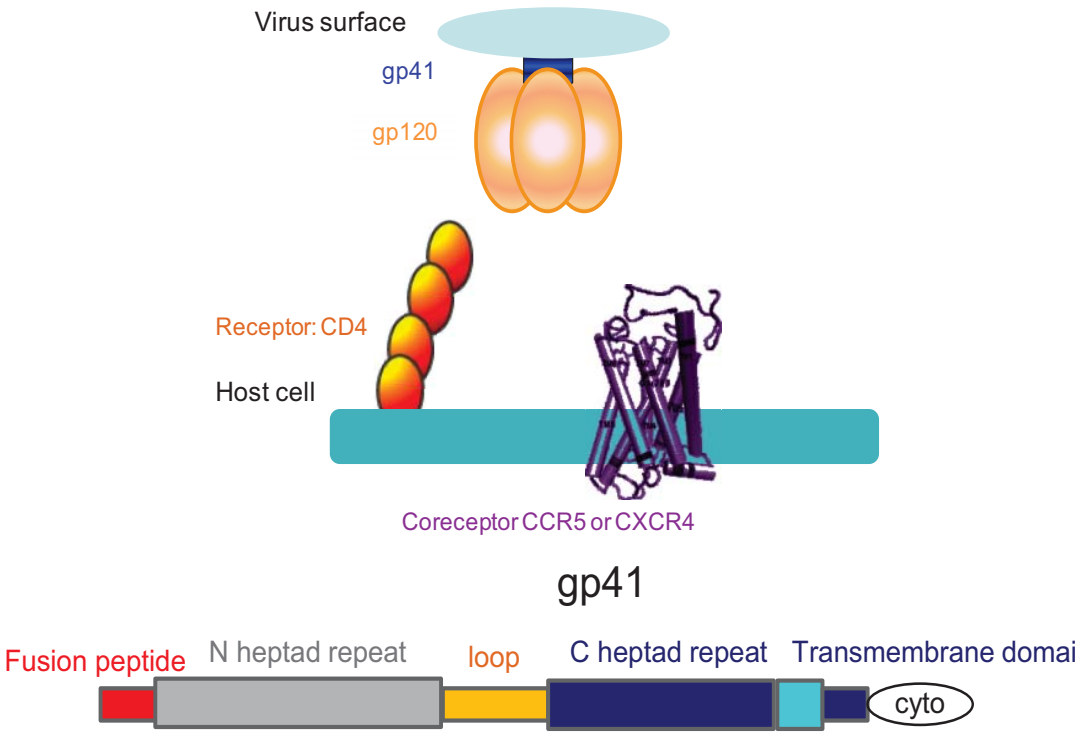

Figure 1-5: HIV envelope protein gp120 and gp41

Top: HIV surface protein gp120 and gp41 about to contact the host cell surface receptor and coreceptor (seven-transmembrane helix).

Bottom: gp41 domains. During HIV entry, fusion peptide anchors into target cell membrane, N heptad repeat folds back and interact with C heptad repeat, forms a six helix bundle, brings the virus close to target cells. As soon as the virus membrane fuses with target cell membrane, virion particles are released into cells.

As noted, gp120 is a glycosylated trimer, non-covalently associated with gp41, which mediates viral fusion. Five variable regions (variable loops) were identified when comparing the gp120 sequence of different primate immunodeficiency viruses, namely the V1 to V5 loops. There are several loops important for HIV entry, particularly the V1/V2 loops and the V3 loop. V1/V2

loops form the so-called bridging sheet and bind to the human cell receptor CD4, while the V3 loop contacts the corecptor and is the major determinant for coreceptor usage. Most recently, the cryo-EM structure of a fully glycosylated soluble HIV-1 gp140 trimer (gp120 plus extracellular domain of gp41) in complex with a CD4 binding site (CD4bs) antibody PGV04 has been solved at 5.8 Å (Figure 1-6) [7]. The gp120 core crystal structure in complex with a CD4 binding site antibody PGV04 was docked into the EM map and further refined. This structure reveals the organization of fully glycosylated gp120 with gp41 extracellular domain in the CD4 bound form, as well as variable loops V1 V2 and V3 which are usually missing in previous published crystal structures. V1 V2 loops are located at the apex of gp120 trimer, and the V3 loop is situated directly beneath the V1/V2 hairpin with the tip pointing toward the trimer axis and interacting with the V2 base from the adjacent protomer (Figure 1-6, V3 loop shown in black). Gp41 forms a pedestal at the base of the trimer (Figure 1-6, purple, magenta and pink showing gp41 trimers) in this “pre-fusion” state, which we will discuss later. The N heptad repeat forms a three-helix bundle with the neighboring protomers in the trimer core (Figure 1-6, black arrow) and the C heptad repeat wraps around the outer periphery of the trimer base, angling downward and with its C terminus proximal to the viral membrane (Figure 1-6, purple arrow).

Gp41 consists of a cytoplasmic domain (CD), transmembrane domain (TM), C-terminal heptad repeat (CHR), N-terminal heptad repeat (NHR), and a fusion peptide that is located on the N-terminus of the protein (Figure 1-5). The N-terminal region contains a hydrophobic sequence, which is known as the 'fusion peptide' since various studies have shown that this segment associates with the target membrane during HIV entry. The C-terminal region contains the membrane-anchoring domain (or transmembrane domain) (Figure 1-5, bottom panel). The gp41 polypeptide also includes the C heptad and N heptad repeats that fold and anneal after receptor and coreceptor binding. Gp41 is originally located at the bottom of the trimeric spikes on the viral membrane (Figure 1-6, purple, magenta and pink helices). When gp120 interacts with the receptor and coreceptor on the target cell surface, the gp120 trimer opens up and forms an “open, activated” state, gp41 flips to the top (target cell side), inserts its fusion peptide to target cell and forms a six helix bundle, thus leading to fusion. However, this “open”, or post-fusion state of trimeric gp120 has not been successfully crystallized yet due to the difficulty to stabilize the complex.

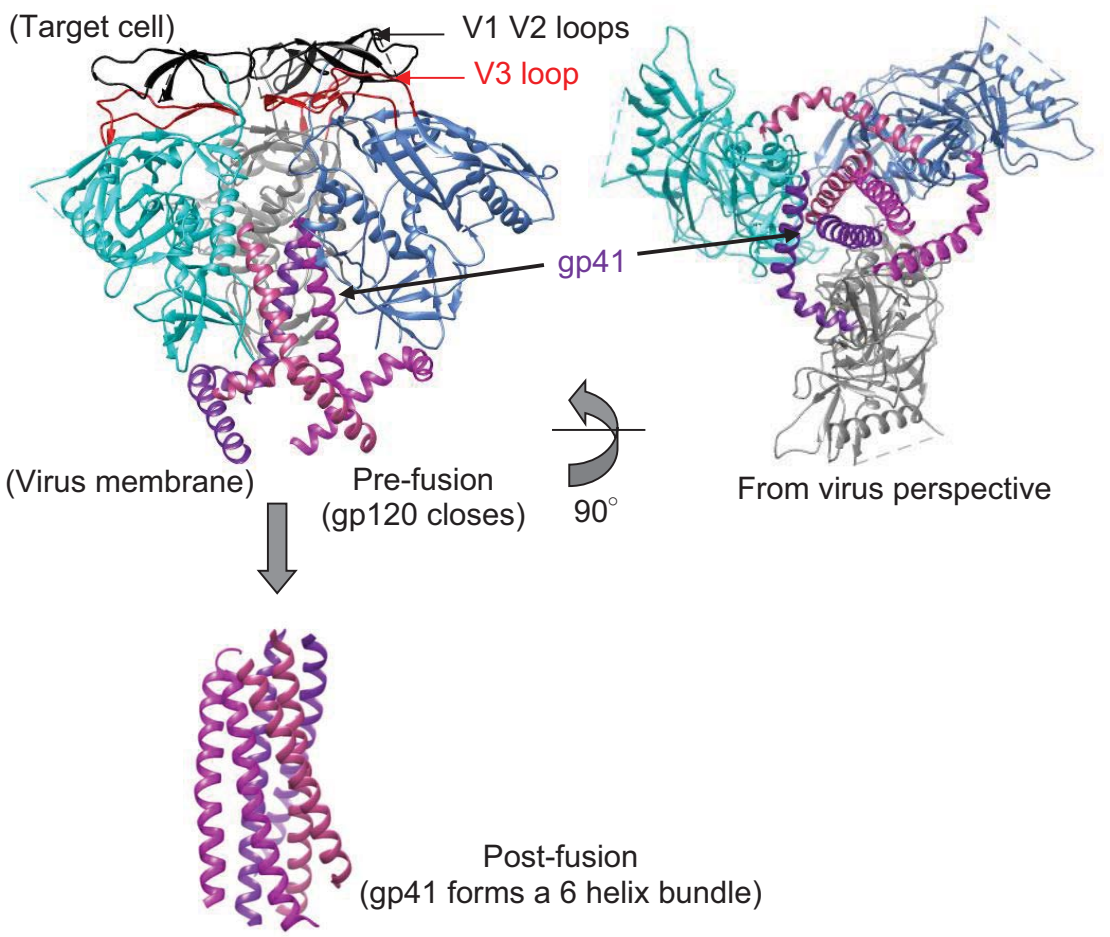

Figure 1-6: Cryo-EM structure of a fully glycosylated soluble cleaved HIV-1 envelope trimer.

Top: A fully glycosylated soluble cleaved envelope trimer in complex with a CD4 binding site antibody PGV04 (not shown here) at 5.8 Å. Env trimer shown here is in closed, pre-fusion state [6]. Gp120 trimers are shown in cyan, blue and grey. Gp41 are shown in purple, pink and magenta. V1 V2 loops are shown in black, V3 loops are shown in red. Left figure shows env trimer, viewed from the perspective of the virus. Structure was made with the program Chimera [5] using PDB structure 3j5m [7]. Notice that in the pre-fusion state, gp41 is at the bottom of the env trimer, on the side of virus membrane.

Bottom: After receptor and coreceptor binding, gp41 flipped to the top and form six-helix bundle. Structure of six-helix bundle was made using PDB 3043 [16].

1.3.4 Gp120 undergoes significant conformational change upon receptor and coreceptor binding

During HIV entry, when gp120 interacts with the CD4 receptor, gp120 undergoes a conformational change by exposing the coreceptor binding site, as well as gp41. The deglycosylated gp120 core structure is folded into two major domains: the inner domain and outer domain (Figure 1-7, Right Panel). The inner domain contains two helices and several β-sandwiches; the outer domain is a stacked double barrel and almost parallel to the inner domain. The outer domain of gp120 has the fewest changes compared to the unligand gp120. CD4 binding induces a conformational change in gp120, which forms a conserved cavity due to the electrostatic potential at the surfaces of CD4 and gp120. One of the most significant conformational changes on gp120 upon binding CD4 is the formation of a "bridging sheet" at the membrane distal domain, which is composed of four antiparallel β strands and mainly derived from V1 V2 loops (Figure 1-7, magenta) [3]. Upon CD4 binding, gp120 goes from a rigid structure to a flexible state, allowing for coreceptor binding (i.e. binding to CCR5 or CXCR4) [3].

For the ligand binding state of gp120, Kwong, P. et al. solved the crystal structure of the monomeric gp120 core in complex with the CD4 receptor and 17b Fab domain, in which 17b is an anti-gp120 antibody that binds the coreceptor binding site (Figure 1-7). The CD4 binding site on gp120 is composed of the interface between the inner and outer domain of gp120, as well as the newly formed "bridging sheet". The V3 loop is located at the distal region of inner domain (Figure 1-7, red). During HIV entry when gp120 undergoes conformational change, the V3 loop is redirected toward the target cell and engages the coreceptor binding site [24] and is the major determinant for coreceptor specificity [25].

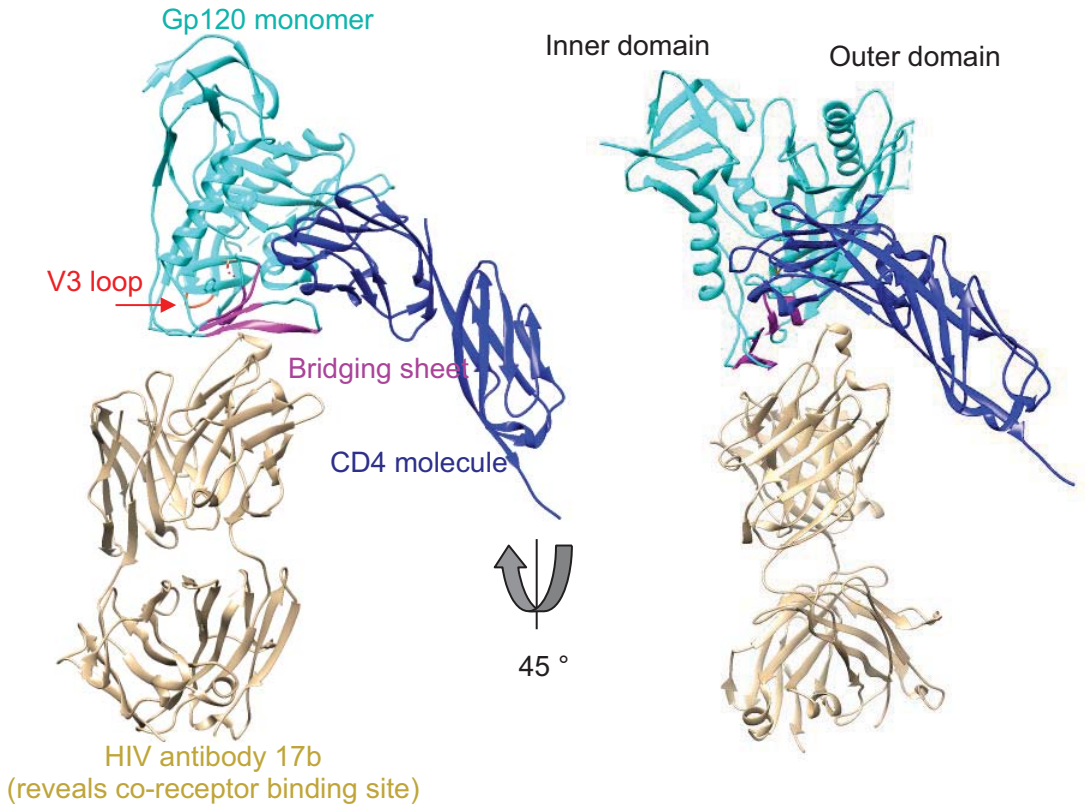

Figure 1-7: Structure of monomeric unglycosylated gp120 in complex with CD4 and 17b.

Gp120 in complex with CD4 and 17b (CCR5 binding site antibody) represents the open, activated conformations [3]. Viral membrane is on top. Monomeric gp120 is labeled in cyan. CD4 molecule is blue, showing the CD4 binding sites. HIV antibody 17b, which binds the co-receptor binding site on gp120 is labeled in gold. In this structure the V1/V2 loops are missing and the V3 loop is labeled in red. The bridging sheet is labeled in magenta. The structure was made with the program Chimera [5] using the PDB structure 1g9m [3].

1.3.5 Structure mechanism of *env* activation

The env trimer undergoes significant conformational change upon receptor and coreceptor binding [3]. Recent studies showed that the CD4 binding site, as well as the bridging sheet formed upon CD4 binding, are slightly different in monomeric and trimeric gp120 structures, probably due to the neighboring protomer restricting CD4's accessibility to the trimeric env structure [7]. The structure of the env trimer in complex with CD4 binding site antibodies reveals that the env trimer shares similar structures when bound to a CD4 binding site antibody, representing a "closed, pre-fusion" form; while env trimer complex with 17b, a coreceptor binding site antibody, reveals a "active, open" form [3, 26]. A comparison of the structures of pre-fusion, closed state and active, open state of env trimer suggests that gp41 serves as an anchor for env trimer (Figure 1-8). Gp120 rotates around the gp41 base and relocates V1 V2 loops to the periphery of the trimer upon coreceptor binding. The outward movement of the V1 V2 loop could uncloak the partially buried V3 loop in the open conformation, possibly facilitating V3 loop for coreceptor binding.

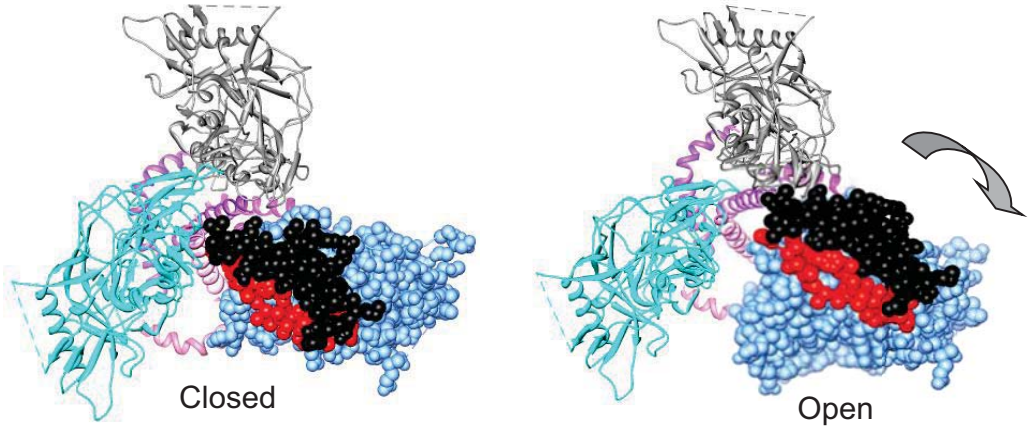

Figure 1-8: Model of env trimer showing pre-fusion, closed form and active, open form.

V1 V2 loops are shown in black, V3 loops is shown in red. Env activation results in outward rotation of gp120 trimer around gp41 stalk. Partially buried v3 loop in pre-fusion state is now exposed and ready for coreceptor binding in the open form. Structure was made using PDB structure 3j5m [7] and 4cc8 [6]. Figure here just show one gp120 subunit, as shown in the blue sphere.

1.3.6 Glycan sites on the gp120 surface

While HIV has relatively few envelope proteins on its surface (few spikes), the HIV env gp120 itself is among the most heavily glycosylated proteins in nature [27], far more heavily glycosylated than envelopes of other retroviruses of

similar size [28]. Not all the potential glycosylation sites on a given HIV-1 Env protein are fully occupied [29]. During viral production, these potential glycosylation sites might be differently glycosylated according to cell type, enzyme accessibility, and transmission stage, etc. [30, 31]; and the glycosylation sites used are major determinants of coreceptor usage [32]. For recombinant HIV gp120, there are usually around 27 glycan sites in gp120, among which around 9-12 are high mannose saccharides, while the rest of them are complex saccharides or hybrid saccharides (>70%complex type glycans) (Figure 1-9). However, in contrast to the recombinant gp120, the N-linked glycans from primary isolates of HIV-1 from clades A, B, and C have been shown to be almost entirely oligmannose, with less than 2% complex type glycans [33].

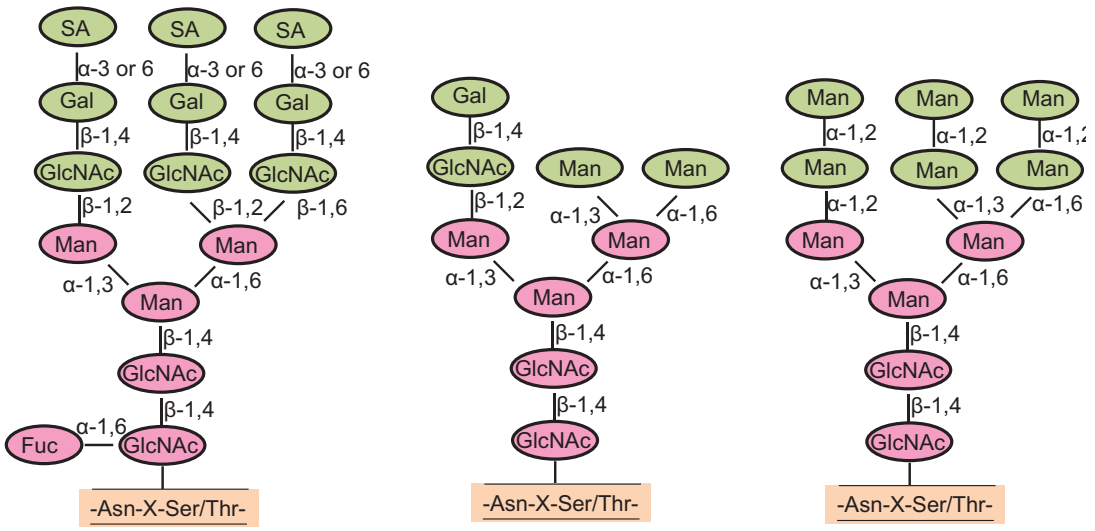

Figure 1-9: Examples of the structural composition of high-mannose-type *N*-glycans.

Left: Complex-type *N*-glycans. Middle: Hybrid-type *N*-glycans. Right: High-mannose-type *N*-glycans that are abundantly present on the envelope glycoprotein gp120 of HIV, but are rare on mammalian glycoproteins. Besides high-mannose-type *N*-glycans, the complex-type and hybrid-type *N*-glycans are also present on gp120. Asn, asparagine; Fuc, fucose; Gal, Galactose; GlcNAc, N-acetylglucosamine; Man, mannose; SA, sialic acid; Ser, serine; Thr, threonine; X, any amino acid except proline.

As stated above, HIV-1 env enters CD4-positive T cells through a series of steps, including binding to both the CD4 protein and a chemokine receptor protein, usually CCR5 (R5 viruses) or CXCR4 (X4 viruses). Some viruses can use either one of the chemokine receptors (R5X4 viruses) [34]. The V3 loop on gp120, which interacts with the chemokine receptor binding site upon CD4

binding and inserts into the ligand binding core of the coreceptor, has been shown to be a determinant of coreceptor usage: complex carbohydrate at N300 was present in all 44 R5 isolates (100%), but only in 4/11 (36%) of the X4 isolates and 7/11 (64%) of the R5X4 dual isolates [35]. Site-directed mutagenesis has shown this site to be associated with coreceptor usage [32, 36].

In addition to coreceptor usage, different glycan patterns have been shown to be important for lectin function. Anti-HIV lectins griffithsin (Grft), cyanovirin-N (CV-N), and scytovirin (SVN), which recognize carbohydrates on gp120's surface, have been shown to be sensitive to certain deletions in glycosylation sites [37-39]. In chapter 3, we analyze the glycosylation pattern on different HIV strains and study the structure of gp120. We also discuss results from our study of the HIV inhibitor Griffithsin (Grft) which is a lectin that binds to gp120 with high affinity, and propose why Grft might be sensitive to these particular glycan sites.

1.4 Structure of the HIV coreceptor

1.4.1 Structure of CCR5

CCR5 (a seven transmembrane chemokine receptor) is the coreceptor for HIV entry, and viruses using CCR5 as the coreceptor for entry are classified as “R5” strains. In addition to CCR5, the HIV virus can also use another seven-transmembrane coreceptor, CXCR4, to enter the cell (X4 strains). During early stages of HIV infection, most HIV viruses are R5 strains, and viruses can switch to X4 during later stages of infection. Patients usually develop syndromes at this later stage [40]. However, some newly discovered HIV strains, mostly from clade C, do not switch to X4 even in later stages of infection [41]. Recently, both the CXCR4 and CCR5 structures have been solved. This is a milestone in the HIV and GPCR (G protein coupled receptor) field, though detailed information about receptor-virus interaction and chemokine recognition is still not well understood.

Figure 1-10 shows the crystal structure of CCR5 in the inactivated state in complex with an HIV entry inhibitor maraviroc, which binds CCR5 as an antagonist and inhibits HIV entry. There are two complexes in each unit (homodimer), with three extracellular loops (ECL) and three intracellular loops (ICL). Previous studies with an N-terminal peptide for CCR5 found that there are several sites important for CCR5 function. The chemokine recognition site and signaling site are separated, and a “two-site” model has been proposed to elucidate the chemokine receptor's function. “Site 1” on the receptor is the chemokine core domain docking site, which interacts with a globular domain after the chemokine's N-terminus. “Site 2” binds the chemokine's N-terminus and triggers signaling.

Here, in the CCR5 structure, the chemokine recognition site (Site 1, green in Figure 1-10) is composed of the N-terminal portion of CCR5 and the ECL2, and

this site recognizes specific ligands for CCR5. During HIV entry, when gp120 undergoes a conformational change and the V3 loop redirects to begin coreceptor binding, this "Site 1" interacts with the gp120 V3 loop and leads to HIV entry. Site 2 (blue residues) with maraviroc (black), is considered the activation site. This site is responsible for ligand binding, and the flexible N-terminus of chemokines is possibly inserted into this binding site.

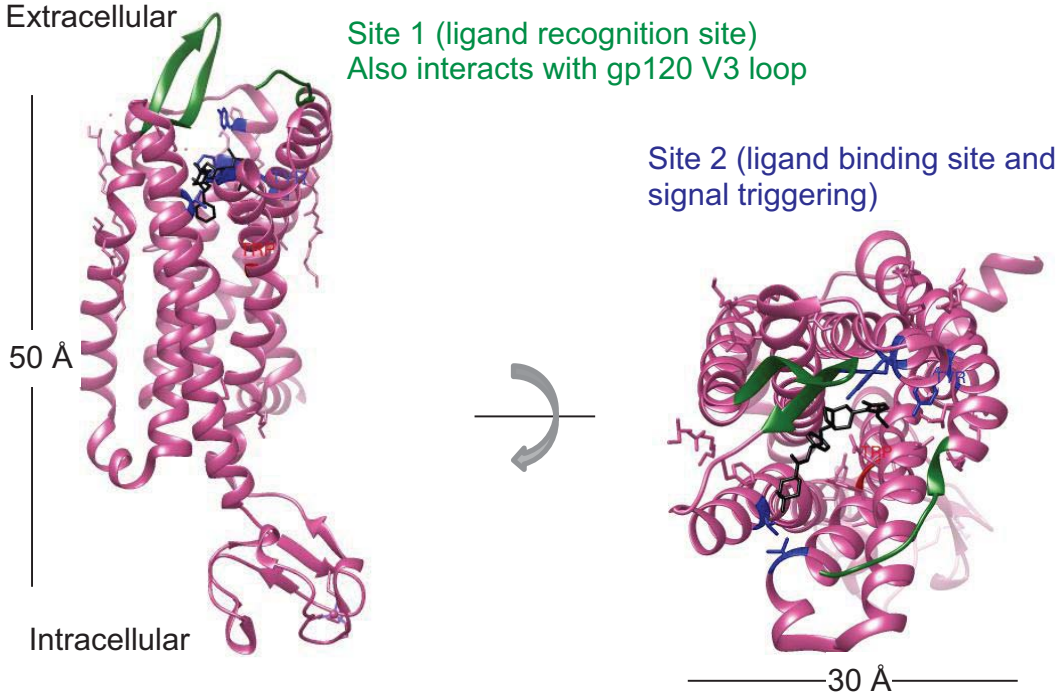

Figure 1-10: Crystal structure of HIV coreceptor CCR5.

Left: Crystal structure of HIV coreceptor CCR5. N-terminus and ECL2 (site 1) are shown in green, while maraviroc is shown in black. Residues Tyr 37 and Trp 248 are important for CCR5 activation and responsible for maraviroc binding, as shown in blue. The structure was made with the program Chimera [5] using PDB structure 4mbs [15].

Right: Top to bottom view of CCR5 from the extracellular. Maraviroc (black) is buried in Site 2, which is the ligand binding site.

1.4.2 Model of chemokine-CCR5 interaction:

The CC chemokine RANTES is a CCR5 ligand that will be described more fully in Chapter 1.5.3. As mentioned, HIV isolates are shown to predominantly use CCR5 for infection at early stage of infection [40], thus RANTES and its derivatives are very promising in preventing HIV transmission. The N-terminus of RANTES has been shown to be important for its function (Figure 1-11, orange), and Y/F13 is shown to be important and conserved among RANTES variants

(Figure1-11, red). Here, we used the published CCR5 structure (PDB: 4mbs) and RANTES structure (PDB: 1hrj) and propose the possible interaction between RANTES and CCR5 (Figure 1-11).

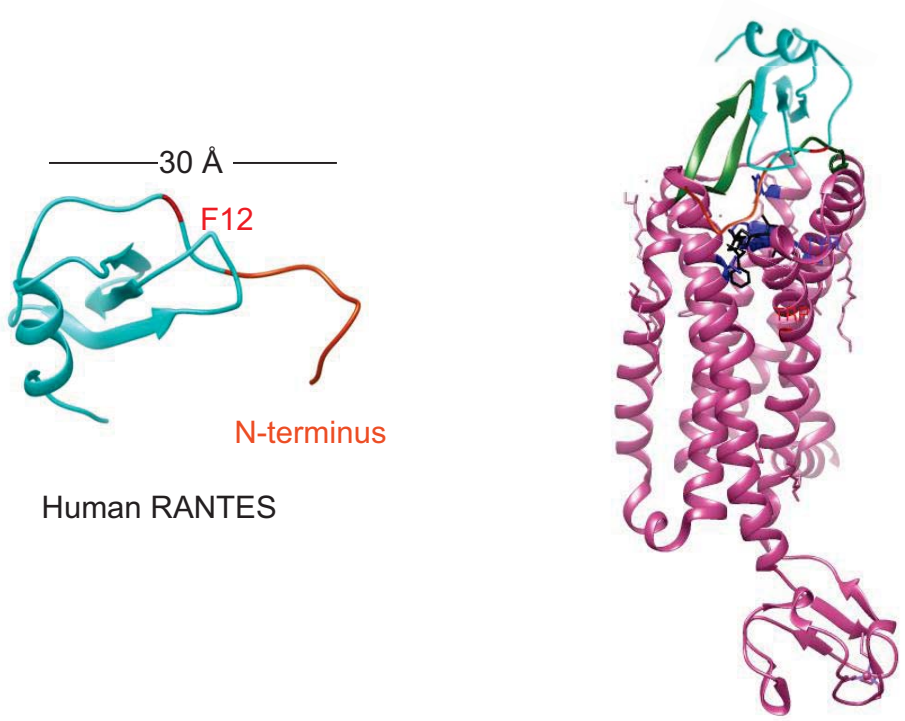

Figure 1-11: Model of chemokine RANTES interaction with CCR5.

Left: Human RANTES structure in cyan. Blue represents the N-terminal 10 amino acids, which is important for receptor binding and downstream signaling. After the N-terminus, chemokine forms core globular domain (cyan), which binds CCR5 N-terminus and extracellular loop 2. Structure was made with the program Chimera [5] using PDB structure 1hrj [12].

Right: Proposed model of RANTES and CCR5 interactions. N-terminus of chemokine RANTES (blue) insert into the core of CCR5 receptor (Site 2), while chemokine globular domain (cyan) interact with CCR5 N-terminus and ECL2 (green).

1.4.3 Structure of HIV coreceptor CXCR4

Crystallization of CXCR4 bound to an antagonist showed that CXCR4 also forms a homodimer and shares many similarities to the CCR5 structure, except that the location of the ligand binding site (Site 2) in CCR5 is higher and the binding area is larger [42]. A comparison between the binding pockets of CCR5

(Site 2, for ligand binding and signal triggering) and CXCR4 showed that CXCR4 has more acidic residues, while CCR5 has mostly uncharged residues [15].

Gp120's V3 loop is heavily glycosylated and determines the coreceptor usage. The stem region of the V3 loop has been reported to be responsible for coreceptor binding. The V3 crown interacts with the co-receptor's ECL2 (Site 1) and residues inside the ligand-binding pocket (Site 2) [43-45]. It has been reported that mutating the uncharged residues on the CCR5 ligand binding pocket (Site 2) greatly reduces interaction with gp120, indicating that these uncharged residues are responsible and critical for gp120 binding [46]. Models of CCR5–R5-V3 and CXCR4–X4-V3 complexes based on the CCR5 structure suggest that the different charge distributions in the ligand binding pockets on the coreceptor may be the major determinants of HIV coreceptor selectivity [15]. Models have been proposed about the CCR5 in complex with the V3 loop from both R5 and X4 HIV strains, as well as CXCR4 in complex with V3 loop from both R5 and X4 strains. Comparison of these interactions showed that complexes from the CCR5-R5 strain's V3 loop has stronger interactions than the CCR5-X4 strain's V3 loop, indicating that the ligand binding sites use different charged residues to select for different HIV virus strains [15].

1.5 HIV entry inhibitors

There are inhibitors targeting different steps during HIV entry based on knowledge regarding the HIV entry mechanism. In our lab, we are focusing on several inhibitors: lectins that bind gp120; RANTES (Regulated on Activation, Normal T cell Expressed and Secreted) and its derivatives that bind CCR5; and fusion inhibitors that inhibit gp41 six helix bundle formation, thus inhibiting HIV fusion with host cells.

1.5.1 Inhibitors that bind glycoprotein gp120

The so-called HIV receptor CD4 on the human cell binds into a cavity at the CD4 binding interface formed between the gp120 inner and outer domains (Figure 1-7) [3]. The cavity on g120 caused by CD4 binding does not contain glycosylated sites, which means it is conserved among different HIV strains since different HIV strains may have different sequence as well as glycosylation sites. Upon CD4 binding, gp120 goes from a rigid structure to a flexible state, allowing for coreceptor binding (i.e. binding to CCR5 or CXCR4) [3]. Inhibition of these interactions includes molecules such as gp120 binding antibodies, carbohydrate binding agents including lectins and antibiotics, etc. Some of these inhibit HIV entry through a simple binding and blocking mechanism, but some may have other mechanisms involved, such as cross-linking gp120 or inducing gp120 conformational change during HIV entry.

1.5.2 Griffithsin (Grft): A protein lectin binds the carbohydrates on gp120

Lectins are carbohydrate binding proteins. They are usually extracted from plants, and recognize specific sugar moieties. Recent studies showed that some lectins exert potent inhibition against HIV entry, as well as against some other enveloped viruses. In chapter 2 and 3, I focus on a protein lectin named griffithsin (GRFT), which binds carbohydrate on gp120 and potently inhibits HIV entry.

Grft is a protein lectin extracted from red alga [47]. It has 121 amino acids and exhibits potent anti-HIV activity (in the nanomolar range), and is the most potent anti-HIV lectin discovered so far. In addition to HIV, Grft is also potent against the hepatitis C virus, the SARS Coronavirus, the Japanese encephalitis virus, and the herpes simplex virus [48-50]. Recent studies showed that Grft could be purified in large amounts (multigram quantities) in tobacco leaves [51], and it showed great safety profiles in cell-based assays, including no activation for T cells, retaining activity while interacting with peripheral blood cells, and inducing only minimal changes in cytokine and chemokine expression in immune cells [48, 52, 53]. In addition to the safety and effectiveness profile, Grft also showed synergy when combined with other HIV antibodies or drugs [54]. Recent studies showed that Grft is also resistant to most proteases [53], making it a very promising therapeutic candidate. However, important biochemical details on the antiviral mechanism of GRFT action remain unexplored.

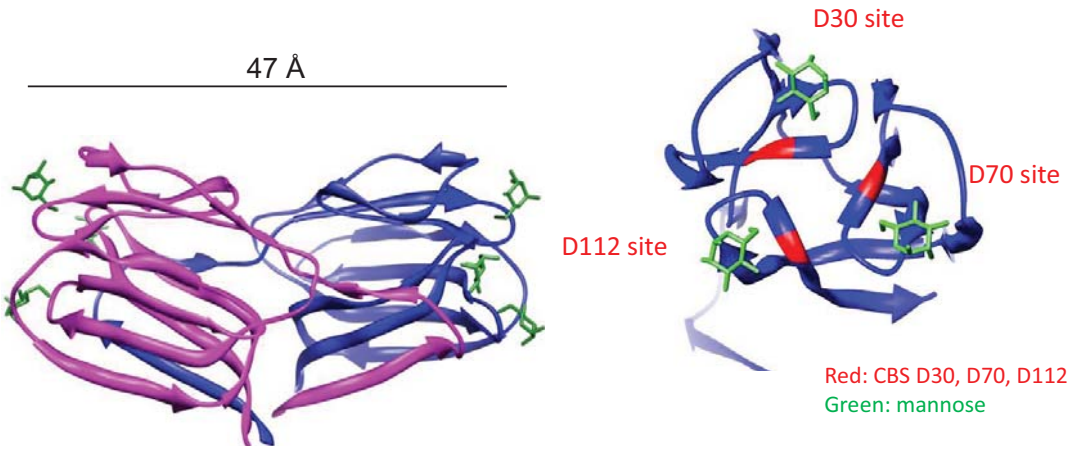

Figure 1-12: Structure of HIV entry inhibitor griffithsin (GRFT) and three carbohydrate binding sites.

Left: Blue and magenta show that Grft forms a domain-swapped dimer structure with 3 carbohydrate binding sites (CBS) on each subunit. Green sticks represent mannose interacting with the Grft dimer. Structure was made with the program Chimera [5] using PDB structure 2gud [1].

Right: Crystal structure showing that each Grft subunit has 3 carbohydrate binding sites; major amino acids at these sites responsible for mannose binding are D30, D70, and D112 (shown in red). The 3 mannose molecules are shown in green.

X-ray crystallography has shown that Grft forms a domain-swapped dimer (blue subunit and magenta subunit, Figure 1-12) [1], and each subunit contains 3 carbohydrate binding sites (CBS). Griffithsin binds to the HIV envelope protein gp120 in a glycosylation-dependent manner [47, 55]. Both ELISA (Enzyme-linked immunosorbent assay) and SPR (surface Plasmon resonance) data showed that Grft binds to glycosylated gp120, but not to deglycosylated gp120 or gp160. Since Grft is such a promising HIV inhibitor, it is intriguing to investigate the carbohydrate binding of Grft to gp120. In addition, different HIV strains exhibit different gp120 sequences, as well as different glycosylation sites. Thus, it is also important to identify how Grft behaves on these highly variable HIV strains. In Chapters 2 and 3, we study the role of individual carbohydrate binding sites, as well as the role of Grft dimerization in its function, and investigate the mechanisms of Grft.

1.5.3 Inhibitors that bind coreceptor CCR5: RANTES and its derivatives

RANTES (Regulated on Activation, Normal T cell Expressed and Secreted, also known as Chemokine C-C motif ligand 5, CCL5) is a CCR5 ligand that binds

coreceptor CCR5 and suppresses HIV infection. In 1995 it was shown by Drs. Robert Gallo and Paulo Lusso's group to be one of the major suppressive factors secreted by $CD8^+$ T cells [56]. Later, its receptor, CCR5, was found to be a fusion cofactor for macrophage-tropic HIV (CCR5 strains) [56-58]. In addition to sterically hindering the essential interaction between the HIV envelope glycoprotein-120 protein and the receptor, chemokines can also induce receptor down regulation from the cell surface thereby removing the essential coreceptor [59, 60]. However, later, enhanced rather than inhibitory activity of RANTES on HIV replication was observed through the course of infection [61, 62]. Failure of chemokines to inhibit HIV replication is probably due to the disadvantage that RANTES triggers the down-stream mucosal inflammation by recruiting HIV target cells to the site of infection, therefore enhancing HIV infection [63]. In addition, because RANTES tends to oligomerize after binding to glycosaminoglycans (GAGs) on both viral and cell membranes, it is able to cross-link enveloped viruses and increase virus attachment to target cells, thus increase enveloped-virus infectivity [64]. Also, RANTES-GAG binding on cell surfaces transduces a downstream signal transduction pathway that makes cells more vulnerable to viral infection [64].

To overcome these disadvantages, several strategies were used to improve the HIV inhibitory properties of RANTES, such as mutations to reduce glycosaminoglycan binding, or using random mutagenesis to produce RANTES derivatives with higher potency but reduced rates of inflammation [65]. N-terminal modifications of RANTES have been particularly well-studied since the N terminus was found to be essential for receptor binding and activity [66, 67]. Both organic modification and random mutagenesis at the N-terminaus of RANTES was used to find RANTES derivatives that had properties such as reduced downstream signaling activity and increased binding affinity and selectivity to CCR5. These studies yielded effective HIV inhibitors such as PSC-RANTES, P2-RANTES, and 5P12-RANTES [66, 68, 69]. In our lab, we covalently linked 5P12-RANTES with a fusion peptide C37 (a fusion inhibitor derived from the C heptad repeat, which we will discuss below) and this chimeric inhibitor showed high efficiency and low HIV resistance [70]. Scientists are also engineering *Lactobacillus jensenii* to secrete a RANTES variant as a live HIV-1 strategy [71].

1.5.4 Inhibitor binds both coreceptor CCR5 and CXCR4: vMIP-II

The protein vMIP-II (viral Macrophage Inflammatory Protein-II) is a chemokine analog produced by human herpesvirus 8 (HHV-8) that has high sequence identity to many chemokines as well as nearly identical tertiary structure [10, 72, 73]. However, this protein is unique among chemokines in its ability to bind but not activate receptors of chemokines from multiple sub-families, including the receptors CCR5, CXCR4, CCR1, and CCR2 [74]. These properties allow vMIP-II to effectively compete with the natural chemokine ligands of these receptors, including MCP-1 (monocyte chemoattractant protein-1), MIP-1α

(macrophage inflammatory protein-1 alpha), MIP-1β (macrophage inflammatory protein-1 beta) and RANTES, and have elicited interest in vMIP-II both as an anti-inflammatory agent and for its ability to inhibit HIV [75]. This 71 amino acid protein is also an agonist (having the ability to bind and to cause an intracellular response) for the receptor CCR3 [74, 76, 77]. Though this chemokine analog is able to bind both CCR5 and CXCR4, it is less potent compared to other HIV inhibitors with EC_{50} in the micromolar range [74, 75]. In chapter 4, we have made a vMIP-II variant, "5P12-vMIP-II" in which the N-terminal amino acids of vMIP-II have been replaced by 10 amino acids that have been shown to greatly enhance the anti-HIV potency of the chemokine RANTES for R5 HIV strains [68].

1.5.5 Inhibitors that bind gp41: Fusion peptides

During HIV infection, when gp41 is exposed after gp120 interacts with the receptor and coreceptor, the N- and C- heptad repeats of gp41 form a 6 helix bundle, bringing the virus close to host cell membrane, thus leading to viral fusion with target cell. N peptides and C peptides are fusion peptide inhibitors derived from the N- or C- heptad repeats of gp41 that target the corresponding binding region and interfere with 6 helix bundle formation, thus inhibiting HIV fusion (Figure 1-14). For example, C peptides are peptides derived from C-heptad repeat, which can bind to the N-heptad repeat. Specific amino acids have been mutated in order to increase the anti-viral activity, and to reduce HIV resistance and protease degradation. C-peptides are the major inhibitors; the N-peptides are also well-studied, but they have several disadvantages, in that they are less potent than C peptides and are also known to aggregate [78].

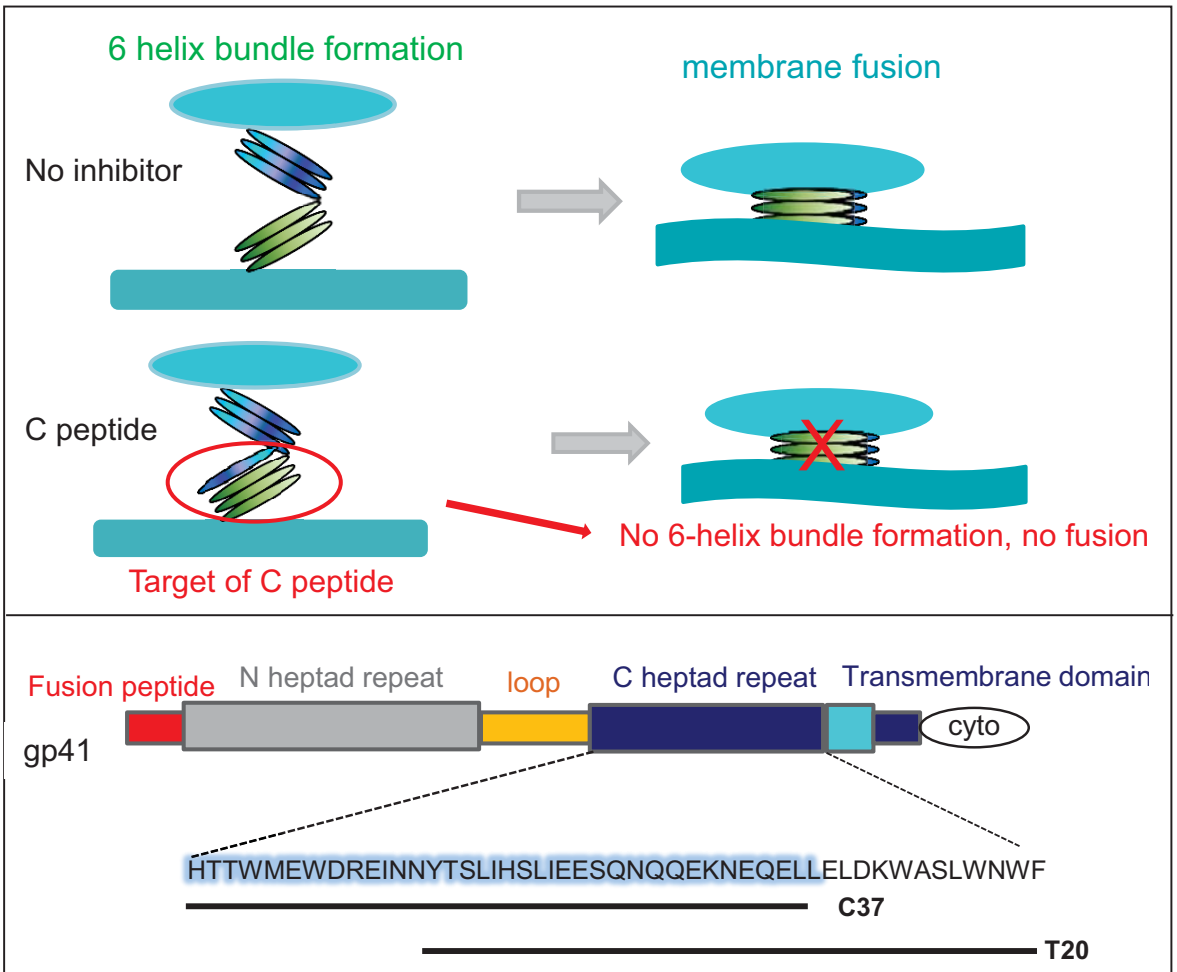

Figure 1-13: Schemes of gp41 structure.

Top: C-peptides are peptides derived from the C-terminus of gp41, which forms the C heptad repeats of the 6 helix bundle. Therefore, c peptides bind to the N-heptad repeat and inhibit 6 helix bundle formation thus interfering with HIV entry.

Bottom: sequence alignment of C37 and T20. Both peptides are derived from C heptad repeats with highly hydrophobic residues.

T20 (enfuvirtide) is a 36-amino acid peptide that binds to the hydrophobic region on N terminus of gp41 and blocks HIV entry. It was approved by the FDA in 2003 as the first entry inhibitor to be used as a drug. However, it causes many side effects such as fever; in addition, since it is a peptide it cannot be ingested as a pill due to susceptibility to degradation by human proteases, and it is prescribed to be injected twice a day, which is an inconvenient therapeutic method for patients. Therefore, it is currently only used as a salvage strategy for

patients failing other therapies. However, studies show that T20-resistant strains may have reduced replication ability, so T20 is promising as a component of a combination treatment or could be used to generate newer inhibitors.

Newer generations of C peptide: T2635 and T1144

Because of drug resistance and side effects of the first generation of C-peptide T20, mutagenesis and HIV-resistant selection have been used to generate newer generations of C-peptides, including T2635 and T1144 [79, 80]. Newer features include less HIV resistance among different strains, longer half-life in animal studies, and higher affinity to HIV gp41.

1.6 Multivalent studies of anti-HIV lectins and antibodies

Unlike other enveloped viruses which generally exhibit a high density of envelope spikes (i.e. gp120, gp41), HIV displays a very low density of spikes [4, 81]. Although similar in size to influenza type A, HIV has an average of 14 spikes per virus particle with longer distance between spikes, while influenza type A virus has ~450 spikes per virus particle [23]. These HIV spikes form clusters on the virus's surface with the closest distance between two spikes being 150 Å [4]. As few as 4 spikes have been shown to be sufficient for HIV entry [82], and possibly even fewer spikes are needed achieve fusion with the target cell membrane [83].

Several models have been proposed for lectins or antibodies binding to gp120, including the possibilities of inter-spike or intra-spike cross-linking [84]. As shown for lectins and some carbohydrate binding antibodies, bivalent binding is necessary for potent function, and multivalency leads to higher activity [85, 86]. Class-switch of anti-gp120 carbohydrate binding antibodies from IgG (two epitope binding sites) to IgM (five epitope binding sites) leads up to 28-fold more efficiency [87, 88].

Enhanced inhibition due to multisite binding can often be explained by the avidity effect of the inhibitor [84, 85]. The effect of avidity on the affinity of a multivalent antibody or lectins can be explained as a two-step reaction. When the first binding site of an antibody molecule is tethered to the surface, the small reaction volume increases the reaction rate of the second binding site and brings the free binding site close to its target. This increased on-rate of the second (later) site after the first site binding leads to overall better binding and less dissociation of the lectin or antibody from the virus [84].

In addition to increased affinity, another important question regarding an inhibitor requiring two arms for function is whether the inhibitor is actually cross-linking two different gp120 subunits, as opposed to binding two sugar moieties on the same gp120 subunit. Alternatively, a bivalent inhibitor may actually bind to two different gp120 trimers on the surface of the virus (i.e. two different viral

spikes). The closest distance between HIV spikes is 150 Å [4], which is very close to the distance between the two antigen recognition sites on Fabs. This way, an antibody might be using two Fabs to cross-link two HIV spikes. For lectins, which are much smaller than antibodies, it may have an "intra-spike" cross-linking mechanism (i.e. binding two gp120 monomers within the same trimer). Gp120 is a trimer on the surface of the virus, and the distance between the two arms of Grft (~47 Å) or two carbohydrate binding site of another potent lectin, cyanovirin (~44 Å) could allow for binding to putative glycosylation sites on two different gp120 monomers within the trimer [1, 89] [90]. Using ELISA assays, my data show that griffithsin can cross-link two separate gp120 subunits, which supports the hypothesis that griffithsin can cross-link the gp120. This will be discussed in Chapter 3. However, due to the limitations of assay, this mechanism needs further investigation.

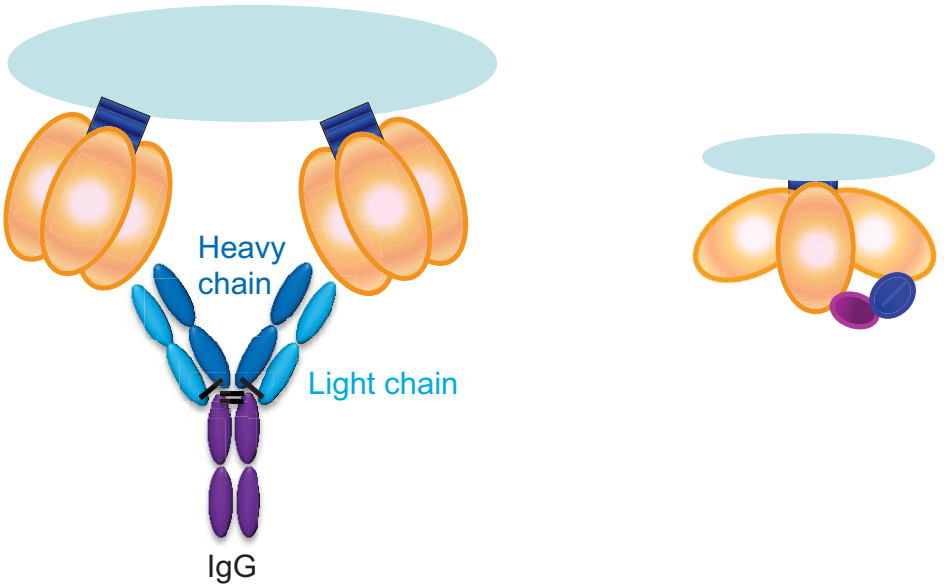

Figure 1-14: A proposed model of antibody or lectin cross-linking gp120 subunits.

Left: An antibody may have an "inter-spike" cross-linking mechanism due to the distance between two antigen binding sites on two Fab domains. When one antigen binding site binds to the epitope, it may increase affinity to the second antigen binding site by decreasing the k_{off} rate, thus achieving higher affinity and potency.

Right: Lectins, or an unusual carbohydrate binding antibody 2G12 that has a shorter distance between two Fab domains than usual Fabs (~45 Å versus 150 Å), may use an "intra-spike" cross-linking mechanism.

1.7 Microbicides

As defined by the World Health Organization (WHO), microbicides are compounds that can be applied inside the vagina or rectum to protect against sexually transmitted infections (STIs) such as HIV. They can be formulated as gels, creams, films, or suppositories. Microbicides may or may not have spermicidal activity (a contraceptive effect). Microbicides need to be easy to apply, cheap to produce, and stable for a long period of time. At present, an effective microbicide is not available. Scientists are working on different combinations of anti-HIV drugs and using them as components of microbicides [91]. For example, the use of a reverse transcriptase inhibitor tenofovir in a topical 1% gel worked to protect against HIV in women in the CAPRISA 004 trial [92]. This was the first proof that a microbicide can protect against sexual transmission of HIV. However, lack of success in later VOICE trials show that many factors need to be considered in designing an acceptable microbicide. Lectins have several features that make them good candidates for components of microbicides: first of all, lectins are usually extracted from plants, and they are very stable against many human proteases and are stable at different pHs and temperatures; secondly, they can be made in large quantities very easily, usually in milligram or gram amounts, and are cheap to produce. Recent studies also showed that lectins have a synergistic effect when combined with anti-HIV antibodies, suggesting a possible combination strategy, using lectins and broadly neutralizing antibodies together [93].

In addition, scientists are also working on different formulations of microbicides to stabilize the active components, making it easy to apply, and studying the time-released capability of potential microbicides. For example, intravaginal rings (IVRs) may improve efficacy by providing long-term sustained drug delivery, and scientists showed that formulated tenofovir in an intravaginal ring completely protects macaques from multiple vaginal simian-HIV challenges [94]. In addition, by using an affinity-based gel, Wang et al. showed that 5P12-RANTES, a derivative of RANTES, can be formulated in a glycosaminoglycan gel that slowly releases active 5P12-RANTES over the course of one month, although this was not tested in an animal model [95]. Our group involved in collaboration to study the use of silk fibroin as a stability matrix for anti-HIV films. These include the use of Grft and 5P12-RANTES as inhibitors, and have been extended to include time release capability.

Chapter 2

The Role of Individual Carbohydrate-Binding Sites in the Function of the Potent Anti-HIV Lectin Griffithsin

This work was published as part of [55]:

Xue J, Gao Y, Hoorelbeke B, Kagiampakis I, Zhao B, Demeler B, Balzarini J, Liwang PJ., "The role of individual carbohydrate-binding sites in the function of potent anti-HIV lectin Griffithsin", *Molecular Pharmaceutics*, 2012 Sep 4;9(9):2613-25. **ACS Articles on Request.**

2.1 Abstract

Griffithsin (GRFT) is a lectin that has been shown to inhibit HIV infection by binding to high mannose glycan structures on the surface of gp120, and is among the most potent HIV entry inhibitors reported so far. However, important biochemical details on the antiviral mechanism of GRFT action remain unexplored. In order to understand the role of the three individual carbohydrate-binding sites (CBS) in GRFT, mutations were made at each site (D30A, D70A, and D112A), and the resulting mutants were investigated. NMR studies revealed that each GRFT variant was folded but showed significant peak movement on the carbohydrate-binding face of the protein. The wild-type and each point mutant protein appeared as tight dimers with a Kd below 4.2 μM. Mutation of any individual CBS on GRFT reduced binding of the protein to mannose, and ELISA assays revealed a partial loss of ability of each GRFT point mutant to bind gp120, with a near-complete loss of binding by the triple mutant D30A/D70A/D112A GRFT. A more quantitative surface plasmon resonance (SPR) examination showed a rather small loss of binding to gp120 for the individual GRFT point mutants (K_D: 123 to 245 pM range versus 73 pM for wild-type GRFT), but dramatic loss of the triple mutant to bind gp120 derived from R5 and X4 strains (K_D > 12 nM). In contrast to the 2- to 3-fold loss of binding to gp120, the single CBS point mutants of GRFT were significantly less able to inhibit viral infection, exhibiting a 26- to 1900-fold loss of potency, while the triple mutant was at least 875 fold less effective against HIV-1 infection. The disparity between HIV-1 gp120 binding ability and HIV inhibitory potency for these GRFT variants indicates that gp120 binding and virus neutralization do not necessarily correlate, and suggests a mechanism that is not based on simple gp120 binding.

2.2 Introduction

In the fight against HIV/AIDS, HIV entry inhibition is increasingly important. To inhibit entry of the virus, general strategies include the development of drugs that interact with the HIV envelope proteins gp120 and gp41, or that interact with human cell surface proteins that are the targets of the virus, such as the co-receptor CCR5 [47, 68, 96]. One important class of potent HIV entry inhibitors is the lectin class, which bind to the glycans that cover the surface of HIV gp120. In particular, the branched mannose oligomers Man-8 and Man-9 on HIV-1 gp120 are the likely target of inhibitors such as cyanovirin-N and griffithsin (GRFT) [1, 11, 90, 97-99]), each of which are highly potent HIV inhibitors in cell culture.

GRFT is a lectin derived from a red algae and is among the most efficient anti-HIV lectins, showing low nanomolar inhibition in cell fusion assays and sub-nanomolar inhibition against single round and replication-competent HIV [47]. GRFT has been shown to be produced easily in gram quantities [51], and to be non-irritating and largely unable to activate cellular receptors under conditions necessary for clinical use [52, 53]. Therefore, this protein is considered as a leading drug candidate to prevent the sexual spread of HIV.

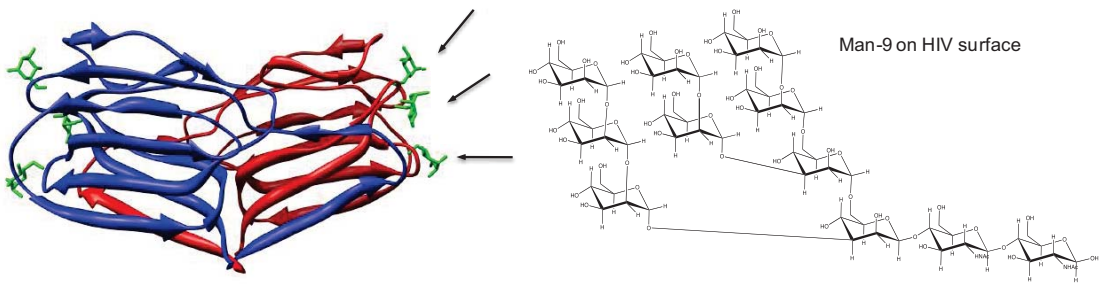

Figure 2-1: Crystal structure of griffithsin (GRFT) and high mannose glycans on HIV surface.

Left: The structure of the GRFT dimer in complex with mannose [1, 2]. The arrows denote the three mannose binding sites of one monomer. Right: The structure of Man-9 [11], an oligosaccharide on the surface of gp120 that is likely bound by GRFT. Structure was made with the program Chimera [5] using PDB structure 2gud [1].

GRFT has been crystallized as a domain-swapped dimer, and several high resolution structures have shown three putative carbohydrate-binding sites (CBS) on each monomer (Figure 2-1) [1, 97, 98]. Each site appears to be able to bind only one glycan unit, but affinity studies with monosaccharides show only a micromolar binding potential. Therefore, some combination of glycan binding by the multiple sites on GRFT, rather than by individual sites, seems to be necessary to achieve high levels of virus inhibition. Mechanistic work on the

particular sites of glycosylation of gp120 reveals the likely importance of N-linked carbohydrates at N295, N234, and N448 in the action of GRFT [38, 39, 100]. Calculations have been carried out suggesting that all three sites on a GRFT subunit could indeed be used simultaneously to bind the three terminal mannose residues of the branched Man-9 of gp120 [101]. However, more recent structural work by these research groups shows that an engineered GRFT monomer "1GS-S" in complex with nona-mannoside does not appear to have all three sites bound simultaneously to the three terminal mannose groups of a high-mannose glycan. In this structure, two of the terminal mannoses bind in two sites on GRFT (Pocket 1 and Pocket 3, using the nomenclature from Ziolkowska 2006 [1]), while the Pocket 2 site was bound by a mannose from another symmetry related nona-mannoside [97]. This work indicated that this Pocket 2 site (with key residue Asp30) was not equivalent to the other two sites within the monomeric subunit, and emphasized the role of the GRFT dimer by showing that a monomeric variant was greatly diminished in its ability to inhibit HIV [97].

Therefore, an outstanding question regarding the mechanism of HIV inhibition by GRFT is the role each of the three putative carbohydrate-binding sites play in the affinity of the protein for its mannose target and subsequent anti-HIV function. Here, we show the effect on the structure and function of GRFT when each individual CBS is mutated. We also present NMR chemical shift assignments of wild-type GRFT and describe further biochemical investigations of the wild-type protein and its mutants, including analytical ultracentrifugation, surface plasmon resonance and assessment of carbohydrate binding and anti-HIV function of wild-type and mutant GRFT.

2.3 Material and Methods

2.3.1 DNA construction

Single site mutations of GRFT (D30A, D70A, D112A) were made using the Stratagene QuikChange® Site-Directed Mutagenesis or using a standard thermocycling strategy. Genes of GRFT variants were cloned into the pET-15b expression vector (Novagen) between the Nco1 and BamH1 cleavage sites. The triple mutation of GRFT (D30A/D70A/D112A) was made using a standard thermocycling strategy and all mutants were confirmed by DNA sequencing.

2.3.2 Protein production and purification

Plasmids with an N-terminal histidine-tag were transformed to *Escherichia coli* BL21(DE3) (Novagen) competent cells and expressed in minimal media with $^{15}NH_4Cl$ as the sole nitrogen source. Each mutant was produced using the following procedure. Protein production was induced upon addition of Isopropyl β-D-1-thiogalactopyranoside (IPTG) with further incubation at 37ºC for 6 hours. Cells were harvested by centrifugation at 6,000xg for 10 min and the pellet was resuspended in 5 M guanidine hydrochloride, 500 mM NaCl, 10 mM benzamidine, and 20 mM Tris pH 8; this allowed complete solubilization of proteins from both the inclusion body and the supernatant upon cell disruption. The solution was French pressed twice at 16,000 psi, and then centrifuged at 15,000 x g for 1 hour. The soluble portion was loaded onto a Ni chelating column (Qiagen) equilibrated with the same resuspension buffer. Proteins that bind nonspecifically were first eluted in the same buffer in the presence of 50 mM imidazole. These were discarded. Finally, GRFT or its variants were then eluted using 500 mM imidazole, 5 M guanidine hydrochloride, 500 mM NaCl and 20 mM Tris pH 8 and refolded by adding dropwise to low salt refolding buffer (50 mM NaCl, 20 mM Tris pH 8) over the course of 30 min. The solution was dialyzed against in the same refolding buffer at 4ºC overnight. The protein solution was then centrifuged at 15,000xg for 1 hour to remove precipitated material, and purified on a C4 reversed-phase chromatography column (Vydac, Hesperia, CA). The fractions were analyzed on a SDS-PAGE gel to confirm the size and then lyophilized in a Labconco freeze-dry system (Labconco Corporation).

For the D30A/D70A/D112A triple mutation, in some preps a slight variation was used. The cell pellet was resuspended in high salt cracking buffer (500 mM NaCl, 20 mM Tris pH 8) without the presence of guanidinium so that only the supernatant was used without further refolding. The purification continued as described above, in buffers lacking guanidinium using a Nickel chelating column, followed by dialysis and C4 column purification.

Concentration of protein was determined using absorbance at 280 nM with an extinction coefficient of GRFT subunit (11920 $cm^{-1}M^{-1}$, from the Expasy program located at http://web.expasy.org/protparam/) except as described for

analytical ultracentrifugation, which also used A_{230}. Results indicate the concentration of GRFT subunits (monomers), except for the surface plasmon resonance, which show the concentration of dimers, since those were established here to be the relevant binding unit.

2.3.3 GRFT binding to D-mannose-agarose column

The D-mannose-agarose column was obtained from Sigma (St. Louis, MO), and is composed of a single mannose saccharide bound to the agarose bead, likely through the C6 hydroxyl. GRFT was made to 15 uM in 50 mM Tris pH 7.4 and bound to the column. Elution was carried out with a gradient up to 200 mM mannose, 50 mM Tris pH 7.4.

2.3.4 ELISA studies of GRFT-gp120 interactions

To test the binding of each GRFT mutant to HIV gp120, ELISA binding assays were carried out as described previously[47, 102]. In brief, 100ng HIV $gp120_{ADA}$ (ImmunoDiagnostic) was coated on each well in a 96 well plate (Maxisorp Immunoplate; Nalge NUNC) overnight at 4 °C. After the plate was washed with 0.5% Tween20 in PBS and blocked with 1% bovine serum albumin for 1 hour, serial dilutions of wild-type GRFT or its mutants were added to triplicate wells and incubated for 2 hours at 37ºC. After the plate was washed, a 1:1000 fold dilution of Horseradish-peroxidase-conjugated Nickel-NTA (Qiagen) (which detects the N-terminal his-tag of GRFT and its mutants) was added according to the company's instructions. Then the substrate for Horseradish-peroxidase (2,2'-azino-bis 3-ethylbenzthiazoline-6-sulphonic acid) (Fisher Scientific) was added and signal was measured by absorbance at 405nm.

2.3.5 Virus isolates

HIV virions deleted in vpr and env were used to make pseudo viral particles as follows. Viral plasmids containing the env gene from HIV-1 were obtained from the NIH AIDS Research and Reference Reagent Program, Division of AIDS, NIAID, NIH as follows: HIV-1 ADA-M (referred to as HIV-1 ADA, R5) from Dr. Howard Gendelman [103-106]. Plasmid pSV-JRFL (R5) was a kind gift from Nathaniel Landau [107]). pCAGGS-SF162-gp160 (R5) was from Leonidas Stamatatos and Dr. Cecilia Cheng-Mayer [108-110]. 293FT cells were kind gifts from Dr. Jennifer Manilay and were originally obtained from Invitrogen. For single round virus production, plasmids with deleted vpr and env (pNL-luc3-R^-E^- containing the firefly luciferase gene; a kind gift from Dr. Nathaniel Landau [107]) were co-transfected into 293FT cells with different HIV strain env plasmids using Roche X-treme HP transfection reagent according to the manufacturer's instructions. Supernatant media containing virions was harvested 48 hours post transfection, centrifuged at 1,000xg, filtered through a 0.45 µM syringe (Millipore) and stored at -80 °C for later experiments. HIV-1(III_B) was provided by R.C. Gallo, at that time at the National Institutes of Health (Bethesda, MD).

2.3.6 Single-round infection assays

TZM-bl cells stably expressing CD4, CCR5 and CXCR4 coreceptors were maintained in Dulbecco's Modified Eagle's Medium (DMEM) with 10% fetal bovine serum (FBS). 10^4 cells per well were first seeded into a 96 well plate for one day. The media was then changed 3 hours before the assay and made to a volume of 50 ul per well, and then a serial dilution of GRFT variants were added from the top row to the bottom row, as follows: 20 ul GRFT variants of different concentration was added into the first row and mixed well with culture media. Then 20 ul media was removed and added into the second row, and so on. Virus was then added into each well containing different GRFT variants. The media was changed in 24 hours and cells were incubated for another 24 hours. PBS containing 0.5% NP-40 was used to lyse the cells and substrate chlorophenol red-D-galactopyranoside [CPRG] (Calbiochem) was added. Signal was measured at 570nm and 630nm (absorbance). The ratio of 570/630 for each well was calculated. EC_{50} values were determined using a linear equation fitted between two data points surrounding 50% inhibition. For presentation purposes, data shown in the figures were plotted and fitted as curves using a four-parameter logistic equation in Kaleidagraph (Synergy Software, Reading, PA).

2.3.7 Anti-HIV assays in CEM cell cultures

CEM cells (5 x 10^5 cells per ml) were suspended in fresh culture medium and infected with HIV-1(III_B) at 100 times the $CCID_{50}$ (50% cell culture infective dose) per ml of cell suspension, of which 100 µl was then mixed with 100 µl of the appropriate dilutions of the test compounds. After 4 to 5 days at 37°C, HIV-1-induced syncytia formation was recorded microscopically in the cell cultures. The 50% effective concentration (EC_{50}) corresponds to the compound concentration required to prevent syncytium formation by 50% in the virus-infected CEM cell cultures. Syncytium formation was recorded microscopically.

2.3.8 Cocultivation assay

Persistently HIV-1(III_B)-infected HuT-78 cells were washed to remove free virus from the culture medium, and 5 x 10^4 cells (50 µl) were transferred to 96-well microtiter plates. Next, a similar amount of Sup-T1 cells (50 µl) and appropriate concentrations of test compound (100 µl) were added to each well. After 2 days of coculturing at 37°C, the EC_{50}s were quantified by microscopic inspection on the basis of the appearance of syncytia.

2.3.9 NMR spectroscopy

GRFT variants were expressed in minimal media with $^{15}NH_4Cl$ as the only nitrogen source or with $^{15}NH_4Cl$ as well as ^{13}C labeled glucose as the sole nitrogen and carbon source. These mutants were produced and purified as described above. To dissolve the protein powder after purification, 20mM

sodium phosphate buffer (pH 7.0) with 5% D_2O was used and 2,2-dimethyl-2-silapentane-5-sulfonic acid (DSS) was added for calibration. Spectra were collected at 25ºC on a four-channel 600-MHZ Bruker Avance III spectrometer. The backbone resonances were assigned using standard spectra: 3D HNCO, HN(CA)CO, HNCACB, CBCA(CO)NH, HNCA, HN(CO)CA [111-114]. Data was processed using NMR Pipe [115]. The programs PIPP, Sparky and NMRVIEW [116-118] were used for visualization and chemical shift assignment. Molecular graphics images were produced using the UCSF Chimera package from the Resource for Biocomputing, Visualization, and Informatics at the University of California, San Francisco (supported by NIH P41RR001081) [5]. Changes in backbone chemical shift ($\Delta\delta_{obs}$) upon mutation or titration with mannose were determined using the weighted average of changes in ^{1}H and ^{15}N, with the equation [10, 119, 120]:

$$\Delta\delta_{obs} = [(\Delta\delta^{2}_{HN} + (\Delta\delta_{N}/5)^{2})/2]^{1/2}$$

2.3.10 Surface plasmon resonance (SPR) analysis

Recombinant gp120 proteins from HIV-1(III_B) strain (ImmunoDiagnostics Inc., Woburn, MA), from HIV-1(ADA) strain (ImmunoDiagnostics) and recombinant gp41 protein from HIV-1(HxB2) (Acris Antibodies GmbH, Herford, Germany) were covalently immobilized on the carboxymethylated dextran matrix of a CM5 sensor chip in 10 mM sodium acetate, pH 4.0, using standard amine coupling chemistry. The exact chip densities are given in the Results section. A reference flow cell was used as a control for non-specific binding and refractive index changes. All interaction studies were performed at 25°C on a Biacore T200 instrument (GE Healthcare, Uppsala, Sweden). The test compounds were serially diluted in HBS-P (10 mM HEPES, 150 mM NaCl and 0.05% surfactant P20; pH 7.4) covering a concentration range between 1.51 and 12.05 nM by using two-fold dilution steps. Samples were injected for 2 minutes at a flow rate of 45 µl/min and the dissociation was followed for 8 minutes. One duplicate sample and several buffer blanks were used as a positive control and for double referencing, respectively. The CM5 sensor chip surface was regenerated with 1 injection of Glycine-HCl pH1.5. The experimental data were fit using the 1:1 binding model (Biacore T200 Evaluation software 1.0) to determine the binding kinetics. In a separate experiment, both monomeric gp120 and trimeric gp140 derived from HIV-1/JR-FL (kind gift from R.W. Sanders, Amsterdam, The Netherlands. [121] was bound on the CM5 sensor chip and interaction of wild-type GRFT was site-by-site investigated against both mono- and trimers as described above. Also recombinant non-glycosylated gp160 (derived from HIV-1/IIIB and expressed in *E.coli* (ImmunoDiagnostics Inc., Woburn, MA)) was covalently immobilized on the CM5 sensor chip as described above, and its interaction with wild-type and mutant GRFT, but also the carbohydrate-binding monoclonal antibody 2G12 (Polymun Scientific GmbH, Vienna, Austria), soluble CD_4 (sCD_4) (ImmunoDiagnostics Inc.), and the α1,3/α1,6-mannose-specific plant

lectin from *Hippeastrum hybrid* (HHA) (provided by E. Van Damme, Ghent, Belgium) was investigated.

2.3.11 Analytical Ultracentrifugation

Sedimentation velocity experiments were carried out to confirm that the mutations did not affect the dimeric oligomerization state of GRFT. All experiments were performed on a Beckman Optima XL-I at the Center for Analytical Ultracentrifugation of Macromolecular Assemblies (CAUMA) at the University of Texas Health Science Center at San Antonio. Sedimentation velocity (SV) data were analyzed with the UltraScan software [122, 123]. Calculations were performed at the Texas Advanced Computing Center at the University of Texas at Austin, and at the Bioinformatics Core Facility at the University of Texas Health Science Center at San Antonio as described in [124]. All GRFT samples were measured in 40 mM sodium phosphate buffer (pH 6.9), except for the Triple mutant D30A/D70A/D112A which also include 50 mM NaCl. To monitor possible mass action in the oligomerization behavior of GRFT, the data were measured in intensity mode both at 0.3 and 0.9 OD at 230 and 280 nm (0.3, 0.6, 0.9 at 230 nm for the Triple mutant D30A/D70A/D112A), giving access to a wide concentration range. All data were collected at 20°C, and spun at 50 krpm, using standard titanium 2-channel centerpieces (Nanolytics, Potsdam, Germany). The protein concentrations ranged from 4.2 uM (0.3 OD_{230nm}) to 75.5uM (0.9 OD_{280nm}). The partial specific volume of GRFT was determined to be 0.7128 cm^3/g for wild-type GRFT and 0.7138 cm^3/g for the D-A mutants by protein sequence according to the method by Durchschlag as implemented in UltraScan. All data were first analyzed by two-dimensional spectrum analysis with simultaneous removal of time-invariant noise [125, 126] and then by enhanced van Holde–Weischet analysis [127] and genetic algorithm refinement [126, 128] followed by Monte Carlo analysis [129].

2.4 Results

2.4.1 NMR chemical shift assignments of wild-type GRFT.

Although several high quality X-ray structures of GRFT have been published [1, 97, 101], limited nuclear magnetic resonance (NMR) data has yet been reported [130]. This technique is quite complementary to X-ray analysis, allowing a quick assessment of whether a protein is folded and the likely structural similarity of a mutant to the wild-type protein. Therefore, the backbone chemical shift determination of wild-type GRFT was carried out using standard methods. We were able to obtain 90.7% assignments, including backbone ^{15}N, $^{1}H^{N}$, ^{13}CO, $^{13}C\alpha$ and 40% $^{13}C\beta$; Figure 2-2 shows an assigned ^{15}N, ^{1}H HSQC (Heteronuclear Single Quantum Coherence) correlation spectrum for GRFT.

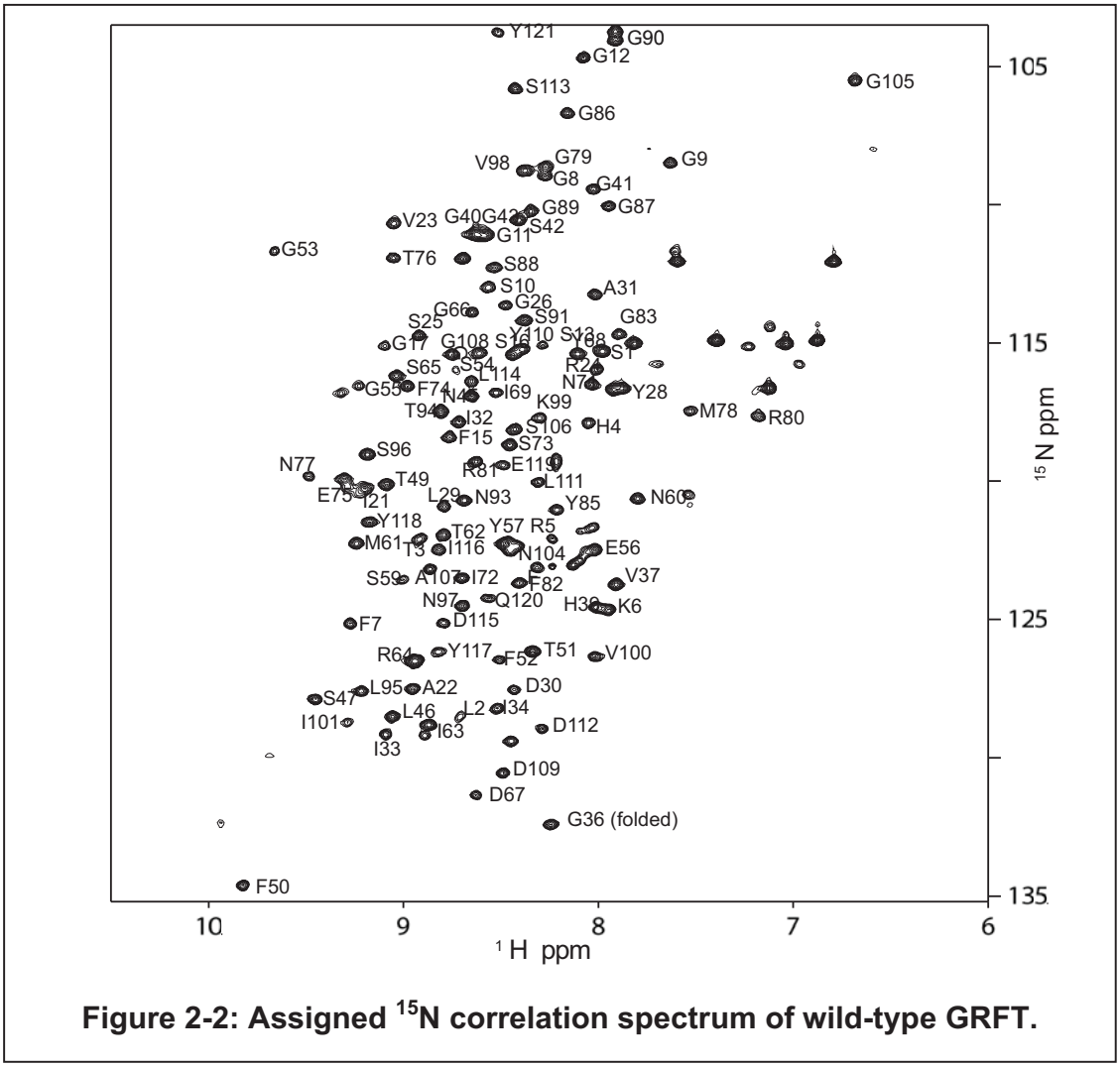

Figure 2-2: Assigned ^{15}N correlation spectrum of wild-type GRFT.

2.4.1 NMR of GRFT with mannose.

A titration was carried out with wild-type GRFT in the presence of mannose. The addition of the monosaccharide caused a significant shift in several peaks, as shown in Figure 2-3A, indicating a changed environment for these amino acids upon mannose binding. The shifted peaks were identified, and as shown in Figure 3B the region most affected by the addition of mannose is the face of the protein containing the three CBS. It was found that 15 residues on this face shifted by at least 1 standard deviation from the average (9 shifted by 1 SD, 6 shifted by 2 SD) while only a small amount of shifting occurred elsewhere in the protein (Figure 2-3B, Appendix Figure A-1). Also, some of the peaks corresponding to residues on the mannose binding face were impossible to follow upon titration with mannose due to broadening, suggesting a change in dynamics indicative of a binding event.

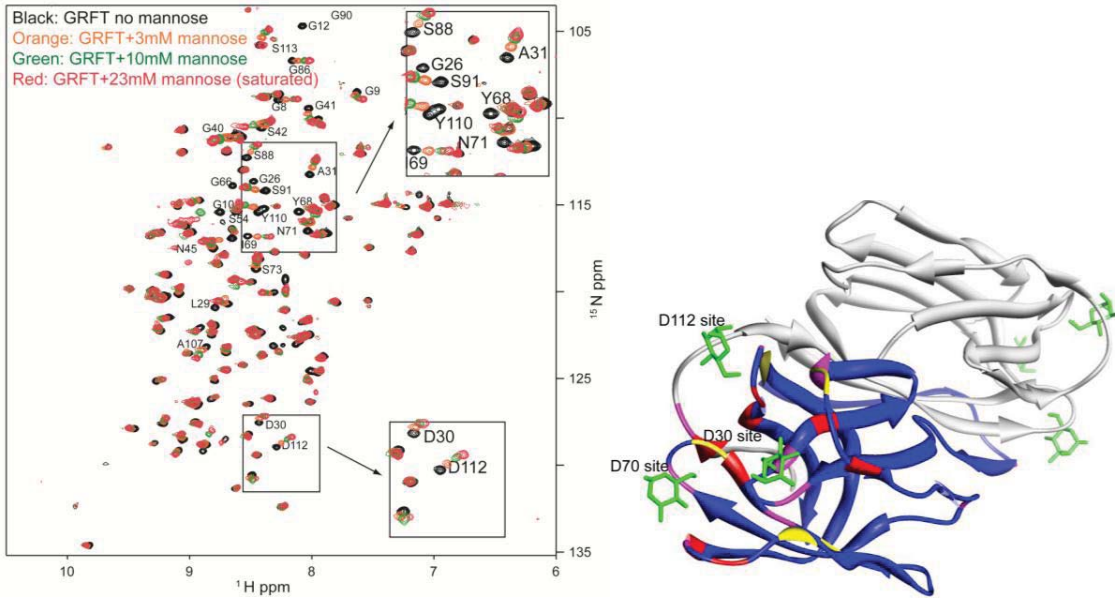

Figure 2-3: Mannose titration of wild-type GRFT.

Left: ^{15}N HSQC of mannose titration of GRFT. Resonances for unliganded wild-type protein are shown in black. Orange peaks represent GRFT in the presence of 3 mM mannose; green peaks show the presence of 10 mM mannose; red peaks show the presence of 23 mM mannose (saturated).

Right: Structure of GRFT showing regions from one subunit of the protein affected by titration with mannose, as determined by NMR spectroscopy. Yellow indicates residues whose chemical shift changed by 1 standard deviation from the average upon addition of mannose, while red indicates residues whose chemical shift changed by 2 standard deviations, and magenta indicates residues that became impossible to follow upon addition of mannose. These residues are listed in Appendix Table A-1. Mannose monosaccharides are shown in green. Residues G8 and G9 are from the domain-swapped other subunit. Structure is PDB 2gud obtained from [1, 2].

2.4.3 Mutations of carbohydrate-binding sites in GRFT.

As shown in Figure 2-4, each mannose moiety interacts with GRFT through several H-bonds [1]. One of the most clear and defined interactions in each carbohydrate-binding site involves the side chain of Asp 30 (and Asp 70 and Asp 112 in the other nearly-identical CBS) and the hydroxyl of O4 and O6 in mannose. It appears very likely that if the Asp were removed by mutation to Ala, the sugar binding capability would be severely impaired, likely without harming the overall structure of the protein. However, it cannot be excluded that individual amino acid side chains also contribute to maintain the protein configuration, and

therefore, a dramatic amino acid change from Asp to Ala may also affect the conformational structure of the protein. To clarify the role of each putative mannose binding site in GRFT, we mutated the key Asp residue at each CBS to Ala. We also made a triple mutant at all three CBS of GRFT. Each variant was first assessed by NMR and shown to be folded (Figure 2-5, Appendix Figure A-2 and A-3). A comparison of HSQC spectra with the wild-type protein indicates that each point mutant has changes that extend further than its individual site, propagating to much of the mannose-binding face of the protein, including usually each of the other two sites, while the remainder of the protein appears to be largely unaffected (Figures 2-5 and Appendix Figure A-2 and A-3). The largest changes in spectra were observed for the triple mutant, having the Asp at each of the three CBS mutated to Ala (Appendix Figure A-4). When this triple mutant D30A/D70A/D112A was titrated with mannose, the HSQC spectra showed essentially no change for any concentration tested, up to 23 mM mannose, indicating no binding (Appendix Figure A-9).

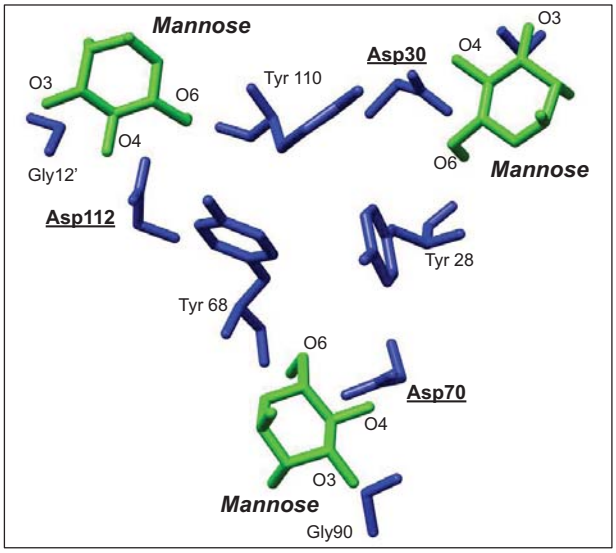

Figure 2-4: The three putative mannose binding sites of GRFT, as determined by [1, 2].

Mannose saccharide is shown in green, selected residues from griffithsin are shown in blue and labeled.

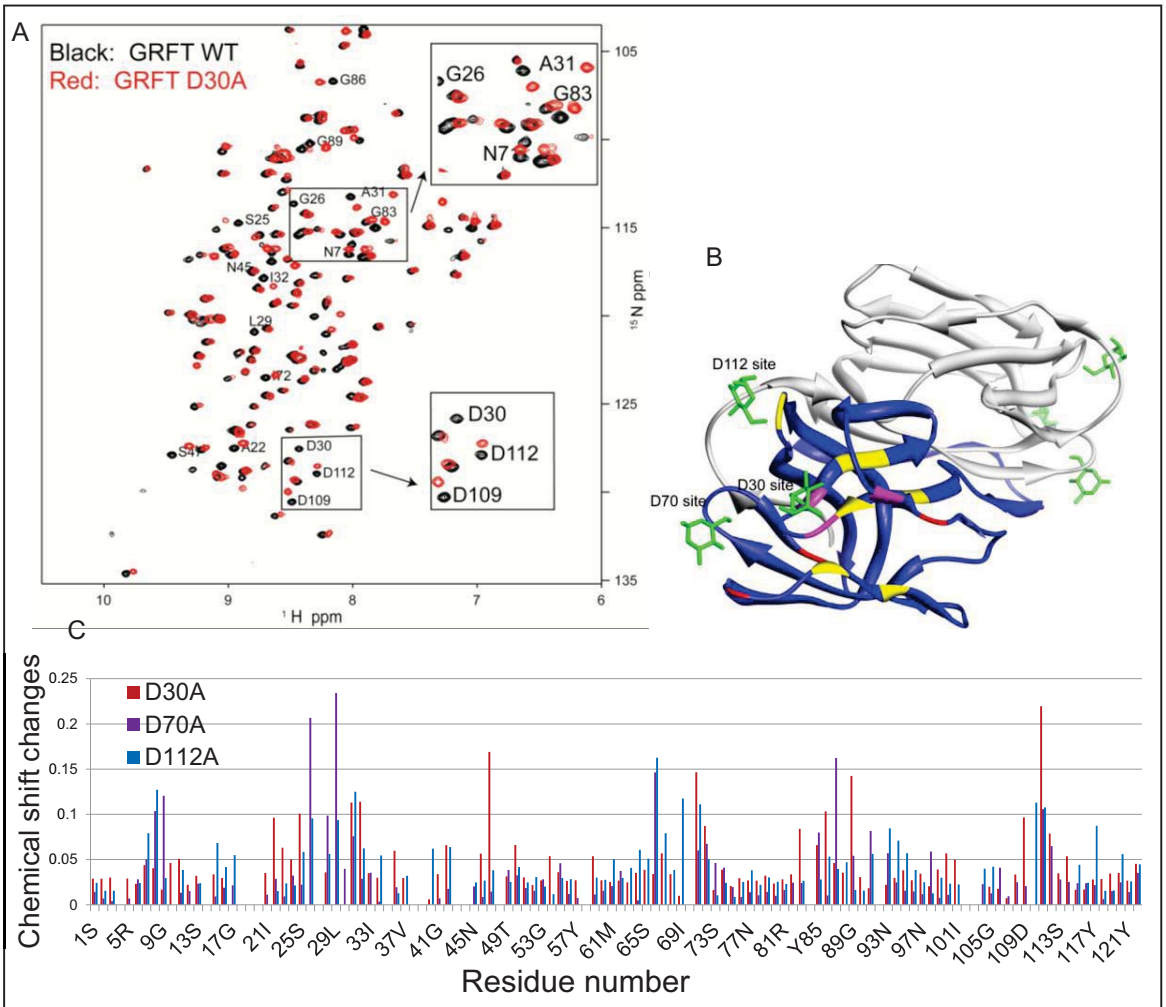

Figure 2-5: Structure of GRFT single point mutants.

Figure 2-5A. ^{15}N HSQC spectrum of GRFT D30A (red) overlaid with the spectrum of wild type griffithsin. Some peaks with significant movement upon mutation are labeled.

Figure 2-5B. Structure of GRFT showing regions that have chemical shift changes upon mutation of the mannose site at D30. Yellow indicates chemical shift change that is 1 standard deviation greater than average, red indicates chemical shift change that is 2 standard deviations greater than average, and magenta indicates peaks that broaden or otherwise have moved too much to assign upon mutation. These residues are listed in Table S1. Mannose residues are shown in green. Structure is 2gud from [1, 2].

Figure 2-5C. Chemical shift changes of GRFT upon mutation of residues at the mannose binding sites. Some residues broaden or move and cannot be visualized upon mutation of one of the sites so they are not shown. Changes for D30A are shown in red; D70A: purple; D112A: blue.

To determine whether the mutations at each CBS in GRFT altered the dimer affinity, analytical ultracentrifugation was carried out on the wild-type protein and each variant using sedimentation velocity analysis. To better ascertain whether any mass action effects were detectable, wild-type and mutant GRFT were measured over a wide concentration range. In each case vertical sedimentation coefficient G(s) distributions were obtained with the enhanced van Holde–Weischet analysis [127], and had nearly identical sedimentation coefficients (see Figure 2-6 and Appendix Figure A-5). Vertical G(s) distributions indicate that all samples were homogenous [131]. 2-dimensional spectrum analysis [132, 133] combined with Monte Carlo analysis [129] resulted in a molecular weight consistent only with the dimer (see Table 2-1), even at the lowest concentration tested (4.2 μM).

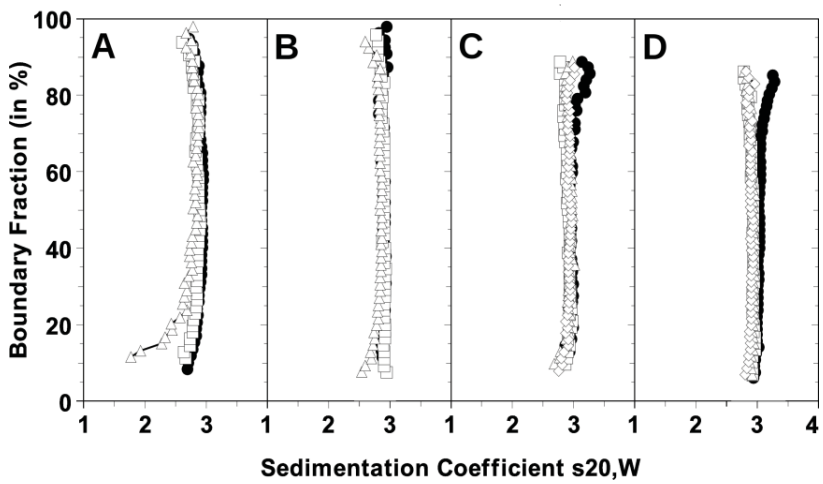

Figure 2-6: Van Holde-Weischet G(s) sedimentation coefficient distributions of GRFT at 4 concentrations.

A: 0.3 OD 230 nm, B: 0.9 OD 230 nm, C: 0.3 OD 280 nm, D: 0.9 OD 280 nm. Filled circles: wild-type, open squares: D30A, open triangles: D112A, open diamonds: D70A. Vertical distributions indicate homogeneity.

Table 2-1. Molecular weight of GRFT and its point mutants determined by analytical ultracentrifugation.

Molecular weight of the major species determined with the 2-dimensional spectrum analysis [125] combined with Monte Carlo analysis [97] for wild-type GRFT and mutant at 4 different loading concentrations. Values in parenthesis refer to the 95% confidence intervals for each fit. In all cases the molecular weight closely matches the molecular weight of the GRFT dimer.

Sample/ Concentration	0.3 OD 230 nm	0.9 OD 230 nm	0.3 OD 280 nm	0.9 OD 280 nm
Wild type	2.71e+04 (1.584e+04, 3.83e+04)	2.73e+04 (2.39e+04, 3.27e+04)	2.83e+04 (2.15e+04, 3.11e+04)	2.98e+04 (2.70e+04, 3.10e+04)
D30A	3.15e+04 (3.03e+04, 3.20e+04)	3.04e+04 (2.81e+04, 3.28e+04)	3.15e+04 (2.35e+04, 3.54e+04)	3.00e+04 (2.73e+04, 3.22e+04)
D112A	3.00e+04 (2.88e+04, 3.04e+04)	2.79e+04 (2.57e+04, 3.01e+04)	3.07e+04 (2.91e+04, 3.23e+04)	3.13e+04 (2.13e+04, 4.11e+04)
D70A	Not measured	Not measured	3.01e+04 (2.81e+04, 3.13e+04)	3.01e+04 (2.89e+04, 3.27e+04)
GRFT D30A/D70A/D112A	Not measured[a]	2.84e+04 (2.72e+04, 2.97e+04)	Not measured[a]	Not measured[a]

[a]For the Triple mutant GRFT D30A/D70A/D112A, other concentrations were also tested and consistent with this data (Appendix Figure A-5)

2.4.4 Mutations in the CBS of GRFT reduce the ability of GRFT to bind mannose and gp120.

The ability of wild-type GRFT and its variants to bind mannose was first assessed by using a commercial mannose column, having mannose monosaccharide bound to a standard bead. This column is a crude method of determining mannose binding, since the attachment of each carbohydrate to the bead at C6 precludes protein binding from that direction. Each protein was loaded onto the column and eluted using a mannose gradient. GRFT bound to the column, requiring 50 mM mannose for elution, while mutation at any single CBS resulted in a protein that flowed through without binding the column (Figure 2-7). This indicates that carbohydrate binding was diminished for each mutant,

but since the column is composed of a single carbohydrate ring that is not freely available at all sites for binding, further interpretation is not possible.

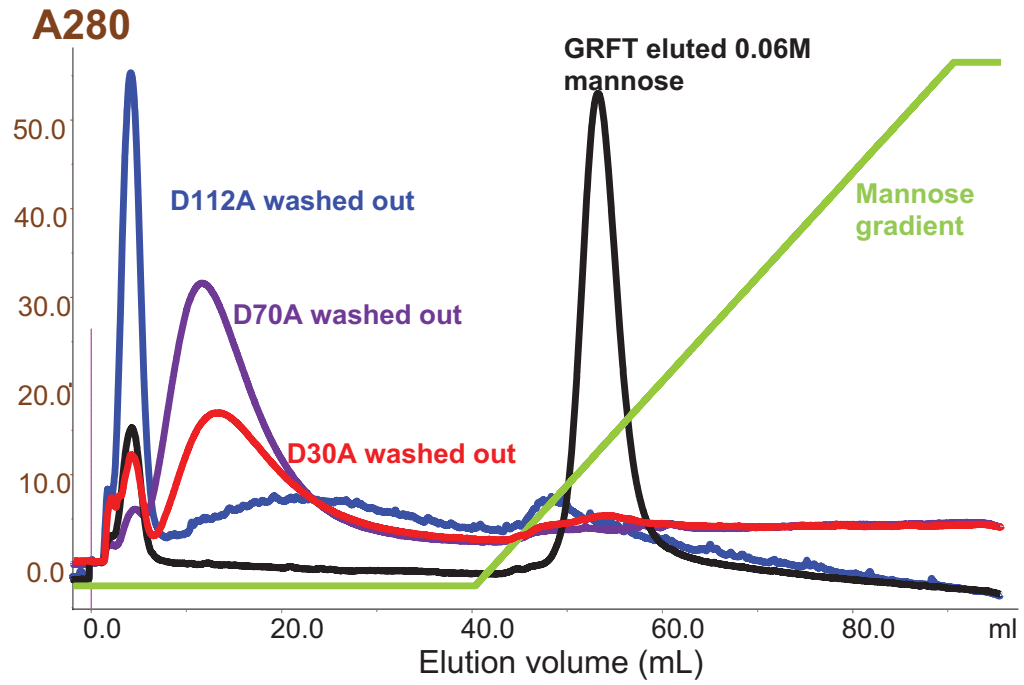

Figure 2-7: GRFT and its variants binding to mannose-agarose column.

Wild-type GRFT was eluted out at 0.06 mM mannose, while the 3 single-point mutants, GRFT D30A (red), D70A (purple) and D112A (blue) could not bind to the mannose-agarose column.

The most relevant binding interaction for GRFT in terms of HIV inhibition is its ability to bind HIV envelope protein gp120. A straightforward way to measure this interaction is the ELISA assay, in which gp120 is bound to a surface, and varying amounts of GRFT or its mutants are exposed to the gp120. The level of binding between GRFT and gp120 is determined by addition of a peroxidase-conjugated protein that is specific for the N-terminal His-tag on GRFT. (We and others have shown that an N-terminal His-tag does not impede the activity of GRFT [47, 130]). As shown in Figure 2-8, wild-type GRFT binds very well to gp120 derived from HIV-1 strain ADA, with clear binding between 10 nM and 100 nM. In contrast, each point mutant binds gp120 less well, requiring 100 nM to 1,000 nM. In general, the GRFT point mutant D70A, having a mutation at the so-called Pocket 3 [97], repeatedly appeared to bind the worst in these experiments under the same conditions, although ELISA experiments are not quantitative. The triple GRFT mutant D30A/D70A/D112A binds very poorly to gp120, showing only a low signal increase at the high-tested amount of 1.28 μM. Therefore,

overall the single point mutants show an approximate 10-fold reduced ability to bind, while the triple mutant binds much more weakly to gp120.

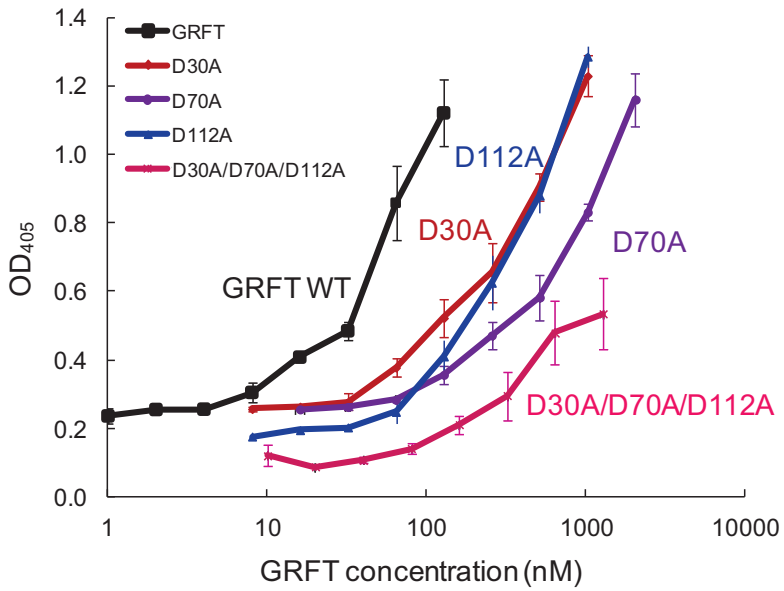

Figure 2-8: ELISA assay indicates the ability of GRFT and its variants to bind to gp120$_{ADA}$.

Wild-type GRFT (black) binds better than any single point mutant (D30A red; D70A purple; D112A (blue). The triple mutation D30A/D70A/D112A (magenta) binds poorly to gp120$_{ADA}$. Typical results are shown from an experiment in triplicate. Each experiment was repeated at least 3 times. Error bars indicate standard deviation from a typical triplicate experiment.

A more quantitative way to determine binding to the HIV-1 envelope is the use of surface plasmon resonance (SPR) [134, 135]. In this experiment, binding properties of GRFT and its mutants were evaluated against monomeric gp120 III$_B$ (X4) and gp120 ADA (R5), and also against the glycosylated HIV-1 (HxB2) gp41 fusion protein. All ligands were covalently immobilized on CM5 sensor chips and 140 RU (~1.17 fmol), 90 RU (~0.75 fmol) and 240 RU (~5.85 fmol) of gp120 density was obtained, respectively. Such low gp120 density chips are required to enable reliable determination of K_D values, since high gp120-density chips may easily allow rebinding of GRFT to another gp120 molecule on the same sensor chip resulting in erroneous k_{off} rate determinations. The binding and release of GRFT (concentration expressed in dimer units) can be measured in real time to provide on- and off- rates as well as affinity constants (K_D values). As shown in Figure 2-9 and Table 2-2, wild-type GRFT binds very tightly to gp120 derived from the X4 strain III$_B$ as well as the R5 strain ADA, with K_D values of 72.7 ± 1.7 pM and 73.2 ± 2.0 pM, respectively. The basis for the tight binding

appears to be a fast on-rate (k_{on}) (about 6.3 x 10^6 M^{-1} s^{-1}) and a slow off-rate (k_{off}) (about 5 x10^{-4} s^{-1}). The binding kinetics for gp120 derived from HIV-1(III_B) and HIV-1(ADA) were very similar regarding the K_D as well as the k_{on} and k_{off} rates (Table 2-2 and Appendix Figure A-6). Since the native form of gp120 is a trimer in the viral envelope, the binding of GRFT to trimeric gp140 has also been evaluated side-by-side, but no significant difference in the K_D value was observed (K_D: 0.111 nM and 0.152 nM, respectively). GRFT also binds well to gp41 with a similar affinity constant compared to gp120 (Appendix Figure A-7), although this viral fusion protein is only exposed at a later stage of the entry process [136, 137] and most likely does not play a relevant role in the eventual anti-HIV activity of GRFT.

While each point mutant of GRFT showed reduced binding to gp120 derived from both X4 and R5 HIV-1 strains, the effect was small, with D30A and D112A generally exhibiting an as little as 2-fold reduction in binding compared to the wild-type protein, while the point mutant D70A showed only a 3-fold reduction in affinity. The triple mutant D30A/D70A/D112A did not show a binding signal when exposed to gp120 at 12 nM (Table 2-2). However, higher concentrations (i.e. 24 and 48 nM) start to show an interaction signal for binding to gp120 and gp41 (Appendix Figure A-8).

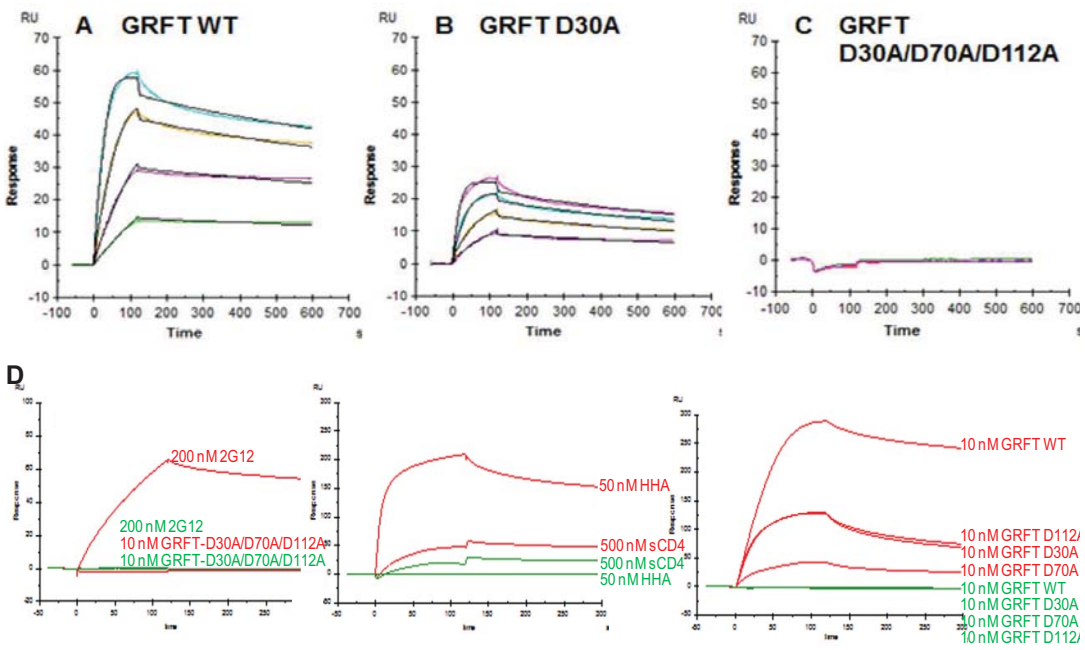

Figure 2-9: SPR of GRFT and its variants binding to gp120.

Figure 2-9A-C. Surface plasmon resonance sensorgrams of GRFT binding to $gp120_{ADA}$ immobilized on the surface. Kinetic analysis of the interactions of GRFT (Panel A), GRFT D30A (Panel B) and GRFT triple mutant (Panel C) with immobilized HIV-1 ADA gp120. Serial two-fold analyte dilutions (covering a concentration range from 1.51 to 12.05 nM) were injected over the surface of the immobilized gp120. The experimental data (colored curves) were fit using the 1:1 binding model (black lines) to determine the kinetic parameters. The biosensor chip density was 90 RU. Concentration shown here is in dimer units.

Figure 2-9D. Surface plasmon resonance binding assay of GRFT binding to immobilized glycosylated HIV-$1/III_B$ gp120 (expressed in CHO) and non-glycosylated HIV-$1/III_B$ gp160 (expressed in *E. coli*). A protein density of 647 RU and 667 RU were obtained for the glycosylated HIV-1/IIIB gp120 and the non-glycosylated HIV-1/IIIB gp160. Binding signals for the interactions of 10 nM GRFT triple mutant and 200 nM 2G12 (Panel A); 500 nM sCD4 and 50 nM HHA (Panel B); and GRFT WT and its single mutants (all at 10 nM) (Panel C) with immobilized glycosylated HIV-1 III_B gp120 (red curves) and non-glycosylated HIV-1 III_B gp160 (green curves).

Table 2-2. Kinetic data for the interaction of GRFT and its mutants with immobilized HIV-1 envelope proteins gp120 and gp41.

Concentration shown here is in dimer units. The p-values for interactions with $gp120_{IIIB}$ strains are 0.0280 (wild-type GRFT: GRFT D30A); 0.0207 (wild-type GRFT: GRFT D70A) and 0.0282 (wild-type GRFT: GRFT D112A).

	gp120 III_B (X4)			gp120 ADA (R5)			gp41 HxB2		
	K_D (pM)	k_{on} (1/M.s)	k_{off} (1/s)	K_D (pM)	k_{on} (1/M.s)	k_{off} (1/s)	K_D (pM)	k_{on} (1/M.s)	k_{off} (1/s)
GRFT WT	72.7 ± 1.7	(6.30 ± 0.94)E+06	(4.57 ± 0.58)E-04	73.2 ± 2.0	(8.45 ±0.68)E+06	(6.17 ± 0.33)E-04	44.9 ± 1.5	(8.01 ± 1.46)E+06	(3.61 ± 0.78)E-04
GRFT D30A	155.6 ± 11.2	(7.89 ± 1.26)E+06	(1.24 ± 0.29)E-03	122.7 ± 7.3	(9.08 ± 0.74)E+06	(1.12 ± 0.16)E-03	137.5 ± 18.0	(1.26 ± 0,07)E+07	(1.72 ± 0.14)E-03
GRFT D70A	244.9 ± 88.7	(4.15 ± 2.59)E+06	(8.58 ± 3.29)E-04	194.3 ± 26.3	(4.44 ± 2.10)E+06	(8.35 ± 2.91)E-04	164.9 ± 37.8	(7.87 ± 0.21)E+06	(1.29 ± 0.26)E-03
GRFT D112A	141.8 ± 9.7	(8.43 ± 3.20)E+06	(1.21 ± 0.54)E-03	122.5 ± 3.6	(9.27 ± 3.37)E+06	(1.14 ± 0.45)E-03	130.9 ± 22.2	(1.41 ± 0.51)E+07	(1.90 ± 0.98)E-03
GRFT D30A/D70A/D112A[a]	no specific binding observed at 12.05 nM			no specific binding observed at 12.05 nM			no specific binding observed at 12.05 nM		

K_D, dissociation equilibrium constant; k_{on}, association rate constant; k_{off}, dissociation rate constant.

[a]At concentrations higher than 12.05 nM (i.e. 24.1 and 48.2 nM), a weak binding signal was observed.

In an attempt to reveal the binding capacity of wild-type GRFT and its mutants to specific sites of gp120 other than the N-glycans, *E.coli*-expressed non-glycosylated gp160 was bound to the sensor chip, and binding of the GRFTs but also the carbohydrate-recognizing mAb 2G12, the α1,3/α1,6-mannose-recognizing plant lectin HHA and sCD_4 were examined in comparison with their binding to the glycosylated gp120. Whereas binding of GRFT, mutant GRFT, 2G12, HHA and sCD_4 to glycosylated gp120 was observed, no significant binding for GRFT, mutant GRFT, 2G12 and HHA was found for non-glycosylated gp160 (Figure 2-9D). Instead, sCD_4 that binds to gp120 without the requirement of the presence of N-glycans could still bind to non-glycosylated gp160 (Figure 2-9D). These data indicate that the interactions of GRFT (and also 2G12 and HHA) are predominantly N-glycan-dependent.

2.4.5 Mutation of the individual CBS markedly reduces the anti-HIV activity of GRFT.

GRFT and its variants were tested against several strains of HIV using single-round viral assays. As shown in Table 2-3 and Figure 2-10, while wild-type GRFT inhibited HIV strain ADA with an EC_{50} of 10.5 pM, the D30A mutant and D112A mutant were about 1,000-fold less potent (20.3 and 6.57 nM, respectively). The D70A mutant was somewhat a better inhibitor than the other point mutants, with an EC_{50} of 2.63 nM. This is in contrast to the ELISA and SPR results, which showed only a very moderate effect of the mutations for the ability of these GRFT variants to bind gp120 derived from the HIV-1 strain ADA. However, since this set of gp120 binding and antiviral data only includes the ADA strain, it is premature to assume that the superior antiviral activity of the D70A mutant *versus* the other mutants is a general phenomenon.

Similar functional results were obtained using R5 HIV-1 strain JR-FL, where wild-type GRFT inhibited single round virus infection with an EC_{50} of 72.5 pM. The D30A and D112A variants were approximately 300-fold lower in anti-HIV potency than wild-type GRFT, and the D70A mutant exhibited about a 10-fold greater antiviral potency than the other two point mutants. Again for R5 HIV-1 strain SF162, both D30A and D112A variants were reduced in potency compared to the wild-type protein by several hundred fold, while the D70A mutant was worse than the wild-type protein, but better than the other point mutants. When viral inhibition assays using X4 HIV-1 strain III_B in CEM cell cultures were performed in which inhibition of virus-induced cytopathicity was recorded at day 4 post infection and post addition of the compounds, wild-type GRFT inhibited the virus-induced cytopathicity at an EC_{50} of 0.109 nM, while the point mutants were much worse, ranging from 4.8 to 6.8 nM (Table 2-3). In this case the D70A variant had quite similar antiviral activity as the other point mutants. In all cases, the triple mutant D30A/D70A/D112A was a very poor antiviral inhibitor, with an EC_{50} of 95.3 nM for the III_B strain, and EC_{50} values being higher than the

maximum concentration tested (500 nM) against the R5 HIV-1 strains (Figure 2-10 and Table 2-3).

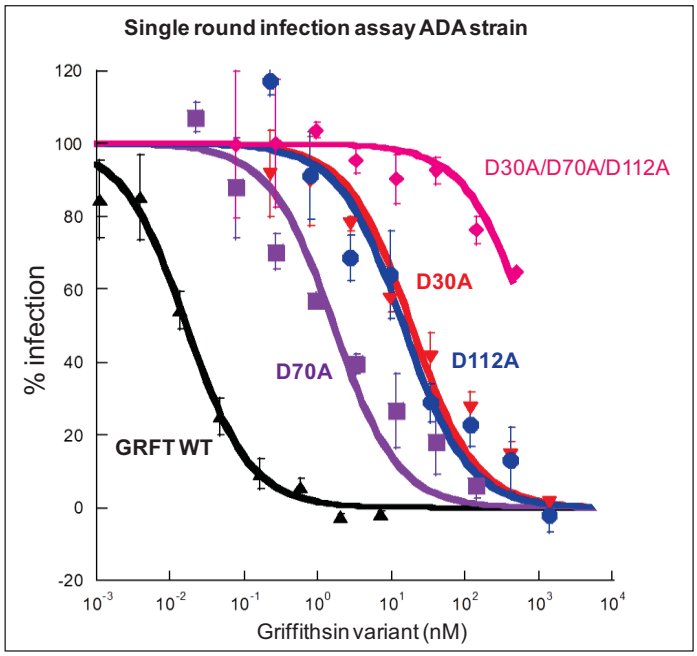

Figure 2-10: Results of inhibition by GRFT mutants in single-round virus assays.

Typical results are shown from an experiment in triplicate. Wild-type GRFT is shown in black; D30A red; D70A purple; D112A blue; triple mutation D30A/D70A/D112A magenta). Each experiment was repeated at least 3 times. Error bars indicate standard deviation from a triplicate experiment.

GRFT neutralizes HIV-1 by binding to specific N-glycans on HIV-1 gp120 rather than those on cells. Therefore, a preincubation experiment was performed in which MT-4 cells were exposed to GRFT for 1 hour prior to infection of the cell cultures. In these experiments, an increased antiviral (5- to 10-fold decreased EC_{50}) efficacy of the compound was observed (data not shown). A similar phenomenon was previously also reported for several plant lectins [138], and might be important in view of the potential of GRFT as an anti-HIV microbicide drug.

Table 2-3. Inhibition of GRFT variants in single-round viral assays or antiretroviral assays.

Each experiment was repeated at least 3 times in triplicate and the values shown are +/- the standard deviation of the EC_{50} from all experiments. The experiments with R5 tropic strains were carried out with TZM-bl target cells. The EC_{50} determination is described in the Methods section and is defined as the compound concentration required to inhibit HIV-induced syncytium formation by 50%. The experiments with X4-tropic strain III_B were carried out with CEM target cells. In this assay system, HIV-induced syncytia formation was examined microscopically at day 4 post infection. “Fold decrease” indicates decrease in potency compared to wild-type GRFT.

Compounds	Inhibition of							
	ADA Strain (R5)		JR-FL Strain (R5)		SF 162 Strain (R5)		III_B (X4)	
	EC_{50} (nM)	Fold decrease	EC_{50} (nM)	Fold decrease	EC_{50} (nM)	Fold decrease	EC_{50} (nM)	Fold decrease
GRFT	0.011 ± 0.01	1	0.073 ± 0.03	1	0.032 ± 0.02	1	0.109±0.0	1
GRFT D30A	20±14	1933	23±23	322	13±2.1	417	6.8±0.6	63
GRFT D70A	2.6± 2.2	250	3.0± 1.7	41	0.8± 0.6	26	6.7±2.2	61
GRFT D112A	6.6± 6.1	625	21± 9	284	8.7± 3.1	276	4.8±0.5	44
GRFT Triple mutant D30A/D70A/D112A	>500	>47600	>500	>6900	>500	>15800	95±33	875

The much poorer antiviral activity of the point mutants and the triple GRFT mutant was also confirmed in cocultivation experiments in which the compounds were exposed to a coculture of persistently HIV-1(III_B)-infected HuT-78 cells and uninfected Sup T1 CD4+ T-lymphocytes. Whereas the wild-type GRFT potently prevented syncytia formation in the cocultures at an EC_{50} of 1.91 ± 1.23 nM, the D30A, D70A and D112A point mutants showed EC_{50} values of 67.4 ± 39.7 nM, 88.6 ± 23.8 nM and 36.1 ± 14.3 nM, respectively. The triple GRFT mutant was only inhibitory in this assay at 340 nM.

2.5 Discussion

GRFT is a protein lectin that potently inhibits HIV entry and infection by binding to gp120 [47]. Since its discovery in 2005, GRFT has been considered a leading candidate for an anti-HIV microbicide, due to its high potency, low toxicity, and good stability to a variety of pH conditions and temperature [47, 52, 53]. This lectin has been shown to be easily produced in gram quantities, leading to the possibility of simple and inexpensive production [51, 139]. It proved also able to inhibit hepatitis C virus infection and dissemination both *in* vitro and *in* vivo by acting on the entry step of the viral life cycle [50].

Several high quality X-ray structures and thermodynamic analyses of GRFT have been carried out, showing a protein dimer and indicating three carbohydrate-binding sites per monomer of protein [1, 97, 98, 101]; Figure 2-1. Competition data and further structural work [47, 101] indicate that each binding site binds one mannose mono-saccharide, which is likely the key to GRFT's ability to inhibit HIV. The HIV envelope protein gp120 contains between 18 and 33 N-linked glycosylation sites (depending on the virus strain), approximately a dozen of which are high mannose type glycans [29, 33, 35, 140]. These high-mannose glycans, in particular their highly clustered appearance on the HIV envelope gp120, are rarely found on mammalian cells, reducing the possibility of adverse host interactions [141] although one study indicates that GRFT can bind to the surface of some cells [52]. High mannose glycans contain several branched carbohydrate chains, having three terminal (α1,2) mannose residues (Figure 1). It is therefore generally assumed that GRFT inhibits viral entry by binding tightly to the mannose on the surface gp120.

Given its relatively high profile and potential for clinical use, it is important that the action of GRFT is biochemically well understood. However, many biochemical details of the role of GRFT in HIV inhibition have not yet been elucidated. For example, while modeling studies suggested three equivalent CBS for each monomer subunit of GRFT, a recent X-ray analysis indicates a subtle lack of equivalence between these sites [97]. Recent studies have used a GRFT mutant with all three CBS mutated to asparagine and this mutant GRFT showed no activity in biological assays against several viruses, including *Coronaviridae* and Hepatitis C [50, 52, 142]. While this triple Asp-to-Asn mutant is likely quite similar to the triple D30A/D70A/D112A mutant reported here, we do see some minimal activity in D30A/D70A/D112A, while none has yet been reported for the Triple Asn construct. It appears that our triple mutant retains some weaker binding activity to gp120 as shown by SPR technology, while these assays were not performed for the Triple-Asn mutation. Also, the lack of activity for the Triple-Asn mutant was reported for viruses other than HIV, which makes direct comparison to our findings not obvious.

In the present work, we have individually mutated each CBS in GRFT, and analyzed the resulting mutants for their ability to dimerize, to bind to mannose, to

bind to gp120, and to inhibit HIV. We found that GRFT and its point mutants form a high-affinity dimer that does not dissociate at the lowest level of detection using analytical ultracentrifugation. Further, while the wild-type protein binds well to a mannose monosaccharide column, mutation at any individual site results in the lack of ability to bind this commercial column. NMR spectroscopy of the wild-type protein in the presence of mannose reveals chemical shift changes across the entire face of the protein containing the mannose binding sites. Single site mutants at each binding site shows localized changes in the chemical shifts at those sites, as well as some changes at more distal locations, but generally on the mannose binding face of the protein rather than in more buried residues.

Disruption of any single CBS in GRFT results in a moderate loss of ability to bind HIV gp120 as shown by ELISA. These assays show a reduction in ability to bind gp120 from strain ADA, requiring concentrations about 10-fold higher from each mutant GRFT compared to the wild-type protein, with the D70A variant appearing to perform several fold worse than D30A or D112A. In more quantitative binding assays using SPR, GRFT and its mutants were tested for binding to immobilized gp120 (from R5 strain ADA and X4 strain III_B) as well as to gp41. These experiments showed picomolar binding by wild-type GRFT and only a 2-3 fold reduction in binding by the point mutants D30A, D112A, and D70A, the latter showing slightly worse binding than the other two mutants.

However, when these mutants were tested in single-round HIV infection assays as well as HIV cytopathicity assays (read-out after 4 days) and co-cultivation assays (24 hr read-out), it was found that their ability to inhibit HIV was much more drastically affected than would be predicted based on their ability to bind gp120 (or gp41). For each virus strain tested, the point mutants showed at least a 26-fold or higher increase in EC_{50} compared to the wild-type protein (although it should be noted that in the context of a dimer, each point mutant results in an overall loss of two CBSs). It was also found that the D70A mutant, while showing lower binding to gp120 in both ELISA and SPR assays, showed better HIV inhibition than the other point mutants in some strains, again indicating a lack of direct correlation between binding to HIV gp120 and viral inhibition.

While the three mannose binding sites of GRFT each use similar amino acid side chains and backbone for carbohydrate binding, a recent crystallography study suggests that two of the sites bind equivalently (Pocket 1, including D112, and Pocket 3, including D70), while the third site binds differently and may have a less optimal binding environment (Pocket 2 including D30) [97, 98]; notation introduced in [2]. The present work directly investigated each CBS, and our data indicate that the D30 and D112 site are largely identical in terms of contribution to binding of gp120 and inhibition of HIV. The loss of the D70 CBS site appears to have a somewhat different outcome, with consistently better HIV inhibition than the other single mutants. Therefore, the present experiments are not completely in agreement with the previous work, so further experiments may be necessary to resolve this issue.

Our results have implications for the mechanism of action of GRFT. Although mutants lacking one of the three mannose binding sites perform well in binding gp120, all three sites are apparently important for efficient antiviral activity. This strongly implies that GRFT does not function simply by binding gp120 and causing a steric blockade, but rather uses multiple binding interactions with glycans to cause an allosteric shift or a structural shift that inhibits infection by compromising the ability of gp120 to efficiently interact with the host cell during infection. In support of this, recent work has shown that binding of GRFT to gp120 enhances the exposure of the CD4 binding site in gp120, while apparently decreasing the ability of the intact virus to bind the coreceptor [143]. In fact, it is well-known from antibody research that binding to gp120 does not guarantee an antiviral effect; binding to gp120 can result in potent neutralization of the virus but may also have poor, if any, effect on viral infectivity, depending on the epitope that is recognized on gp120 by these antibodies [144, 145]. Thus, it seems that the GRFT mutants bind nearly as efficiently to gp120 as wild-type GRFT (as found in our ELISA and SPR experiments) but are not necessarily equally efficiently neutralizing the virus. The efficient capacity of cross-linking of glycans or glycan parts on gp120 by wild-type GRFT may have been markedly decreased by the mutants, explaining the substantially decreased antiviral potential of the mutants versus wild-type protein. Although this hypothesis has still to be proven by direct experimental evidence, these observations suggest that binding as such to gp120 is not necessarily predictive for eventual antiviral activity of the agents and cross-linking of glycans on gp120 may be a key event to efficiently inhibit virus infectivity. The importance of glycan cross-linking for eventual potent antiviral activity by carbohydrate-binding agents has also been suggested earlier by Moulaei et al. [97] for GRFT, who showed that a monomeric form of the protein is able to bind two different carbohydrate moieties, and also that the monomer itself is not sufficient for anti-HIV function. The possibility of lectin function based on glycan cross-linking has also been raised for cyanovirin-N, which can bind multiple carbohydrates and requires two active sites for its antiviral function [11] [86].

The tight GRFT dimer is also likely critical for anti-viral function, leading to a total of 6 mannose binding sites. Indeed, an engineered GRFT monomer was recently shown to have low antiviral potency despite retaining binding ability to gp120 [97]. We are currently investigating the role of the GRFT dimer in HIV inhibition, where it is possible that the protein uses both arms to alter the conformation of a gp120 subunit or to bind two separate gp120s. The commercially obtained gp120 used in our ELISA and for most SPR experiments is a monomer, while the viral surface contains trimeric gp120 [89, 146]. However, when binding of wild-type GRFT (and its individual point mutants) to trimeric gp140 was compared with monomeric gp120, no significant differences were observed. Nevertheless, these findings leave open the possibility that the anti-viral activity of GRFT involves cross-linking of separate gp120 subunits on the virus particle.

2.6 Conclusion

The potent HIV inhibitor GRFT has been shown to be a tight dimer, with three nearly-equivalent mannose binding sites that are each critical for full potency of the anti-HIV activity of the protein. Mutation of any of the three sites results in a loss of at least 26-fold in ability to inhibit HIV, even though these single mutations only moderately affect the ability of GRFT to bind gp120 or gp41. Overall, this suggests that the antiviral mechanism of GRFT action is not simply to bind and sterically block the action of gp120, but rather to use the binding of mannose residues on g120 to affect the gp120 structure or its oligomeric state, possibly by cross-linking gp120 glycans, resulting in a loss of viral infectivity.

Chapter 3

The Griffithsin Dimer Is Required for High-Potency Inhibition of HIV-1: Evidence for Manipulation of the Structure of gp120 as Part of the Griffithsin Dimer Mechanism

This work was published as part of [147]:

Xue J, Hoorelbeke B, Kagiampakis I, Demeler B, Balzarini J, Liwang PJ., "The griffithsin dimer is required for high potency inhibition of HIV-1: Evidence for manipulation of the structure of gp120 as part of the griffithsin dimer mechanism", *Antimicrobial Agents and Chemotherapy,* 2013 Aug;57(8):3976-89.

3.1 Abstract

Griffithsin (Grft) is a protein lectin derived from red algae that tightly binds the HIV envelope protein gp120 and effectively inhibits virus infection. This inhibition is due to the binding by Grft of high-mannose saccharides on the surface of gp120. Grft has been shown to be a tight dimer, but the role of the dimer in Grft's anti-HIV function has not been fully explored. To investigate the role of the Grft dimer in anti-HIV function, an obligate dimer of Grft was designed by expressing the protein with a peptide linker between the two subunits. This "Grft-linker-Grft" is a folded protein dimer, apparently nearly identical in structural properties to the wild-type protein. A "one-armed" obligate dimer was also designed (Grft-linker-Grft OneArm), with each of the three carbohydrate binding sites of one subunit mutated while the other subunit remained intact. While both constructed dimers retained the ability to bind gp120 and the viral surface, Grft-linker-Grft OneArm was 84- to 1,010-fold less able to inhibit HIV than wild-type Grft, while Grft-linker-Grft had near-wild-type antiviral potency. Furthermore, while the wild-type protein demonstrated the ability to alter the structure of gp120 by exposing the CD4 binding site, Grft-linker-Grft OneArm largely lost this ability. In experiments to investigate gp120 shedding, it was found that Grft has different effects on gp120 shedding for strains from subtype B and subtype C, and this might correlate with Grft function. Evidence is provided that the dimer form of Grft is critical to the function of this protein in HIV inhibition.

3.2 Introduction

HIV is a devastating disease affecting at least 33 million people worldwide, leading to a critical need for multiple strategies to prevent HIV infection. One such strategy is the development of a microbicide to prevent the sexual spread of HIV. While the CAPRISA 004 clinical trial showed partial success for the HIV reverse transcriptase inhibitor tenofovir in gel form, the subsequent VOICE trials were not successful, likely due in part to non-compliance [92, 148]. This underscores the need for a continued study of a variety of different microbicides, and the likelihood that most success will occur with combinations of drugs with different mechanisms of action (and possibly different formulations) to achieve maximal effectiveness and to avoid potential development of drug resistance [149].

Several highly effective proteins are being studied as possible microbicides, particularly lectins that bind the glycosylated surface of gp120. Many reports confirm the importance of lectins in binding gp120 and inhibiting HIV [47, 97, 101, 134, 135, 150, 151], and it has also been shown that viral escape by deglycosylation leads to a higher viral susceptibility to plasma antibodies [152]. Griffithsin (Grft), a 121 amino acid lectin derived from the red alga Griffithsin sp. [47] is among the most promising lectins yet discovered. This protein has a combination of (i) higher potency than other lectins [39, 47], (ii) excellent pre-clinical properties including low/no toxicity and lack of significant activation of a variety of cell types [52, 53], (iii) inexpensive production in gram quantities [51], and (iv) synergy when combined with antibodies and a variety of other lectins [93]. Recently, Grft has also been shown to be active against other viruses including the Hepatitis C virus [48-50, 142], and it is resistant to digestion by many commercially available proteases (although it is susceptible to elastase) [153]. Recent work specifically addressing lectin cellular toxicity showed that Grft does not activate T cells, minimally alters gene expression, and minimally induces cytokine secretion [52]. Further, while Grft can bind some human cells, it still retains antiviral activity [52]. These positive characteristics make Grft a very promising microbicide candidate, and underscore the importance of elucidating the biochemical details of the role of Grft in HIV inhibition [13, 52]. There is a critical gap, however, in an understanding of how Grft functions so effectively to inhibit HIV infection. Crystal structures of Grft have been reported showing a dimer [1, 98, 101], and lower antiviral potential of a monomeric variant [97]. More recently, analytical ultracentrifugation confirmed a tight Grft dimer [55]. However, the mechanism of action of Grft is not fully known. In particular, no work has yet investigated the Grft dimer itself or shown how it might function to achieve such unusually high potency.

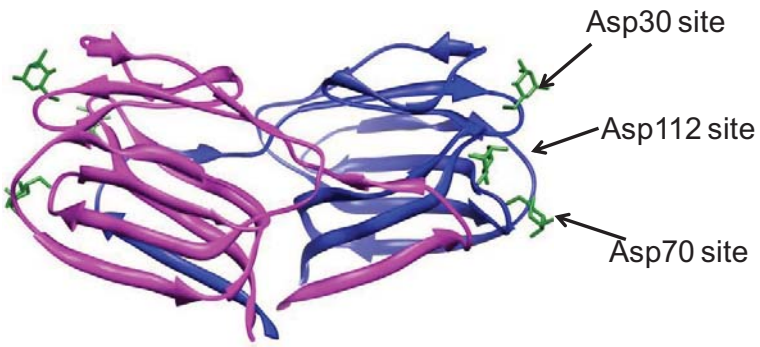

Figure 3-1: The structure of the GRFT dimer in complex with mannose [1].

The arrows denote the three mannose binding sites of one monomer: D30, D70 and D112 sites. Structure was made with the program Chimera [5, 6] using PDB structure 2gud [1].

Figure 3-1 shows the structure of Grft as determined by X-ray crystallography [1]. The protein is a dimer, having three putative carbohydrate-binding sites (CBS) per subunit. Competition data and further structural work [47, 101] indicate that each binding site binds one mannose mono-saccharide, making it very likely that Grft inhibits viral entry by binding mannose on the surface of gp120. Grft has been shown to also bind gp41 [47], although it has not been proven yet whether this binding is through N-glycan interaction and/or to direct protein interaction. However, the gp41 glycoprotein is obscured during the first part of HIV entry and mutations that affect Grft sensitivity tend to be contained on gp120, not gp41 [152]. The HIV envelope protein gp120 contains between 18 and 33 N-linked glycosylation sites (depending on the virus strain), approximately a dozen of which are high-mannose sites [29, 33, 35, 140]. These high-mannose saccharides contain several related branched glycans, often having three terminal mannose residues rarely found on mammalian cells (reducing the possibility of mannose-specific lectin-host interaction), although it has been shown that Grft can bind to PBMC but retains antiviral activity [13, 52]. Other work has demonstrated that several high mannose glycans on the subtype C gp120 surface, in particular those on N234 and N295, have important roles in Grft effectiveness. HIV strains lacking both of these glycan sites on gp120 show significantly lower sensitivity to Grft, and introducing these two glycans by adding back the glycosylation sites at these locations on gp120 increased Grft sensitivity [39]. Similarly, glycosylation at site N448 is likely important for Grft function [38]. Interestingly, Grft has been shown to alter the conformation of gp120 by exposing the CD4 binding site on gp120 in both HIV-1 subtype B and C strains [143]. This raises the possibility that the importance of some N-glycan sites on

gp120 in Grft potency is related to the ability of Grft to utilize these sites to alter the conformation of gp120, thereby interfering with virus entry.

Two outstanding questions regarding the mechanism of HIV inhibition by Grft have been (i) what role do each of the three putative carbohydrate-binding sites play in the affinity of the protein for its mannose target and subsequent anti-HIV activity, and (ii) what is the role of the dimer in the function of Grft for anti-HIV activity? We have recently shown that while loss of an individual carbohydrate binding site by substitution leads to only several-fold loss of ability to bind gp120, such individual-site variants show orders of magnitude loss of HIV inhibitory potency [55]. Therefore there is a clear lack of correlation between simple ability to bind gp120 and ability of Grft to inhibit the virus.

Since there appears to be a lack of direct correlation between carbohydrate binding and anti-HIV activity, the question arises as to what structural features and interactions contribute to the effectiveness of Grft. This leads to the second question, whether the role of the dimer may be critical for efficient Grft function. For the lectin cyanovirin-N, anti-HIV activity could be restored with only slightly reduced activity when two non-functional CV-N units (each containing only one carbohydrate binding site) were cross-linked [86]. Similarly, linking higher order multimers of cyanovirin could increase its anti-HIV activity [85].

To address the role of the dimer in Grft function, we have made an obligate dimer of Grft as well as an obligate dimer with all three CBS in one subunit intact, but the three CBS on the second subunit (“arm”) removed by substitution. In a direct comparison of the “two armed” dimer and the “one armed” dimer, we show that while the obligate dimer behaves very similarly in all respects to the wild-type protein, the one-armed obligate dimer has quite different properties. The one-armed obligate dimer exhibits only a modest loss of ability to bind gp120, yet its ability to inhibit the virus is reduced by orders of magnitude compared to the wild-type protein and the obligate dimer. Further, both the wild-type Grft and the obligate dimer demonstrate the ability to alter the conformation of gp120, while the one-armed obligate dimer is markedly reduced in this ability. Overall, this work provides evidence that the mechanism of Grft involves multiple subunits binding to gp120, and suggests that the need for two subunits may be related to the ability of Grft to alter the conformation of gp120, reducing the potential of gp120 to mediate viral infection. This mechanism may be applicable to other multi-subunit lectin inhibitors of HIV.

3.3 Material and Methods

3.3.1 DNA construction

Genes of Grft variants were cloned into the pET-15b expression vector (Novagen). Grft-linker-Grft was constructed using a 16 amino acid Gly-Ser linker: SSSGGGGSGGGSSSGS. One-Armed obligate dimer constructs were made similarly and all variants were confirmed by DNA sequencing.

3.3.2 Protein purification

Plasmids with an N-terminal histidine-tag were transformed to *Escherichia coli* BL21(DE3) (Novagen) competent cells and expressed in minimal media with $^{15}NH_4Cl$ as the sole nitrogen source. Each variant was produced using the following procedure. Protein production was induced upon addition of Isopropyl β-D-1-thiogalactopyranoside (IPTG) with further incubation at 37 ℃ for 6 hours. Cells were harvested at 6,000 x g for 10 min and the pellet was resuspended in 5 M guanidine hydrochloride, 500 mM NaCl, 10 mM benzamidine, and 20 mM Tris pH 8; this allowed complete solubilization of proteins from both the inclusion body and the supernatant upon cell disruption. The solution was French pressed twice at 16,000 psi, and then centrifuged at 15,000 x g for 1 hour. The soluble portion was loaded onto a Nickel chelating column (Qiagen) equilibrated with the same resuspension buffer. Proteins were eluted using 500 mM imidazole, 5 M guanidine hydrochloride, 500 mM NaCl and 20 mM Tris pH 8 and refolded by adding dropwise to low salt refolding buffer (50 mM NaCl, 20 mM Tris pH 8) over the course of 30 min. The solution was dialyzed against in the same refolding buffer at 4ºC overnight. The protein solution was then centrifuged at 15,000 x g for 1 hour to remove precipitated material, and purified on a C4 reversed-phase chromatography column (Vydac, Hesperia, CA). The fractions were analyzed on a SDS-PAGE gel to confirm the size and then lyophilized in a Labconco freeze-dry system (Labconco Corporation).

3.3.3 NMR spectroscopy

Grft variants were expressed in minimal media with $^{15}NH_4Cl$ as the only nitrogen source. These variants were produced and purified as described above. To dissolve the protein powder after purification, 20 mM sodium phosphate buffer (pH 7.0) with 5% D_2O was used and 2,2-dimethyl-2-silapentane-5-sulfonic acid (DSS) was added for calibration. Spectra were collected at 25 ℃ on a four-channel 600-MHZ Bruker Avance III spectrometer. The data were processed using NMR Pipe [115] and analyzed using PIPP [116]. For two-dimensional HSQC spectra, a sweep width of 9615 Hz (^1H) and 1939 Hz (^{15}N), with 640* points in ^1H and 128* points in ^{15}N were used.

3.3.4 Analytical Ultracentrifugation

To identify the oligomerization state of the Grft-linker-Grft construct, the molecule was studied by analytical ultracentrifugation using sedimentation velocity (SV) analysis. To determine if mass action effects could affect the oligomerization state, the experiments were carried out at multiple concentrations. Enhanced van Holde – Weischet analysis [127] resulted in vertical sedimentation coefficient G(s) distributions, identifying a major species with identical sedimentation coefficients for each concentration, suggesting that the major species is homogeneous, and not subject to mass-action induced oligomerization (see Fig. 1C). To determine the molecular weight of this major species, and ultimately identify the oligomerization state of Grft-linker-Grft, 2-dimensional spectrum analysis [125, 132, 133] and genetic algorithm analysis [126, 128], combined with Monte Carlo analysis [129] resulted in a molecular weight consistent only with the dimer (24.4 kDa for the 0.3 OD_{230nm} species, 27.8 kDa for 0.6 OD_{230nm}, and 26.6 kDa for 0.9 OD_{230nm}, see Fig. 1D). These values are in good agreement with the theoretical molecular weight of 28.9kDa. All experiments were performed on a Beckman Optima XL-I at the Center for Analytical Ultracentrifugation of Macromolecular Assemblies (CAUMA) at the University of Texas Health Science Center at San Antonio. Sedimentation velocity (SV) data were analyzed with the UltraScan software [122, 123]. Calculations were performed at the Texas Advanced Computing Center at the University of Texas at Austin, and at the Bioinformatics Core Facility at the University of Texas Health Science Center at San Antonio as described in [124]. All Grft samples were measured in 20 mM sodium phosphate buffer containing 50 mM NaCl. All data were collected at 20 ℃, and spun at 60 krpm, using standard titanium 2-channel centerpieces (Nanolytics, Potsdam, Germany). The protein concentrations ranged from 4.2 uM (0.3 OD_{230nm}) to 12.6 uM (0.9 OD_{230nm}). The partial specific volume of the Grft-linker-Grft construct was determined to be 0.711 cm^3/g by protein sequence according to the method by Durchschlag as implemented in UltraScan. All data were first analyzed by two-dimensional spectrum analysis with simultaneous removal of time-invariant noise [154] and then by enhanced van Holde–Weischet analysis [127] and genetic algorithm refinement [126, 128], followed by Monte Carlo analysis [129].

3.3.5 ELISA studies of Grft obligate dimer interaction with HIV gp120

To test the binding of each Grft variant to HIV gp120, ELISA binding assays were used as described previously [47, 102]. In brief, 100 ng HIV ADA gp120 (ImmunoDiagnostic) was coated in each well of a 96 well plate (Maxisorp Immunoplate; Nalge NUNC) overnight at 4 ℃. Then the plate was blocked with 1% bovine serum albumin for 1 hour. Serial dilutions of wild-type Grft as well as variants were added to triplicate wells and incubated for 2 hours at 37 ℃. After the plate was washed, 1:1000 fold dilution of Horseradish-peroxidase-conjugated Ni-NTA (Qiagen, Valencia, CA), which can detect the N-terminal his-tag on Grft,

was added according to the company's instructions. Then the substrate for Horseradish-peroxidase (2,2'-azino-bis 3-ethylbenzthiazoline-6-sulphonic acid, ABTS) (Thermo Fisher Scientific) was added and signal was measured by absorbance at 405 nm.

3.3.6 Surface plasmon resonance (SPR) analysis

All interaction studies were performed with a Biacore T200 instrument (GE Healthcare, Uppsala, Sweden) at 25 ℃ in HBS-P running buffer (10 mM HEPES, 150 mM NaCl and 0.05% surfactant P20; pH 7.4). Recombinant gp120 proteins from HIV-1(III_B) strain (ImmunoDiagnostics Inc., Woburn, MA), from HIV-1(ADA) strain (ImmunoDiagnostics) and recombinant gp41 protein from HIV-1(HxB2) (Acris Antibodies GmbH, Herford, Germany) were covalently immobilized on the carboxymethylated dextran matrix of a CM5 sensor chip in 10 mM sodium acetate, pH 4.0, using standard amine coupling chemistry. A reference flow cell was used as a control for non-specific binding and refractive index changes. The test compounds were serially diluted in running buffer using two-fold dilution steps. Grft samples were injected for 2 minutes at a flow rate of 45 µl/min and the regeneration pulse was 1 injection of Glycine-HCl pH1.5. The experimental data were fit using the 1:1 binding model (Biacore T200 Evaluation software 1.0) to determine the binding kinetics.

3.3.7 Viral Reagents

Viral plasmids containing the env gene from HIV-1 were obtained from the NIH AIDS Research and Reference Reagent Program, Division of AIDS, NIAID, NIH. HIV-1 ADA-M (referred to as HIV-1 ADA, R5) was received from Dr. Howard Gendelman. Plasmid pSV-JRFL (R5) was a kind gift from Nathaniel Landau [107]. pCAGGS-SF162-gp160 (R5) was from Leonidas Stamatatos and Dr. Cecilia Cheng-Mayer. PVO, clone 4 (SVPB11), AC10.0, clone 29 (SVPB13) were from Dr. David Montefiori and Dr. Feng Gao [155], pWITO4160 clone 33 (SVPB 18) was from Drs. B. H. Hahn and J. F. Salazar-Gonzalez [155]. DU156 clone 12 (SVPC3) was from Drs D. Montefiori, F. Gao, S. Abdool Karim and G. Ramjee; and DU422 clone 1 (SVPC5) was from Drs. D. Monteriori, F Gao, Williamson and S. Abdool Karim [41, 156]. ZM53M.PB12 (SVPC11), ZM109F.PB4 (SVPC13) and ZM135M.PL10a (SVPC15) were from Drs. E. Hunter and C. Derdeyn [157]. pSG3Δenv was from Drs. John C. Kappes and Xiaoyun Wu [158, 159]. Recombined human soluble CD4 and HIV antibodies were obtained from the NIH AIDS Research and Reference Reagent Program, Division of AIDS, NIAID, NIH as follows: Soluble Human CD4 from Progenics; HIV-1 gp120 Monoclonal Antibody (IgG b12) from Dr. Dennis Burton and Carlos Barbas [160, 161].

3.3.8 Virus capture ELISA

Different concentrations of Grft variants were coated on a 96 well plate at 4˚C overnight. The wells were then washed 3 times with PBS-Tween20 and blocked with BSA for 1 hour. Virus in DMEM (Dulbecco's Modified Eagle's Medium) was added into each well and incubated at 37 ℃ in a 5% CO_2 atmosphere for 4 hours followed by washing the wells 3 times using DMEM. Viruses were lysed using 0.5% Triton X-100 at room temperature for 15 min and the supernatant containing viral lysate was transferred to a commercial p24 Capture ELISA plate (Immuno Diagnostic) and incubated at 4 ℃ overnight. The detector was added according the manufacturer's instructions. The signal was measured by absorbance at $OD_{450\ nm}$.

3.3.9 Single round infection assays

TZM-bl cells stably expressing CD4, CCR5 and CXCR4 coreceptors were maintained in DMEM with 10% fetal bovine serum (FBS). 10^4 cells per well were first seeded into a 96 well plate for one day. The medium was then changed 3 hours before the assay and made to a volume of 50 µl per well, and then a serial dilution of Grft variants were added from the top row to the bottom row, as follows: 20 ul Grft variant was added into the first row and mixed with culture medium. Then 20 µl medium was removed and added into the second row, and so on. Virus (50–100 ng p24) was then added into each well containing different Grft variants. The medium was changed after 24 hours and cells were incubated for another 24 hours. PBS containing 0.5% NP-40 was used to lyse the cells and substrate chlorophenol red-D-galactopyranoside (CPRG, Calbiochem) was added. The absorbance signal was measured at 570 nm and 630 nm. The ratio of 570/630 for each well was calculated. EC_{50} values were determined using a linear equation fitted between two data points surrounding 50% inhibition. For presentation purposes, data shown in the figures were plotted and fitted as curves using a four-parameter logistic equation in Kaleidagraph (Synergy Software, Reading, PA).

3.3.10 Anti-HIV Assays in CEM Cell Cultures

CEM cells (5×10^5 cells per ml) were suspended in fresh culture medium and infected with HIV-1(III_B) at 100 times the $CCID_{50}$ (50% cell culture infective dose) per ml of cell suspension, of which 100 ul was then mixed with 100 ul of the appropriate dilutions of the test compounds. After 4 to 5 days at 37 ℃, HIV-1-induced syncytia formation was recorded microscopically in the cell cultures. The 50% effective concentration (EC_{50}) corresponds to the compound concentration required to prevent syncytium formation by 50% in the virus-infected CEM cell cultures.

3.3.11 Grft-induced CD4 binding site exposure

CD4 binding site exposure in gp120 was carried out as described [143]. Briefly, anti-gp120 antibody b12, which detects the CD4 binding site on gp120, was coated onto a 96 well plate at 4 ℃ overnight. The next day, the plate was washed and blocked with BSA. Different concentrations of Grft variants (3.2nM, 16nM, 80nM) were pre-incubated with HIV virions at 37 ℃ for 1 hour and then added to the b12-coated plate. After 2 hours of incubation, the plate was washed, and bound virus was lysed using 0.5% Triton X-100. The virus lysate was then transferred to a commercial p24 ELISA plate (Immuno Diagnostic) and p24 was measured following the manufacturer's instructions. Figure 3A and 3B show data from the 16nM Grft incubation.

3.3.12 Cell surface gp120 shedding

Cell surface gp120 shedding was carried out as described [144, 162]. Briefly, 293FT cells were transfected with the HIV JRFL, PVO.4, ZM53M.PB12 or ZM109M.PB4 plasmid using the Roche X-treme transfection reagent. 48 hours post-transfection, cells were collected, washed with PBS and concentrated to $2x10^7$ per ml. Cells were then aliquoted to microcentrifuge tubes (200 ul per tube). Cells were then centrifuged at low speed for 5 min, then 160 ul supernatant was removed. Different concentrations of soluble CD4 or Grft variants were added and mixed gently with cells. The mixture was then put into a 37 ℃ incubator for 1 hour and gently mixed every 20 min. The cells were then centrifuged, and the supernatant containing shed gp120 was collected and separated using SDS-PAGE. Western blots were carried out using the mouse anti-HIV gp120 antibody (Immuno Technology) detecting a linear epitope on gp120, followed by detection using anti-mouse IgG antibody HRP conjugate (Promega). Metal enhanced DAB substrate (Thermo Fisher) was then added and the resulting image was processed using the Bioimaging system (UVP).

3.3.13 Grft cross-linking separate gp120 subunits

5 uM of Streptavidin (Invitrogen, NY) were coated in each well of a 96 well plate overnight at 4 ℃. The plate was then washed 3 times with PBS-Tween20 and blocked with 3% BSA for 1 hour. 0.5 ng/ul biotin-conjugated recombinant gp120 III_B (or ADA strain) (ImmunoDX, MA) were then added to each well and incubate at room temperature for 1 hour. Different concentrations of inhibitors were then added and incubate at room temperature for 2 hours. 0.5 ng/ul HRP-conjugated recombinant gp120 III_B (or ADA strain) (ImmunoDX, MA) were then added into each well followed by incubation at room temperature for 1 hour. Then the substrate for Horseradish-peroxidase (3,3',5,5'-Tetramethylbenzidine, TMB) (Thermo Fisher Scientific) was added according the manufacturer's instructions. The signal was measured by absorbance at $OD_{450\ nm}$.

3.4 Results

3.4.1 Design of the obligate Griffithsin dimer.

To study the role of the Grft dimer, we designed an obligate dimer, in which the C-terminus of one monomeric subunit was covalently linked by a 16 amino acid (Gly-Ser) linker to the N-terminus of a second subunit (Figure 3-2). This "Grft-linker-Grft" was expressed and purified. The ^{15}N correlation spectrum (HSQC; Heteronuclear Single Quantum Coherence) of the protein shows it to be very similar to that of the wild-type protein, strongly indicating that the obligate dimer has the same structural properties (Figure 3-4). To confirm that Grft-linker-Grft is indeed a dimer and has not associated with other units to make a higher order oligomer, analytical ultracentrifugation was carried out, with the results being consistent with a single dimer unit of 28.9 kDa (Figure 3-3A and 3-3B). As noted above and shown in Figure 3-1, each Grft monomer has three carbohydrate-binding sites (CBS). Thus, this obligate dimer has 6 CBS (carbohydrate binding site), 3 on each monomer, with the distance between the carbohydrate binding faces on each subunit being around 47 Å [1].

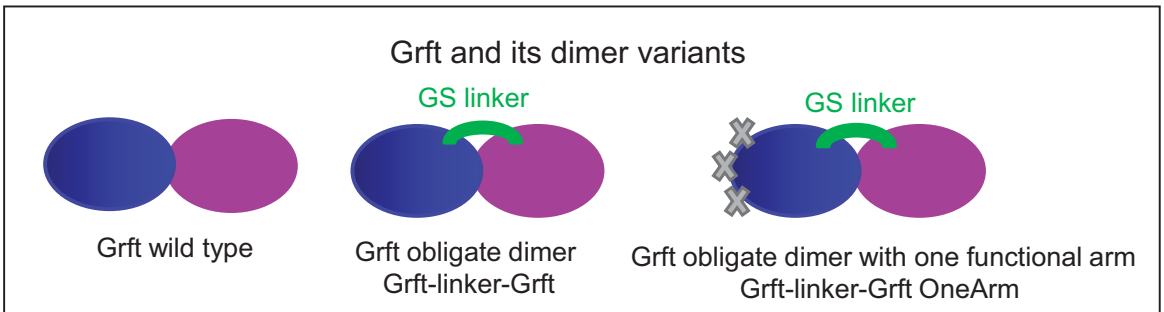

Figure 3-2: Constructs of Grft dimer variants.

Cartoon showing color coded Grft domains, with one domain in magenta and the other domain in blue, Gly-Ser linker in green. Grey cross indicate that the 3 carbohydrate binding sites were substituted to eliminate the carbohydrate binding ability of that domain.

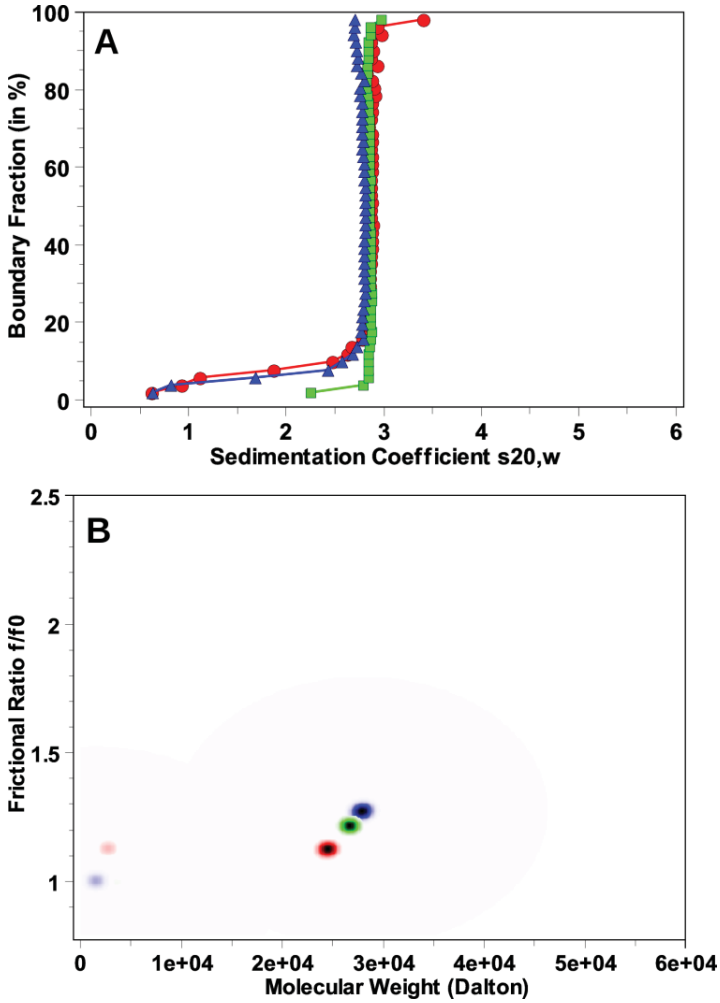

Figure 3-3: Analytical ultracentrifugation showing Grft-linker-Grft forms a dimer.

3-3A: van Holde - Weischet G(s) sedimentation coefficient distributions of Grft-linker-Grft at 3 concentrations (0.3 OD_{230nm}, red circles, 0.6 OD_{230nm}, blue triangles, 0.9 OD_{230nm}, green squares). Vertical distributions indicate homogeneity.

3-3B: Genetic Algorithm Monte Carlo analysis. Combined overlay of all samples using the same color scheme as in 3-3A. The density of color is proportional to partial concentration. A small amount of a contaminating species is apparent in the lower s-value range in both figures. The major species from all concentrations appear to have a low anisotropy, consistent with the globular shape proposed by the X-ray structure, with frictional ratios in the range of 1.1-1.3, and agree very well with the linked Grft dimer molecular weight.

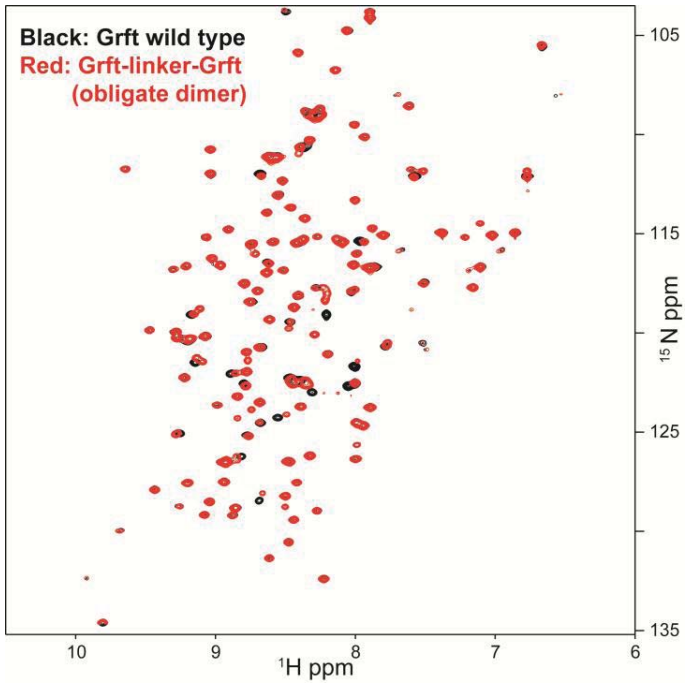

Figure 3-4: The ^{15}N HSQC spectrum of the obligate dimer Grft-linker-Grft (red) overlaid with the spectrum of wild-type Grft (black).

To determine the role of two subunits in the dimer versus one, all three carbohydrate binding sites were removed from one of the monomers in the Grft-linker-Grft by mutating the critical Asp at each site in one of the monomers. This variant, "Grft-linker-Grft-OneArm" has one wild-type subunit and one subunit containing the substitutions D30A/D70A/D112A in its CBS. We have previously shown that this triple substitution essentially removes the ability of the subunit to bind mannose [55]. In order to determine whether substitutions on each of the two subunits of Grft dimer are equivalent, the 3 CBS on either the N-terminal or C-terminal subunit were triply mutated. It was found that the triple substitution on the N-terminal subunit of the Grft obligate dimer behaved the same as the triple substitution of the C-terminal subunit of the obligate dimer, both in pseudo viral assays and ELISA binding assays (Appendix Figure B-3 and B-4). Similarly, the NMR characteristics of the two one-armed variants were very similar as judged by ^{15}N HSQC spectra (Appendix Figure B-1). This indicates that the two Grft subunits are equivalent so we proceeded to work with the triple substitution on the C-terminal domain of Grft-linker-Grft (leaving the N terminal domain in its wild-type form), and refer to this as "Grft-linker-Grft OneArm". ^{15}N correlation spectra of this one-armed variant show a folded protein with peaks similar to both the wild-type protein (likely from the wild-type subunit) and the triple variant reported previously (from the other subunit [55]; Appendix Figure B-7), indicating that this One-Armed dimer does have one subunit as a wild-type Grft subunit,

and the other subunit as a triply mutated Grft subunit. As a negative control, the three carbohydrate binding sites for each monomer of the linked dimer were also mutated (i.e. all six sites were mutated to Ala; Appendix Figure B-2) and this protein was nicely folded. This Grft-linker-Grft with two defective functional arms had very little function in a pseudo viral assay at the highest concentration tested (>1000 nM). The HSQC spectra of this NoArm dimer also showed similar spectral characteristics as the unlinked Grft Triple variant D30A/D70A/D112A (Appendix Figure B-2), so for convenience of purification, the unlinked triple variant is used in this work (except for the SPR studies) as a negative control [55].

3.4.2 Obligate Grft dimer binding to gp120.

ELISA assays were carried out to determine the ability of the obligate Grft dimers to bind to immobilized, recombinant gp120 (strain ADA). As shown in Figure 3-5, Grft-linker-Grft and Grft-linker-GrftOneArm bind about as well as wild-type Grft to HIV-1 ADA, while the triple variant, Grft Triple D30A/D70A/D112A binds poorly, as expected.

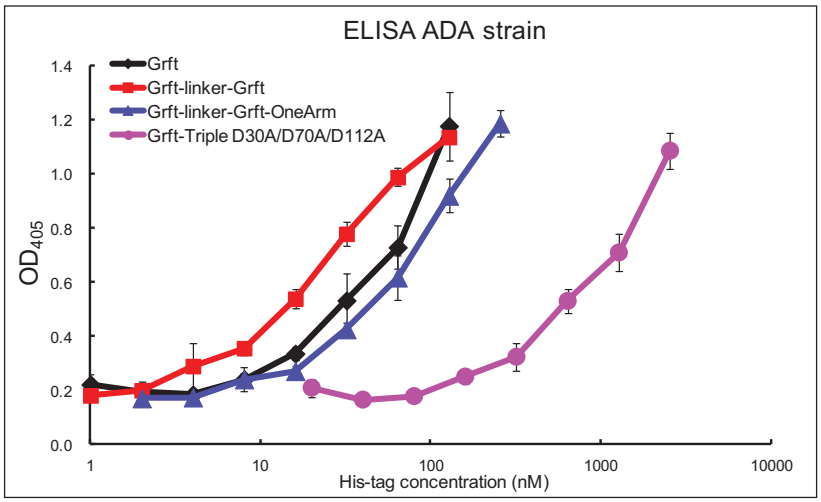

Figure 3-5: ELISA assay indicating the ability of Grft and its dimer variants to bind to immobilized commercial HIV-1 $gp120_{ADA}$.

Wild-type Grft (black) and the obligate dimer Grft-linker-Grft (red) bind well to $gp120_{ADA}$. The One-Armed obligate dimer, Grft-linker-GrftOneArm (D30A/D70A/D112A in one subunit; blue), also binds fairly well to $gp120_{ADA}$. The triple variant D30A/D70A/D112A (with both arms substituted in an unlinked dimer, magenta) binds poorly to $gp120_{ADA}$. Typical results are shown from an experiment in triplicate. Each experiment was repeated at least 3 times. Error bars indicate standard deviation from a typical triplicate experiment. Binding was detected using an HRP-conjugated Ni-NTA.

To obtain more quantitative results, surface plasmon resonance (SPR) analysis was carried out. These experiments showed that Grft-linker-Grft binds immobilized, monomeric gp120 derived from strain ADA and strain III_B quite well, about 2- to 2.5-fold worse than wild-type Grft (Table 3-1, Figure 3-6, Appendix Figure B-5 and B-6). Interestingly, Grft-linker-Grft OneArm also binds well to gp120 compared to Grft-linker-Grft, with a dissociation constant K_D about 2-fold higher (382-386 pM *versus* 164-176 pM, respectively). Also, wild-type Grft and Grft-linker-Grft bind at equally high affinity to gp41 as to gp120, whereas the Grift-linker-Grft OneArm binds gp41 less well, at about 20-fold lower efficacy than wild-type Grft. (Table 3-1).

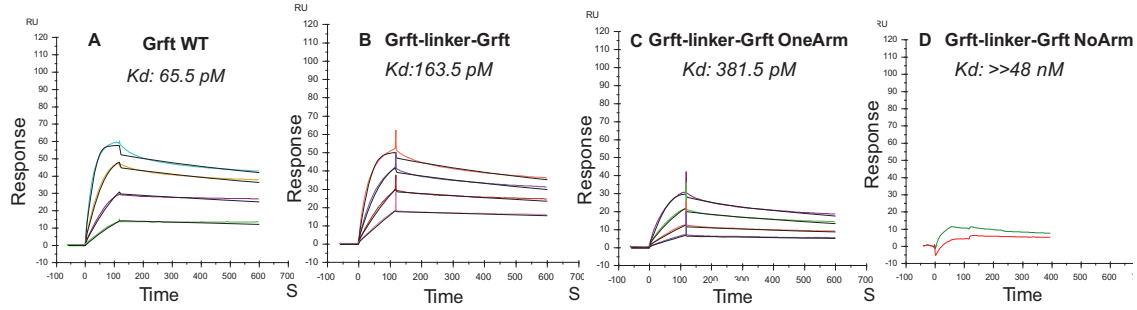

Figure 3-6: Surface plasmon resonance sensorgrams of Grft variants binding to immobilized $gp120_{ADA}$.

Kinetic analysis of the interactions of Grft (Panel A), obligate dimer Grft-linker-Grft (Panel B), Grft-linker-Grft-OneArm (Panel C) and the negative control (obligate dimer with no functional arms, i.e. the D30A/D70A/D112A substitutions in both subunits; Panel D) with immobilized HIV-1 ADA gp120. Serial two-fold analyte dilutions (covering a concentration range from 1.5 to 12 nM in panels A to C and 24 to 48 nM in panel D) were injected over the surface of the immobilized gp120. The experimental data (colored curves) were fit using a 1:1 binding model (black lines) to determine the kinetic parameters. The biosensor chip density of gp120 was 90 RU.

Table 3-1: Kinetic data for the interaction of Grft and its variants with immobilized HIV-1 envelope proteins $gp120_{ADA}$, $gp120_{IIIB}$ and $gp41_{HxB2}$.

	gp120 IIIB (X4)			gp120 ADA (R5)			gp41 HxB2		
	K_D (pM)	k_{on} (1/M.s)	k_{off} (1/s)	K_D (pM)	k_{on} (1/M.s)	k_{off} (1/s)	K_D (pM)	k_{on} (1/M.s)	k_{off} (1/s)
Grft WT	69.3± 5.5	(1.93± 1.51)E+07	(1.29± 0.96)E-03	65.5± 9.2	(2.15± 1.52)E+07	(1.30± 0.79)E-03	64.9± 18.7	(1.47± 0.62)E+07	(1.04± 0.62)E-03
Grft-linker-Grft	175.7± 22.6	(4.91± 0.27)E+06	(8.61± 1.17)E-04	163.5± 21.5	(5.98± 1.19)E+06	(9.97± 3.26)E-04	101.2± 2.4	(6.63± 0.40)E+06	(6.70± 0.36)E-04
Grft-linker-Grft OneArm	386.2± 121.7	(5.15± 2.07)E+06	(1.92± 0.98)E-03	381.5± 79.4	(5.67± 1.24)E+06	(2.12± 0.50)E-03	1299± 1148	(7.42± 2.33)E+06	(1.11± 1.13)E-02
Grft-linker-Grft NoArm [1]	no specific binding observed at 12 nM			no specific binding observed at 12 nM			no specific binding observed at 12 nM		

K_D, dissociation equilibrium constant; k_{on}, association rate constant; k_{off}, dissociation rate constant.

The p values for interactions with $gp120_{IIIB}$ are 0.0001 (wild-type Grft: *versus* Grft-linker-Grft); 0.0027 (wild-type Grft *versus* Grft-linker-Grft OneArm). For interactions with $gp120_{ADA}$: 0.0007 (wild-type Grft *versus* Grft-linker-Grft); 0.0019 (wild-type-Grft *versus* Grft-linker-Grft OneArm).

The above data were obtained with recombinant gp120 (which is a monomer) whereas gp120 occurs as a trimer in the envelope of the native virus particle [4, 81, 163, 164]. However, it was recently shown that the kinetic interactions obtained for several carbohydrate binding agents (including Grft) with monomeric gp120 were virtually similar if trimeric gp120 was used in SPR-based assays [165]. To further probe the ability of Grft variants to bind trimeric gp120, we used virus capture ELISA assays to measure the ability of the obligate dimers to bind to trimeric gp120 [166]. In these experiments, the Grft variant was coated on a plate, followed by incubation with pseudo virus. The amount of virus that the Grft was able to bind was measured by a subsequent p24 ELISA assay. As shown in Figure 3-7, both Grft-linker-Grft and Grft-linker-Grft OneArm bound well to the pseudo virus (strain ADA). The negative control containing the triple substitution D30A/D70A/D112A (in both arms) bound poorly to trimeric gp120 by SPR as expected. Testing of binding of some Grft variants to trimeric gp140 by SPR analysis generated similar data as with monomeric gp120 [165], indicating that both forms of gp120 provide relevant results.

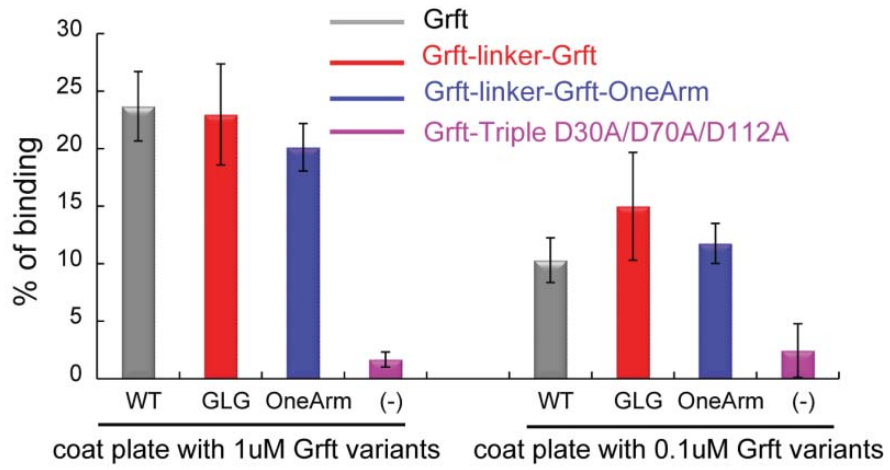

Figure 3-7: Virus capture ELISA indicates the ability of Grft and its variants to bind to the viral surface.

Wild-type Grft (gray) and the obligate dimer Grft-linker-Grft (red) bind well to the HIV spike. The one-armed obligate dimer Grft-linker-Grft-OneArm (blue) also binds well to the viral spike, with very little, if any apparent loss of binding affinity. The Grft containing the triple substitution D30A/D70A/D112A (in both arms) shows essentially no virus binding, as expected (magenta). Experiment was repeated 3 times. Error bars indicate the standard deviation from a triplicate experiment.

3.4.3 Anti-HIV function of the obligate dimer.

Inhibition assays were carried out against several HIV-1 strains of single round pseudo virus. As shown in Table 3-2, Grft-linker-Grft showed pronounced inhibition against the HIV-1 strains that were tested, including a variety of subtype B and subtype C strains. For example, the obligate dimer inhibited HIV infection at an EC_{50} of 0.012 nM (compared to 0.011 nM for the wild-type protein) against HIV-1 strain ADA. However, the one-armed obligate dimer variant was much less potent for each strain tested, with EC_{50} values being 84- to 609-fold worse than for the wild-type protein in single-round infection assays for R5 strains. For strain ADA, in which SPR showed reduced binding by Grft-linker-Grft OneArm by only 5-fold, the antiviral inhibition potency was reduced by 609-fold (Tables 3-1 and 3-2, Figure 3-8). In replication competent viral assays using CEM cells, a 1,010-fold decrease in antiviral activity was observed for the OneArm obligate dimer compared to the wild-type dimer with X4 strain III_B. Together with the binding data, these functional data strongly suggest that Grft binding to gp120 needs only one functional arm to bind with high affinity to HIV-1 gp120, but it requires both arms to exert full antiviral function.

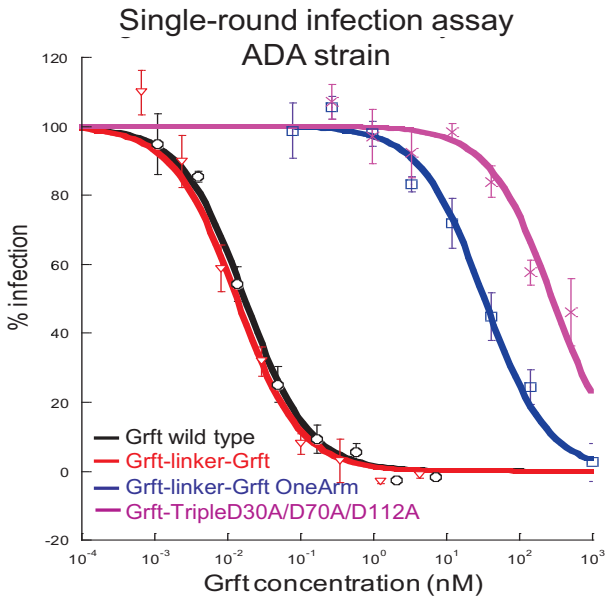

Figure 3-8: Inhibition of HIV-1 infection by Grft variants in single-round virus assays.

Typical results are shown from an experiment in triplicate using R5 subtype B strain ADA. Wild-type Grft is shown in black; obligate dimer Grft-linker-Grft in red; Grft-linker-Grft OneArm in blue; triple substitution D30A/D70A/D112A in magenta. Each experiment was repeated at least 3 times. Error bars indicate the standard deviation from a triplicate experiment.

Table 3-2: EC_{50}s for Single-round infection assay for Grft wild-type, obligate Grft-linker-Grft dimer and One-Armed Grft dimer[a].

Strain/compounds		Grft	Grft-linker-Grft (obligate dimer)		One-Armed dimer	
		EC_{50} (nM)	EC_{50} (nM)	Fold worse than WT	EC_{50} (nM)	Fold worse than WT
Subtype B	ADA	0.0105± 0.0084	0.0118 ±0.0046	1	6.39 ±2.5	609
	JRFL*	0.0725± 0.030	0.0533± 0.016	0.7	8.26 ±3.7	114
	SF162	0.0316± 0.015	0.0253± 0.030	0.8	9.63± 4.8	305
	AC10.0	0.0458±0.022	0.0567±0.050	1.2	13.1±3.7	286
	PVO.4	0.0445± 0.0066	0.0292± 0.0013	0.7	6.28±2.5	141
	pWITO4160.33*	0.0484±0.015	0.0509±0.087	1	10.9±2.6	225
	III_B (X4)	0.06 ± 0.0	0.06 ± 0.00	1	60.6±19	1010
Subtype C	DU156.12$^{\Delta}$	0.276± 0.015	0.205± 0.010	0.7	25.8± 8.8	93
	DU422.1$^{\Delta}$	0.619± 0.079	0.613± 0.028	1	51.9±5.0	84
	ZM53M.PB12$^{\Delta}$	1.39±0.31	1.43±0.12	1.0	133 ±12	96
	ZM109F.PB4$^{\Delta}$*	20.6±1.5	16.1±3.14	0.8	>1000	>49
	ZM135M.PL10a$^{\Delta}$*	15.2±2.9	13.1±1.5	0.9	>1000	>66

* Indicates missing glycan site on N234.

Δ Indicates missing glycan site on N295.

[a]Each experiment was independently repeated at least 3 times in triplicate and the values shown are +/- the standard deviation of the EC_{50} from all experiments. The experiments were carried out with TZM-bl target cells. The experiments with the X4-tropic strain III_B were carried out with CEM target cells. In this assay system, HIV-induced syncytia formation was examined microscopically at day 4 post infection. “Fold worse than WT” indicates decrease in potency compared to wild-type Grft.

Alexandre et al. [39] have shown that the two high mannose glycans at N234 and N295 are important for Grft function, with data suggesting that deletion of these two glycans could lead to marked loss of sensitivity to Grft. Here, using largely different HIV-1 strains, Grft and its variants were tested against a variety of HIV strains from both subtype B and subtype C (subtype C strains usually lack the N295 site). Table 3-2 shows the antiviral EC_{50} values against each strain in single round viral assays, while Table 3-3 lists the predicted high-mannose glycan sites for each strain. In the HIV strains tested, there appears to be a high antiviral potency by Grft against HIV-1 strains lacking the glycosylation site at N234, while strains with the glycan site at N295 missing show a somewhat lower sensitivity to Grft (but still have EC_{50} values of about 1 nM or better). Strains lacking both sites at N234 and N295 show a higher than two orders of magnitude loss of sensitivity to Grft than HIV-1 strains having both N-glycan sites preserved (Table 3-2 and Table 3-3).

Table 3-3: Predicted high-mannose glycosylation patterns of HIV-1 strains[a].

Reagent Name	clade	total predicted number of high-mannose sites	glycosylation sites											total glycan sites
			230	234	241	262	289	295	332	339	386	392	448	
ADA	B	9	*				*							22 [106]
JRFL	B	8	*	*			*							23 [167]
SF162	B	9	*				*							21 [168]
AC10.0	B	8	*					*			*			24
PVO.4	B	9	*									*		28
pWITO4160.33	B	9		*			*							25
III_B	B	11												24
Du156.12	C	8						*		*		*		22
Du422.1	C	8						*		*	*			24
ZM53M.PB12	C	8						*	*	*				25
ZM109F.PB4	C	8		*				*				*		23
ZM135M.PL10a	C	8		*				*				*		23

***** Indicates this glycosylation site is not present.

[a] Predicted glycosylation sites from:
http://www.hiv.lanl.gov/content/sequence/GLYCOSITE/glycosite.html

3.4.4 CD4 binding site exposure on gp120 by Grft variants.

A potentially important aspect regarding the mechanism of Grft is whether the Grft dimer is able to affect the conformation of HIV-1 gp120, and whether this effect on the gp120 conformation is related to Grft potency. One way to detect conformational changes is to use antibodies that bind to specific sites on the surface of gp120, such as the CD4 binding site that is accessible only at some stages during the course of viral entry [26, 146]. It has been reported that wild-type Grft is able to affect the structure of gp120 by exposing the CD4 binding site for 6 strains from subtype B and subtype C upon binding [143]. While the relationship between this action and inhibition of HIV is not yet known, it strongly suggests that Grft may function not simply by binding to gp120, but also by altering its conformation.

The ability of wild-type Grft to expose the CD4 binding site of gp120 was examined by virus capture: Briefly, a plate was coated with the antibody b12 that binds to gp120 at the CD4 binding site [143]. Then single round virus was pre-incubated with Grft or its variants, and then allowed to bind to the antibody on the plate. The amount of virus bound was measured by subsequent p24 assays. As shown in Figure 3-9, wild-type Grft induced CD4 exposure quite well in a variety of clade B strains, including ADA, JRFL, SF162, AC10.0 and PVO.4. Grft-linker-Grft obligate dimer showed similar effects in inducing CD4 binding site exposure as wild type Grft on 4 strains tested (Figure 3-9, red bars). However, Grft-linker-Grft OneArm was significantly less effective in this property for each virus strain, resulting in CD4 binding site exposure in the presence of this protein similar to that of the negative control with virus alone. This suggests that Grft requires both arms of the dimer to facilitate CD4 binding site exposure on gp120 in clade B strains.

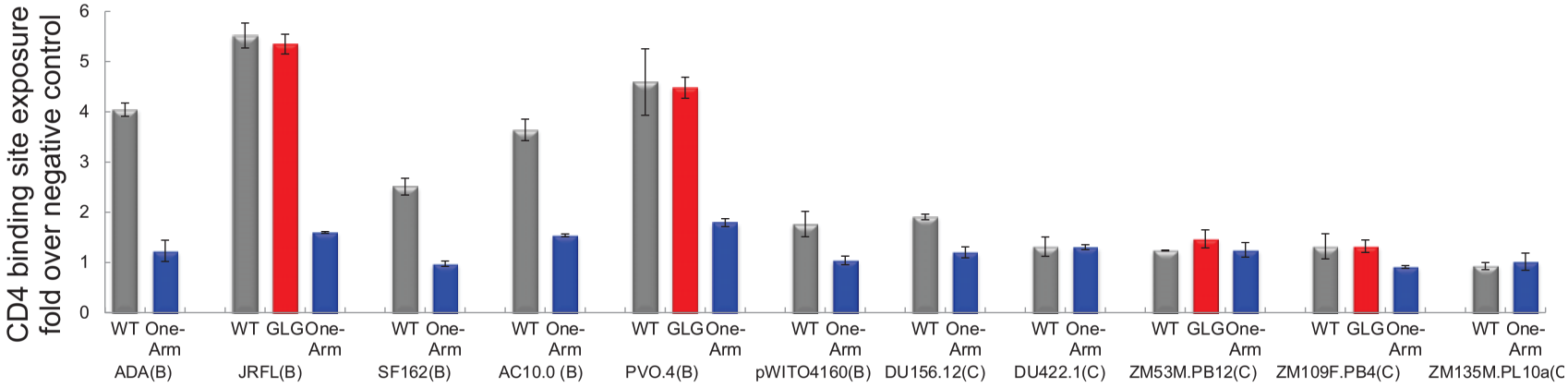

Figure 3-9: Bar graph showing CD4 binding site exposure in HIV-1 gp120 mediated by Grft or its dimer variants.

HIV-1 capture by MAb b12 (which binds to gp120 at the CD4 binding site) is shown for several strains that were pre-incubated with 16 nM Grft (diagonal stripes) or Grft-linker-Grft OneArm (white bars). The data are shown as a fold-difference to the negative control, which is the amount of virus captured by the b12 antibody with no pre-incubation of the virus with Grft.

The present work and other investigators have shown that HIV strains lacking glycan sites at N234 and N295 on gp120 are less sensitive to Grft [39]. Therefore, we explored whether HIV strains lacking these glycan sites affect the ability of Grft to mediate CD4 binding site exposure on gp120. Experiments were carried out with several strains from both subtype B and subtype C. As shown in Figure 3-9, it appears that the lack of the glycosylation site at position N-234 of gp120 does not markedly affect the ability of Grft to mediate CD4 exposure. However, in HIV-1 strains lacking the glycosylation site at position 295, the ability of Grft to mediate CD4 binding site exposure in gp120 was greatly reduced: in three separate strains (Du156.12, DU422.1 and ZM53M.PB12), wild-type Grft showed little or no ability to expose the CD4 binding site. In HIV strains lacking both the N234 and N295 glycosylation sites (ZM109F.PB4, ZM135M.PL10a), Grft was unable to significantly mediate the exposure of the CD4 binding site in gp120, even at the highest concentration of Grft used (80nM, data not shown). In each viral strain, Grft-linker-Grft One-Arm was only able to induce very low (if any) CD4 binding site exposure in gp120 above the control (Figure 3-9).

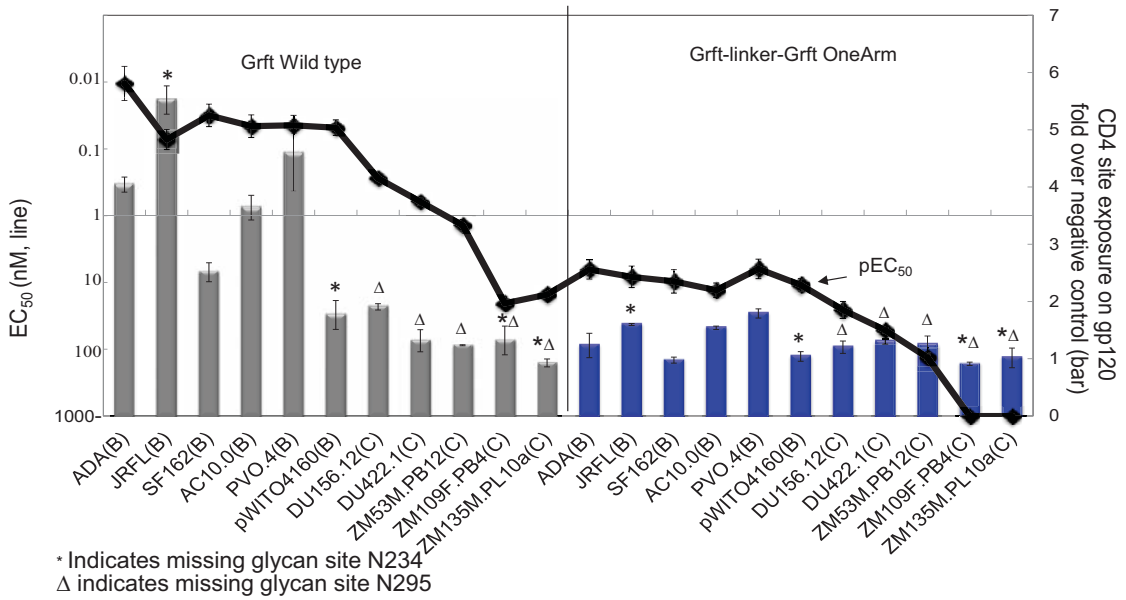

Figure 3-10: Correlation of antiviral activities of Grft dimer variants to the level of CD4 binding site exposure induced by Grft.

Correlation of the antiviral EC_{50} of wild-type Grft and Grft-linker-Grft OneArm (line) to the level of gp120 CD4 binding site exposure that is induced by Grft (grey bars; fold over negative control) or Grft-linker-Grft OneArm (blue bars; fold over negative control). The EC_{50} value is plotted on a log scale. For strains have high mannose glycans N234 and N295, Grft exhibit potent antiviral activity as well as induces high CD4 binding site exposure; for strains lacking these two sites, Grft have very low activity and could not induce CD4 binding site exposure, indicating no or little conformational change on gp120.

Anti-HIV assays were carried out with single round virus from each of these strains to determine whether there is a correlation between the ability of Grft to induce CD4 binding site exposure and Grft antiviral potency. Figure 3-10 shows that in each case where CD4 exposure is relatively high (i.e. more than about 2.5-fold higher than the control), Grft was very potent (EC_{50} of 0.07nM or lower). In cases where the Grft-mediated CD4 binding site exposure was low (less than 2-fold above the control), the antiviral potency of Grft was also lower, exhibiting a marked loss of potency compared to the average potency of the "high CD4-exposure" HIV-1 strains. This was particularly true for HIV-1 strains lacking both glycosylation sites at N234 and N295, which showed the least sensitivity to Grft. However, one notable exception was the clade B strain pWITO4160, which was highly sensitive to Grft (EC_{50}=0.048 nM) but showed only a small amount of CD4 binding site exposure (Figure 3-10). In all cases, as a rule, Grft-linker-Grft OneArm showed a very low ability to mediate CD4 exposure

(as previously described) and also showed reduced antiviral potency, being 84- to 609-fold worse than the wild-type inhibitor (Table 3-2).

3.4.5 The effect of Grft on gp120 shedding.

It has been reported that soluble CD4 induces dissociation of gp120 from HIV viral particles and that this CD4-induced env shedding may impair the functional trimeric spike [169], though the exact role of CD4-induced shedding during viral entry is not clear [170, 171]. Broadly neutralizing antibodies have also been reported to have different effects on gp120 shedding [162, 172, 173]. Here, Western Blot analysis was carried out on supernatants of cells transfected with HIV-1 gp120 from both clade B and clade C and incubated with Grft variants. Figure 4 shows that the sCD4 control is able to induce shedding from the surface of each strain, as expected. For clade B strains (JRFL and PVO.4), Grft also induces shedding. The subtype B strain JRFL lacks a high-mannose glycan site at N234, but still shows high amounts of shedding in the presence of Grft. The obligate dimer Grft-linker-Grft also induces *env* shedding from the cell surface (Appendix Figure B-8) on strains JRFL (subtype B), PVO.4 (subtype B), ZM53M.PB12 (subtype C) and ZM109F.PB4 (subtype C). Grft-linker-Grft OneArm generally had less effect on shedding, particularly for the PVO.4 strain, despite using concentrations for the One-Armed dimer that are 10-fold higher than for wild-type Grft to account for differences in the ability to bind virus. For clade C strains (ZM53M.PB12, ZM109F.PB4), Grft itself induces less shedding compared to soluble CD4, while the One-Armed dimer is even less effective at mediating gp120 shedding (Figure 3-11).

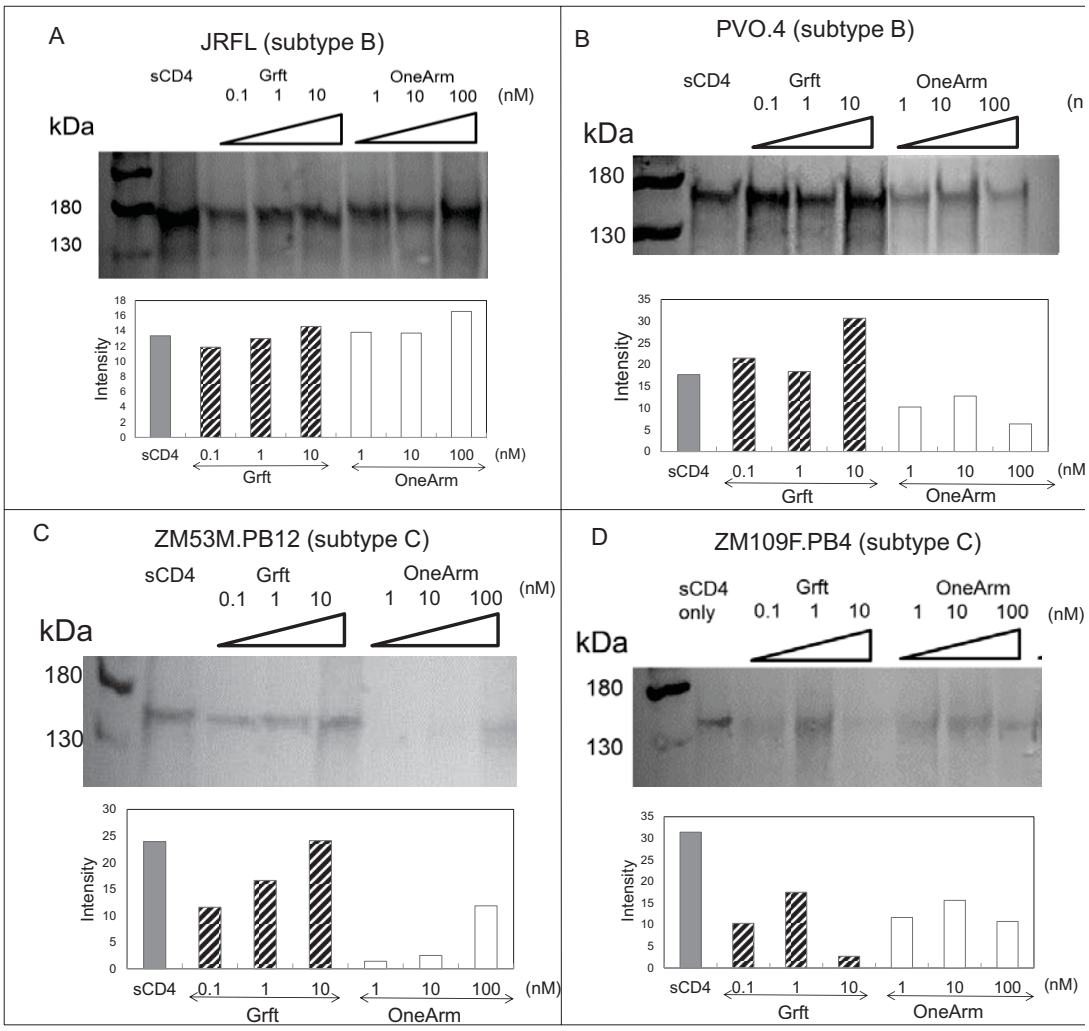

Figure 3-11: Shedding of env from HIV transfected cells for JRFL (subtype B), PVO.4 (subtype B), ZM53M.PB12 (subtype C) and ZM109F.PB4 (subtype C).

Left lane is the molecular weight ladder. sCD4 (25ug/ml) was incubated with transfected 293FT cells (Lane 2) and used as a positive control. Different concentrations of wild-type Grft (0.1nM, 1nM, 10nM) or Grft-linker-Grft OneArm (1nM, 10nM, 100nM) were incubated with env-transfected 293FT cells. Bottom of each panel: Intensity of bands as shown by densitometry, calculated from the program ImageJ [9].

3.4.6 WT Grft and the obligate dimer are able to cross-link two separate gp120 subunits

Our results that the Grft dimer is able to manipulate the conformation of gp120 suggest that the dimer binds to two different glycosylation sites on gp120. But the question arises whether Grft binds two sites on one gp120 subunit or rather is able to crosslink two different gp120 subunits. We tested the ability of Grft to crosslink gp120 using ELISA assay. To test this, streptavidin were used to coat 96-well plate, followed by a BSA block and application of biotin-conjugated gp120s from strains III_B or ADA. Different concentrations of Grft were then added into each well. After incubation and washing, HRP-conjugated gp120s from corresponding III_B or ADA strains were added into plates, substrates were then added to develop signals. If Grft is able to cross-link two separate gp120s, then the HRP conjugated gp120 would remain on the plate and provide signal. This assay showed that Grft and the obligate dimer Grft-linker-Grft are able to cross-link two gp120 subunits, but the One-Armed dimer is not (Figure 3-12, top panel). The data suggest that Grft cross-linking is possibly also a mechanism involved in Grft function, and that the One-Armed Grft is not able to cross-link gp120, which correlates with its poor ability to inhibit HIV.

We also tested other carbohydrate binding lectins or small molecules obtained from the Prof. Jan Balzarini group. Hippeastrum hybrid agglutinin (HHA) is a plant lectin predominantly recognizing α(1,3) or α(1,6)Mannose on gp120 [174]. It has been reported to be composed of four subunits (tetramer). Each subunit is 12.5 kDa and contains one carbohydrate binding site [175]. Urtica dioica agglutinin (UDA) is a monomeric protein lectin of 89 amino acids. It has two carbohydrate binding sites, one with high affinity and the other with low affinity (dissociation constant in uM and mM range). Pradimicin-S (PRM-S) is a non-peptidic antibiotic which binds carbohydrates on gp120 and also inhibits HIV entry. Figure 3-12 shows that both HHA and UDA are able to cross-link two separate gp120 subunits, probably due to multiple carbohydrate binding sites, although the tetramer cross links at much lower concentration. Higher concentration of UDA also showed higher signal to cross-link gp120, and this concentration is close to the Kd of the lower carbohydrate binding site, suggesting that UDA could use both carbohydrate binding sites to binds two gp120 at the same time. PRM-S (one putative binding site) is not able to cross-link gp120 subunits, even at the highest concentration we tested (526000 nM). The ability of these lectins to cross link may correlate with their ability to inhibit HIV, although direct proof of cross-linking in their mechanism of action is not able to be obtained with this experiment.

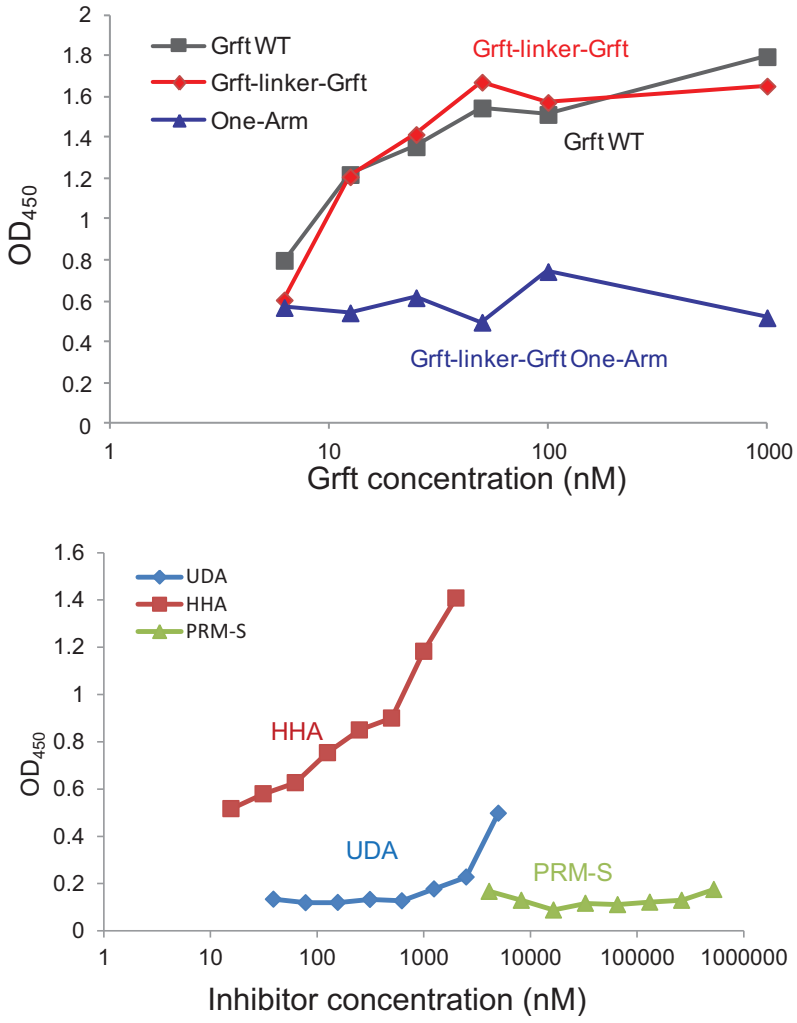

Figure 3-12: ELISA showing Grft and other lectins cross-link two separate gp120 subunits.

Top: Preliminary data showing the ability of WT Grft (Black), obligate dimer Grft-linker-Grft (red) and one-armed Grft variant Grft-linker-GrftOneArm (blue) to bind two gp120 subunits. Controls with no Grft, no beads, or no second gp120 subunit showed negative-control levels of signal (data not shown).

Bottom: Plant lectins HHA (a tetramer), UDA (a monomer with two carbohydrate binding sites) are able to cross-link two separate gp120 subunits, while the single site non-peptide antibiotic PRM-S is not.

Both gp120 subunits are from strain III_B. Signal in this experiment is provided by horseradish peroxidase-conjugated gp120 III_B. A similar ELISA assay with the ADA strain also showed similar result as these III_B strain.

3.5 Discussion

Griffithsin (Grft) is a lectin with broad activity against a variety of viruses, including HIV, hepatitis C virus, the SARS Coronavirus, Japanese encephalitis virus, and herpes simplex virus [48-50, 142]. Grft binds high-mannose structures on viral envelope surfaces, such as HIV gp120. Structural work [1] and biochemical studies [55] confirm that the protein is a tight dimer, with each subunit containing three mannose binding sites that are critical for function. A monomeric variant of Grft was shown to be unable to effectively inhibit HIV, underscoring the importance of the dimer form [97]. Its high antiviral activity against HIV in particular makes Grft a highly promising candidate for a microbicide, which could be used to prevent the sexual spread of the virus. The present work elucidates an important component of the mechanism of Grft, namely that its mode of inhibition of HIV is not simply based on its ability to bind gp120, but that it also requires two functional dimer subunits.

Investigations have been carried out on other carbohydrate-binding HIV inhibitors. The prokaryotic lectin cyanovirin-N has two carbohydrate binding sites per monomer and has been observed as both a dimer and a monomer, both of which are apparently very potent [176, 177]. At least two carbohydrate binding sites are necessary for activity because mutated monomers having only one CBS are not functional unless two defective monomers are cross-linked (containing in total two functional CBS) [86]. Moreover, the covalent linking of the two functional monomers of cyanovirin (giving 4 CBS) also led to a moderately increased potency over the wild-type protein although higher order oligomers apparently did not result in an increased potency [85]. The neutralizing antibody 2G12 binds high-mannose carbohydrates on gp120 [160, 161, 178, 179] and has an unusual domain swapped structure that has a shorter distance between the two primary binding sites (35 Å compared to 150 Å for a typical IgG antibody) and which leads to 2 additional potential CBS [84, 180]. Dimeric and polymeric 2G12 has also been reported to be more effective in neutralizing HIV [87, 181, 182]. The distance between CBS may be important in optimal HIV inhibition because the apparent ideal distance between 2 CBS involved in cyanovirin appears to be around 40 Å [86], the 2G12 primary binding sites are 35 Å apart, and the X-ray structure of Grft shows about a 47 Å distance between the two carbohydrate binding arms [1]. Therefore, effective HIV inhibition appears in these cases to arise from multisite carbohydrate binding of defined (around 40 Å) distance, though these various proteins (which do tend to effectively compete with each other [39, 93, 160, 183]) may not always bind at the same high-mannose glycan sites.

Mechanistically, three major types of action could be envisioned for Grft function against HIV: First, tight binding to the surface of gp120 could sterically impede gp120 from binding the host cell by blocking key interactions with CD4

and/or the co-receptor. This could occur with Grft binding at various locations on gp120, with some mannose-containing glycan sites being more important than others. Avidity gained from multisite binding could be an important factor in this. Second, Grft could alter the conformation of gp120 so that gp120 is less effective at mediating entry by the virus. The conformational change could affect CD4 binding, co-receptor binding, or some other entry processes. Finally, Grft could potentially crosslink two different gp120 subunits by binding a glycan unit on each subunit. Gp120 is a trimer, so this could conceivably occur with two separate trimer spikes (less likely) or with two different gp120 monomers within a single trimer. It is likely that more than one of these mechanisms concomitantly occurs with Grft inhibition. For example, a mechanism involving a structural change in gp120 and/or cross-linking of individual gp120 molecules may be a major inhibitory mechanism and can occur with binding at particular glycan sites, while Grft could sometimes simply block other necessary interactions when it is bound at other mannose glycan sites. The relative importance of each mechanism for inhibition may depend on the viral strain and its individual glycosylation pattern.

In the present work, we have examined the role of the Grft dimer in HIV inhibition by making an obligate dimer, Grft-linker-Grft and a one-armed obligate dimer, Grft-linker-Grft OneArm (with one functional subunit and one subunit having all three mannose-binding sites mutated). These were tested for various aspects of function, including the ability to bind gp120, to inhibit HIV, and to afford a structural change in gp120. It was found that the obligate dimer Grft-linker-Grft very much resembled the wild-type protein both in structure and in function, indicating that, as expected, native Grft likely acts as a dimer. However, while Grft-linker-Grft OneArm was minimally reduced in ability to bind gp120, this Grft variant showed a dramatic reduction in inhibitory functions both in single-round and replication competent viral assays. While quantitative testing of Grft binding to gp120 is presented here with two strains (either from X4 and R5 origin), other work (unpublished) shows similar binding constants to gp120 from at least one other HIV-1 strain. Given that Grft binds to surface high-mannose glycans and that all known HIV-1 strains contain between 18 and 33 potential N-glycosylation sites, it is reasonable to expect that high binding affinity would be observed between Grft and most HIV-1 strains. In fact, only a few well-defined N-glycan locations on HIV-1 gp120 (viz. N234, N295 and N448) have been identified to result in a marked decrease of antiviral activity of Grft when deleted (absent) from the viral envelope [39] [38].

Our results demonstrate that both subunits of the Grft dimer are critical for its optimal anti-HIV function, but not for gp120 binding, suggesting that inhibition is not simply a “bind and block” phenomenon. Enhanced inhibition due to multisite binding can often be explained by the avidity effect of the inhibitor [84, 85]. This is generally due to the increased on-rate of the second (later) site after binding at the first site that leads to overall better binding and less dissociation of

the lectin from the virus [85]. The present results are consistent with a contribution of avidity to the eventual effectiveness of Grft. Specifically, the One-Armed obligate dimer has 3 fewer CBS and much lower HIV neutralization capability. However, the on-rate for the One-Armed dimer to gp120 is only 2- to 4-fold lower than the wild-type or the obligate dimer in SPR studies with gp120 (Table 3-1).

In addition to avidity effects, Grft might have additional functions which involve altering the conformation of gp120 to decrease viral entry ability. Grft may require two sites of (glycan) binding to affect the structure of gp120, in such a way enforcing a conformation that is somehow not competent to facilitate HIV entry to the host cell. To probe this possibility, we examined several possible structural conversions in gp120 and the effect of Grft on these. When initiating infection, gp120 first binds CD4 at a site that seems not to be fully accessible until CD4 is present; broadly neutralizing antibodies have different effects altering the gp120 conformation [26, 89], and it was recently shown that the presence of Grft allows a higher level of virus capture at the CD4 binding site [143]. In our experiments, we show that Grft indeed affords higher levels of virus capture by the b12 antibody that binds gp120 at its CD4 binding site, while Grft-linker-Grft OneArm only mediates viral capture at the level of the negative control (Figure 3-9). In virtually every viral strain tested, Grft's ability to cause CD4 binding site exposure is strongly correlated with antiviral function. This indicates a correlation between the ability to manipulate the structure of gp120 and the anti-HIV activity of the protein, and implicates both arms of the dimer as being necessary for these functions. While this does not prove that mediating a conformational change in gp120 plays a role in Grft inhibition, the data are consistent with the possibility of such a role for Grft in addition to high affinity binding. Further experiments in this regard should clarify this issue.

The exposure of the CD4 binding site on gp120 is obviously important in productive infection by HIV, but given Grft's role as an inhibitor, it is clear that the exposure of the CD4 binding site by Grft either does not facilitate actual CD4 binding or that Grft somehow blocks entry after this step. It is also possible that this "exposure" is just part of a larger, overall conformational change to interfere with viral entry in a manner that is not yet known. Interestingly, different effects were observed for different HIV strains in the CD4 exposure experiments. In general, Grft showed higher levels of CD4 exposure in gp120 strains that retained glycosylation sites at positions N234 and N295, and lower levels of CD4 exposure relative to the negative control in gp120 for strains that lacked glycosylation at N295 or at both N234 and N295. There was also a consistent correlation with the ability to mediate CD4 binding site exposure and the inhibition potency of Grft, with only one exception (clade B strain pWITO4160). In all cases, the OneArmed dimer of Grft was largely unable to mediate exposure of the CD4 binding site and was also as much as 600-fold less potent in HIV

inhibition. Therefore, it seems reasonable that this conformational change of gp120 may be related, at least in part, to Grft function.

An important question regarding an inhibitor that requires two arms for function is whether the inhibitor is actually cross-linking two different gp120 subunits. Gp120 is a trimer on the surface of the virus, and the distance between the two arms of Grft (about 47 Å) could allow binding to putative glycosylation sites on two different gp120 monomers in the trimer [1, 89, 184]. The role and importance of gp120 shedding in infection efficiency has not been defined, although shedding can occur as part of the conformational change in gp120 [170, 185, 186]. Some HIV inhibitors apparently impair gp120 shedding and increase gp41 exposure, while other work indicates that CD4-induced shedding of gp120 does not correlate with subsequent membrane fusion [170, 171]. The broadly neutralizing antibody b12 was shown to increase viral shedding (although there is some disagreement) while the recently discovered broadly neutralizing antibody VRC01 could not induce gp120 shedding [162, 173].

While it is not known whether an effect on gp120 shedding itself is a mechanism of drug inhibition, such a function could provide data regarding the ability of Grft to affect the gp120 conformation. We have measured the amount of gp120 that has been shed in the presence or absence of Grft (and CD4 which does induce shedding) using Western blots [144, 187]. The results show that Grft in general does induce gp120 shedding while the One-Armed Grft dimer appears to be reduced in this ability, indicating that two arms of the dimer are more effective in causing shedding, and suggesting that multisite binding or crosslinking by Grft may play a role in gp120 shedding. However, different effects were observed for different HIV strains suggesting that Grft-induced env shedding may correlate with different glycan patterns on the viral surface.

Our findings that Grft is a highly active anti-HIV agent that inhibits infection of susceptible target cells by a broad variety of X4 and R5 HIV-1 strains, blocks syncytia formation between virus-infected and non-infected cells, prevents capture of virus particles by DC-SIGN-expressing cells and blocks the subsequent transmission of such captured virus to $CD4^+$ T-lymphocytes makes it a prime candidate drug for microbicide development [55]. In addition, it has an outstanding safety profile as a potential microbicide [52]. Indeed, recently, griffithsin has been proposed as the first antiretroviral drug in non-clinical use to be included in a microbicide trial for women living with HIV. This protein has been expressed in tobacco plants using transgenic plant technology, and it has been calculated that an environmentally controlled greenhouse producing 3,000 kg of leaf tissue per acre could yield > 2 million doses per year, making the use of such candidate microbicide a realistic tool (Hiller, Presentation at the Forum for Collaborative HIV Research meeting on Future of PrEP and Microbicides, Washington DC, 7 January 2013) [139]. It is therefore important to understand the mechanism of action of this lectin, both to further its development and to understand the properties that lead to the most valuable inhibitors. The

combination of tight binding properties to gp120 and the use of multiple subunits to mediate inhibitory changes in gp120 by griffithsin may be used by other lectins or broadly neutralizing antibodies, and may also be a desirable property to design future HIV inhibitors.

3.6 Conclusion

This work provides evidence that both arms of the Grft dimer are necessary for its optimal anti-HIV function and that, in addition to allowing an increase in avidity, their role may be to manipulate the structure of gp120, thereby inhibiting the process of viral entry (possibly by binding at two different carbohydrate sites). Grft inhibition correlates with glycan patterns on the viral surface, and with its ability to mediate CD4 binding site exposure in gp120. This work helps to explain previously reported results that HIV strains lacking glycosylation at both positions N234 and N295 are less sensitive to Grft [39]. While the clade B strains (that are prevalent in North America and Western Europe) tend to retain both these sites, clade C strains (which are prevalent in Africa and Asia [41, 157]) tend to lack the glycosylation site at position N295. There may also be a relationship between Grft-mediated env shedding and viral inhibition. Our results have implications for the development of Grft as a microbicide.

Chapter 4

A Comparison of 5P12-vMIP-II and vMIP-II as HIV-1 Entry Inhibitors

This work was published as part of:

Xue J, Kuo NW, Schill MS, LiWang PJ, “A comparison of 5P12-vMIP-II and vMIP-II as HIV-1 entry inhibitors”, Journal of Biochemistry&Physiology, 2013, S2-005: 2168-9652.

4.1 Abstract

vMIP-II (viral macrophage inflammatory protein-II) is a chemokine analog expressed by human herpesvirus-8 that has the unique ability to bind multiple human chemokine receptors, including CCR5 and CXCR4, representative receptors of two major chemokine subfamilies. This broad binding ability gives vMIP-II powerful anti-inflammatory properties, which have been demonstrated in vitro and in vivo. In addition, vMIP-II is of great interest due to its ability to inhibit HIV infection by both major HIV strains: R5 (strains that enter the host cell using CCR5 as a co-receptor), and X4 (strains that use CXCR4). We have made a vMIP-II variant, “5P12-vMIP-II” in which the N-terminal amino acids of vMIP-II have been replaced by 10 amino acids that have been shown to greatly enhance the anti-HIV potency of the chemokine RANTES for R5 HIV strains. This 5P12-vMIP-II is shown by NMR to be fully folded and similar in structure to wild type vMIP-II. Both vMIP-II and 5P12-vMIP-II showed the ability to inhibit multiple strains of HIV, including several R5 strains and an X4 strain. While the 5P12 N-terminus did not improve the potency of the protein, our results suggest that vMIP-II does not bind CCR5 in the same way as human chemokines. Rather, vMIP-II has sacrificed some binding ability to particular chemokine receptors in order to obtain the ability to bind a broader array of receptors.

4.2 Introduction:

Chemokines (chemotactic cytokines) are small proteins that mediate chemotaxis and activation of immune system cells, with importance both in immune development and inflammation. In addition, some chemokine receptors have been shown to be “co-receptors” for HIV-1 (human immunodeficiency virus type 1) entry, making the chemokine system relevant for both its role in human health and in disease. The protein vMIP-II (viral Macrophage Inflammatory Protein-II) is a chemokine analog produced by human herpesvirus 8 (HHV-8) that has high sequence identity to many chemokines as well as nearly identical tertiary structure [10, 72, 73]. However, this protein is unique among chemokines in its ability to bind but not activate receptors of chemokines from multiple sub-families, including the receptors CCR5, CXCR4, CCR1, and CCR2 [74]. These properties allow vMIP-II to effectively compete with the natural chemokine ligands of these receptors, including MCP-1 (monocyte chemoattractant protein-1), MIP-1α (macrophage inflammatory protein-1 alpha) and RANTES (regulated on activation normal T cell expressed and secreted), and have elicited interest in vMIP-II both as an anti-inflammatory agent and for its ability to inhibit HIV [75]. This 71 amino acid protein is also an agonist (having the ability to bind and to cause an intracellular response) for the receptor CCR3 [74, 76, 77].

Regarding its role in inflammation, vMIP-II has shown significant promise as an anti-inflammatory agent in animal models, including prolonging cardiac and corneal allograft survival [188, 189]. vMIP-II also effectively reduced damage and neurological deficit in a spinal cord injury model [190-192] and could be safely injected into the mouse brain in order to attenuate inflammation and thereby reduce injury from cerebral ischemia [193].

The process of HIV infection begins with the interaction of HIV surface protein gp120 with human cell surface protein CD4 (Figure 4-1A). This interaction allows conformational change in gp120, leading to the binding by gp120 of the co-receptor on the cell surface, CCR5 or CXCR4. These co-receptors are chemokine receptors that normally play a role in immune activation and cell chemotaxis. The role of vMIP-II as an anti-HIV agent is based upon its unique ability to act as an antagonist of both chemokine receptors CCR5 and CXCR4 [74, 75] (Figure 4-1B). Human chemokines, by contrast, are able to bind only receptors from one sub-class, so that MIP-1α, MIP-1β, and RANTES (also called CCL3, CCL4, CCL5 respectively) tightly bind the CCR5 receptor (and are able to inhibit infection with HIV strains that use this receptor), but have no effect on the CXCR4 receptor [58, 194, 195]. This receptor is bound by the natural ligand SDF-1 (CXCL-12), which in turn has no ability to bind CCR5 [196, 197].

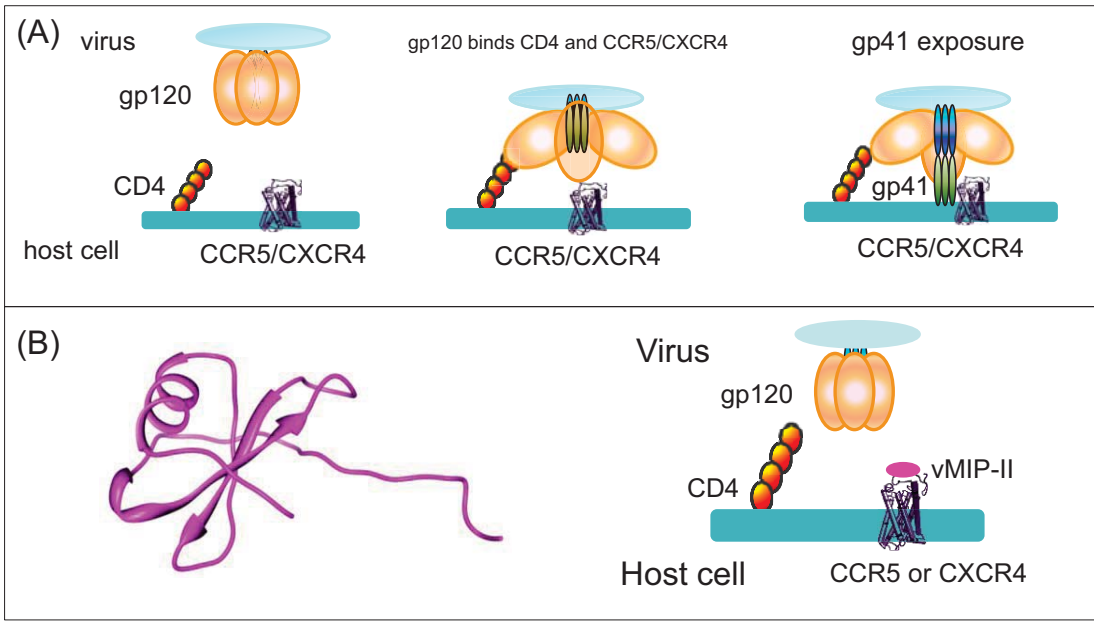

Figure 4-1: vMIP-II binds CCR5 or CXCR4 and inhibits HIV entry.

(A) Left: HIV entry process. On the HIV surface, the envelope protein gp120 (gold) interacts with receptor CD4 (orange) and coreceptor CCR5 or CXCR4 (purple) on the host cell surface. Middle: When viral gp120 binds to the receptor CD4 and coreceptor (CCR5 or CXCR4; purple, 7-transmembrane helix), gp120 undergoes a conformational change and exposes gp41 (cyan and green). When gp41 is exposed, the N-terminus and C-terminus of gp41 form a 6-helix bundle, assisting fusion with the host cell membrane. (B) Left: Solution structure of vMIP-II as determined by NMR spectroscopy (magenta ribbon). Right: vMIP-II (magenta) binds to HIV coreceptor CCR5 or CXCR4 (purple) and blocks HIV entry. The structure was made with the program Chimera [5] using PDB structure 1VMP [14].

Chemokine variants have been developed that are among the most potent HIV entry inhibitors known, with much of the work having been done on the chemokine RANTES. In particular, chemical synthesis at the N-terminus of the protein has allowed the potent RANTES variants AOP-RANTES and PSC-RANTES to be developed, revealing nanomolar activity in *in vitro* [66, 198] and, for PSC-RANTES, effectiveness in protection from HIV in the macaque *in vivo* [199-201]. N-terminal modification of the chemokine has been shown to be transferrable, as AOP-MIP-1α was produced and also shown to be a potent HIV inhibitor [202].

The chemokine variant that currently has the highest potential for clinical use is undoubtedly 5P12-RANTES. This protein was obtained by random mutagenesis at the N-terminus of RANTES, replacing the wild type 9 amino acids

with an N-terminus containing 10 amino acids. There are no further synthetic additions, so this protein can be made by recombinant techniques [68]. In addition to being highly potent (with antiviral activity in the sub-nanomolar range for most strains tested), this protein neither activates nor internalizes the CCR5 receptor, alleviating concerns about immune activation, which is not desirable in the context of HIV inhibition [68]. Later work also demonstrated that viral escape from 5P12-RANTES is extremely difficult, unlike many small molecule inhibitors [203], solidifying the position of 5P12-RANTES as a potential therapeutic that could be expected to remain potent despite a large variation in viral sequence. However, despite the nearly uniform positive properties of 5P12-RANTES, one drawback is its inability to bind the CXCR4 co-receptor, leading to inactivity against HIV viral strains that use this receptor (so-called X4 HIV strains).

Here in Chapter 4 I collaborate with Dr. Naiwei Kuo in our lab and study a vMIP-II variant, 5P12-vMIP-II. We hypothesized that the ability of vMIP-II to inhibit HIV could be enhanced by replacing its native N-terminus with the 5P12 N-terminus that was successfully used for RANTES. This region of the protein is largely unstructured until it binds the receptor, and as mentioned vMIP-II shares significant sequence identity and structural properties with RANTES, MIP-1β, and MIP-1α [14, 204-206]. There is also the possibility with this mutation to obtain dual-acting HIV entry inhibitors that would be effective against both R5 and X4 strains of HIV. In addition, such work could add to our understanding of the manner in which vMIP-II is able to bind chemokine receptors. Our results show that while 5P12-vMIP-II retained activity against both R5 and X4 HIV strains, the activity was not improved by the 5P12 N-terminus compared to the wild type N-terminus. This result suggests that vMIP-II does not bind the chemokine receptor in the same manner as wild type chemokines, a possibility that has been previously suggested [10, 207].

4.3 Materials and Methods

4.3.1 Construction of 5P12-vMIP-II

The gene for vMIP-II was constructed and cloned into pET32a(+) as described [10]. 5P12-vMIP-II was made by replacing the first ten amino acid of vMIP-II (protein sequence: LGASWHRPDK) with the first ten amino acids of 5P12-RANTES (protein sequence: QGPPLMATQS). The replacement was carried out using oligonucleotide primers and PCR to replace the sequence coding for the N-terminal amino acids.

4.3.2 Protein Production

vMIP-II and 5P12-vMIP-II were expressed in the pET32a(+) vector with a thioredoxin fusion tag (Novagen, Madison, WI). The plasmids were transformed into *Escherichia coli* BL21(DE3) (Novagen, Madison, WI) cell and expressed in ^{15}N minimal medium using $^{15}NH_4Cl$ as the sole nitrogen source. The protein induction was carried out with 1 mM IPTG (Isopropyl β-D-1-thiogalactopyranoside) as final concentration when the $O.D._{600}$ reached 0.6-0.8 at 37 °C. The minimal medium was then shifted to 16 °C and shaking continued for 16 hours. The cells were harvested by centrifugation at 6000 ×*g* for 10 min. The cell pellet was resuspended in 50 mM Tris, 50 mM NaCl, 3 mM EDTA, 5 M Guanidinium/HCl, pH 8 with fresh 10 mM benzamidine and then passed through a French Press twice at 16,000 psi. β-mercaptoethanol was then added to a final concentration of 5 mM, and the resulting solution was incubated at room temperature with stirring for 1 hour. Then, the solution was centrifuged at 20,000 × g for 1 hour. The supernatant containing the denatured protein was added dropwise to 10x volume of low salt buffer (50 mM Tris, 50 mM NaCl, pH8) with fresh 5 mM β-mercaptoethanol and stirring. Then, the solution was incubated at room temperature without stirring for 2 hours. The solution was then centrifuged at 20,000 × g for 30 min and the supernatant was dialyzed against 4L high salt buffer (20 mM Tris, 500 mM NaCl, 5 mM Imidazole, pH 8) twice overnight at 4 °C. After dialysis, the solution was applied to a Nickel chelating column and eluted with a gradient of imidazole (50 mM to 500 mM). The resulting purified protein was dialyzed against 4 L 20 mM Tris, 50 mM NaCl, 2 mM $CaCl_2$, pH 7.4 overnight at 4 °C. The solution was made to 0.02% NaN_3 to inhibit bacterial growth. To remove the thioredoxin fusion tag, 10 units of recombinant enterokinase (Novagen, Madison, WI) were added. The solution was incubated at room temperature for 3-5 days to allow protease cleavage. Precipitated material was removed by adjusting the solution to contain 10% acetonitrile and 0.1% trifluoroacetic acid followed by centrifugation at 15,000 × g for 30 min. The supernatant was purified by a C4 reversed-phase chromatography column (Vydac, Hesperia, CA) using the Akta purification system (GE Healthcare, Pittsburgh, PA). The protein was dried to powder using the Labconco freeze dry system (Labconco Corporation, Kansas City, MO).

4.3.3 Nuclear Magnetic Resonance

All NMR samples were prepared in a buffer of 20 mM potassium phosphate, 10 μM DSS, 5% D_2O, and 0.02% NaN_3 at pH 5.5 or pH 7. All 2D HSQC experiments were carried out on a Bruker 600 MHz AVANCE III spectrometer equipped with a TCI cryoprobe at 25 ° C. HSQC experiments were run with carrier positions of 4.75 ppm for ^{1}H and 119.3 ppm for ^{15}N, sweep widths of 9615.385 Hz (15.9 ppm) for ^{1}H and 1938.672 Hz (31.8) ppm for ^{15}N with 672* (* complex points) points in ^{1}H and 128* points in ^{15}N. All chemical shifts were referenced to internal DSS (2,2-dimethyl-2-silapentane-5-sulfonic acid). Data were processed using NMRPipe and viewed using NMRDraw and PIPP [115, 116] and Sparky [117]. The chemical shift changes compared to wild type protein were calculated as described previously [10].

4.3.4 Viral reagents

Viral plasmids containing the *env* gene from HIV-1 were obtained from the NIH AIDS Research and Reference Reagent Program, Division of AIDS, NIAID, NIH as follows: PVO, clone 4 (SVPB11), AC10.0, clone 29 (SVPB13) was from Dr. David Montefiori, Dr. Feng Gao and Dr. Ming Li [155]; pWITO4160 clone 33 (SVPB18) was from Drs. B. H. Hahn and J. F. Salazar-Gonzalez [155]; DU156.12 (SVPC3) was from Drs. D. Montefiori, F. Gao, S. Abdool Karim and G. Ramjee [41, 156]; CAP210.2.00.E8 (SVPC17) was from Drs. L. Morris, K. Mlisana and D. Montefiori [156]; ZM109F.PB4 (SVPC13) was from Drs. E. Hunter and C. Derdeyn [157]; pHxB2-env was from Dr. Kathleen Page and Dr. Dan Littman [208]; pSG3Δenv was from Drs. John C. Kappes and Xiaoyun Wu [158, 159].

4.3.5 Single-round HIV infection assay

Single-round infection assays were performed as described [55]. Briefly, TZM-bl cells stably expressing CD4, CCR5 and CXCR4 coreceptors were maintained in DMEM (Dulbecco's Modified Eagle's Medium) with 10% FBS (fetal bovine serum). The cells were seeded in 96-well plate and serial dilutions of vMIP-II, 5P12-vMIP-II and 5P12-RANTES were added from the top row to the bottom row, as follows: 20 ul ligand of different concentration was added into the first row and mixed well with culture media. Then 20 ul media was removed and added into the second row, and so on. Virus was then added into each well containing different ligands. The cells were incubated at 37° C for 24 hours, at which time the medium was changed, and the cells were then incubated for another 24 hours. PBS containing 0.5% NP-40 was used to lyse the cells and substrate chlorophenol red-D-galactopyranoside (CPRG, Calbiochem, CA) was added into each well. The absorbance signal was measured at 570 nm and 630 nm. The ratio of 570/630 for each well was calculated. EC_{50} values were determined using a linear equation fitted between two data points surrounding 50% inhibition. For presentation purposes, data shown in the figures were plotted and

fitted as curves using a four-parameter logistic equation in Kaleidagraph (Synergy Software, Reading, PA).

4.4 Results

4.4.1 Construction and structure of 5P12-vMIP-II.

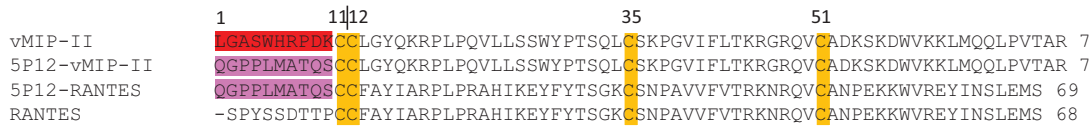

Figure 4-2: Sequence comparison of vMIP-II, 5P12-vMIP-II, 5P12-RANTES and RANTES.

Conserved cysteine residues are highlighted in yellow. The first ten residues in the N-terminus of vMIP-II are highlighted in red. The first ten residues in the N-terminus of 5P12-vMIP-II are highlighted in magenta. The sequence number is according to vMIP-II.

The “5P12” chemokine N-terminus consists of a 10 amino acid sequence directly before the conserved Cys-Cys of the chemokine: QGPPLMATQS (Figure 4-2). Thermocycling techniques with overlapping oligonucleotide primers were used to replace the existing N-terminus of vMIP-II with DNA encoding these amino acids. The gene was placed into a pET32a(+) expression vector with an N-terminal thioredoxin fusion tag, and the protein was produced and purified as described in Methods. Figure 3 shows the ^{15}N-^{1}H correlation spectra of ^{15}N-labeled 5P12-vMIP-II. At pH 7, the protein showed good chemical shift dispersion and homogeneous peak height, indicating a nicely behaved protein that is not likely experiencing multiple conformations (Figure 4-3A). Chemical shift assignments of wild type vMIP-II have been carried out at pH 2.5 [14] and pH 5.4 [10], so spectra were also obtained of 5P12-vMIP-II at pH 5.5, and a comparison is shown in Figure 4-3B. The assignments were adapted from Zhao et al. [10]. 5P12-vMIP-II showed similarity to the wild type protein in most regions of the spectrum, but the spectrum contains no matching peaks for the N-terminal residues, as expected. However, seven new peaks could be observed in the 5P12-vMIP-II spectrum (red) that were not close to any assigned peaks from the wild type vMIP-II spectrum (black). These likely correspond to the 7 non-Pro amino acids that are different between the variant and wild type vMIP-II (Figure 4-2 and Figure 4-3B). Moreover, peaks in the variant spectrum near the resonances in the wild type spectrum for G2, Q33, and K37 could be observed when the contour level is lowered indicating that these are likely the analogous resonances of the variant (data not shown). Finally, the 5P12 variant contains two additional glutamines, Q1 and Q9; in the HSQC spectrum two additional pairs of side-chain peaks are observed, indicating the presence of Q1 and Q9 in 5P12-vMIP-II. Therefore, the HQSC spectrum is fully consistent with a folded 5P12-vMIP-II.

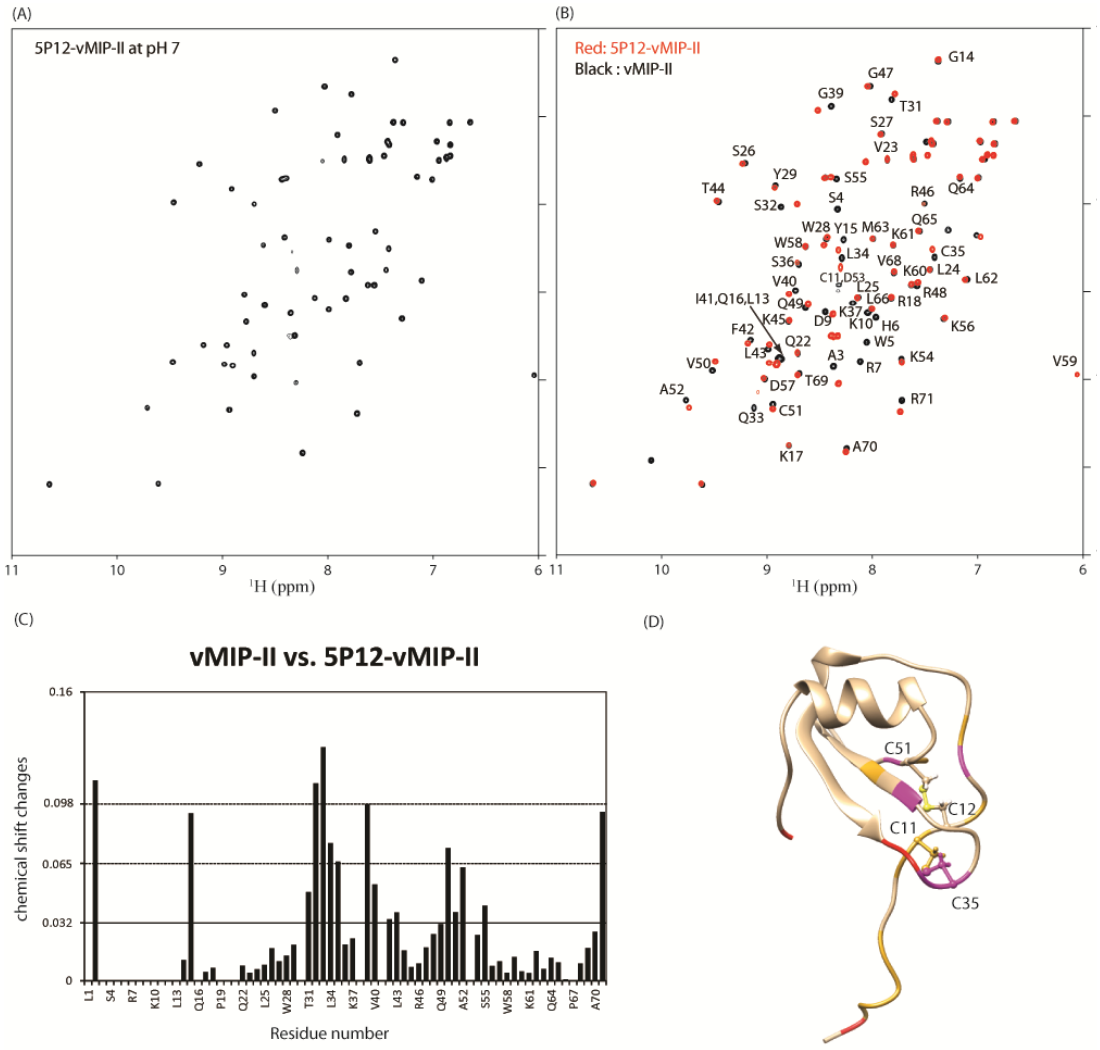

Figure 4-3: Structure study of 5P12-vMIP-II.

(A) ^{15}N HSQC spectrum of 5P12-vMIP-II at pH 7. (B) Overlay of ^{15}N HSQC spectrum of vMIP-II (black) and 5P12-vMIP-II (red) with the assignment adapted from Zhao et al [10] at pH 5.5. (C) Chemical shift changes of each reside after the replacement at the N-terminal region of wild-type vMIP-II. The sequence is according to wild-type vMIP-II. The blank region indicates the peaks have shifted too much to be assigned. (D) vMIP-II structure (PDB: 1VMP) showing the residues with significant chemical shift changes. Pink indicates chemical shift changes above 1 standard deviation greater than average and red indicates chemical shift changes above 2 standard deviations greater than average. Yellow indicates the peaks have shifted too much to be assigned. The disulfide bonds are showed as ball and stick with side-chains.

While a comparison of the wild type and variant spectra indicate an overall similar structure, some regions with significant changes compared to the wild type protein were observed in 5P12-vMIP-II. These include amino acids near Cys 35 (that participates in a disulfide bond with Cys 11 that is adjacent to the mutated N-terminus) and amino acids near Cys 51 (that participates in a disulfide bond with Cys 12). Figure 4-3C shows chemical shift changes at each residue in 5P12-vMIP-II compared to wild type vMIP-II. Figure 3D maps these onto the structure of the wild type protein and shows the structure of the wild type protein. Most significant changes occur near these N-terminus adjunct disulfide bonds. Nine out of 71 residues (residues: 2, 15, 32, 33, 34, 35, 39, 50, and 71) showed chemical shift changes that were bigger than 2 standard deviations from the average. One of these (residue 2) is in the mutated region and the other (residue 71) is at the C-terminus. Overall it can be concluded that 5P12-vMIP-II is a folded protein that is quite similar in tertiary structure to wild type vMIP-II.

4.4.2 Anti-HIV function of vMIP-II and 5P12-vMIP-II.

While the anti-HIV properties of vMIP-II have been known for some time, few studies have reported assays against multiple viral strains. For this work we used single-round HIV infection assays, in which a viral particle lacking key elements of the HIV genome (but having a functional HIV envelope) is used to infect target cells. The viral particle is therefore the same size and has the same surface proteins (and is presumed to have a similar ability to infect the host cell) as replication-competent HIV, but is not able to replicate. This type of assay is therefore highly useful as an efficient, accurate test of inhibition of HIV entry into the host cell, with each different “pseudovirus” defined by the different sequences of the envelope proteins (i.e. gp120) on the surface [107].

We tested wild type vMIP-II against seven strains of pseudotyped HIV: R5 strains PVO.4, AC10.0 and pWITO4160 clone 33 (SVPB18) (all from subtype B, which tends to be common in North America and Europe) [155]; R5 strain ZM109F.PB4, DU156.12 and CAP210.2.00.E8 (all from subtype C, which tends to be common in Asia and Africa) [156]; and X4 strain HxB2 (subtype B). Strain PVO.4 also has been categorized as a “Tier 3” HIV strain, indicating low sensitivity to antibody-mediated neutralization, and adding significance to the search for inhibitors for such “difficult to inhibit” viruses [209]. Strain ZM109F.PB4 is also particularly significant because it has shown orders of magnitude less sensitivity than most strains to another major type of HIV inhibitor, namely the lectin griffithsin [39].

As shown in Figure 4-4 and Table 4-1, vMIP-II was able to inhibit these strains at high nanomolar or low micromolar levels. We then tested 5P12-vMIP-II against these strains. It also showed effectiveness at high nanomolar or low micromolar levels, but did not show improvement over the wild type protein (Table 4-1). As a control, 5P12-RANTES was tested, where it showed excellent

potency against R5 strains as expected, but no effectiveness against the X4 strain (Figure 4-4 and Table 4-1).

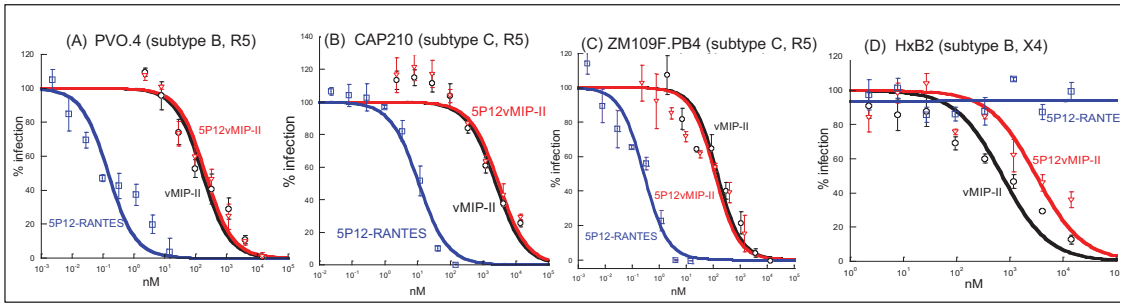

Figure 4-4: Inhibition of HIV-1 infection by vMIP-II, 5P12-vMIP-II and 5P12-RANTES in single-round infection assays.

(A) PVO.4 (subtype B, R5); (B) CAP210.2.00.E8 (subtype C, R5); (C) ZM109F.PB4 (subtype C, R5); (D) HxB2 (subtype B, X4). Wild type vMIP-II is shown in black; 5P12-vMIP-II is shown in red; 5P12-RANTES is shown in blue. A typical experiment is shown. Each experiment was repeated at least 3 times. Error bars indicate the standard deviation from a triplicate experiment.

Table 4-1: EC_{50} values for single-round infection assays for vMIP-II, 5P12-vMIP-II and 5P12-RANTES.

Strains/Compounds	vMIP-II		5P12-vMIP-II		5P12-RANTES
	EC_{50} (nM)	Fold difference from WT	EC_{50} (nM)	Fold difference from WT	EC_{50} (nM)
PVO.4 (subtype B, R5)	88.3±17	1	109±10	1.2	0.049±0.015
AC10.0.29 (subtype B, R5)	2450±530	1	2360±730	1	0.70±0.19
WITO4160.33 (subtype B, R5)	8220±1600	1	10100±1800	1.2	2.36±0.57
CAP210.2.00.E8 (subtype C, R5)	2630±790	1	2570±530	1	1.14±0.27
DU156.12 (subtype C, R5)	8540±1400	1	9850±1800	1.2	1.32±0.095
ZM109F.PB4 (subtype C, R5)	199±36	1	154±43	0.8	0.065±0.016
HxB2 (subtype B, X4)	931±210	1	1010±320	1.1	No activity

Each experiment was repeated at least 3 times in triplicate and the values shown are +/- the standard deviation of the EC_{50} from all experiments. The experiments were carried out with TZM-bl target cells.

4.5 Discussion

Since its discovery in 1996-1997 [74, 75, 210], vMIP-II has been the focus of a variety of studies, based on its ability to bind multiple chemokine receptors. Most of these studies dealt with the potential of this virally-encoded chemokine homolog to inhibit inflammation. Indeed, vMIP-II has been shown in various animal models to attenuate cellular infiltration after spinal cord injury [190-192], to protect the brain against focal cerebral ischemia [193], and to protect allograft survival in both the heart and the cornea [188, 189]. However, from the earliest reports, it was also clear that vMIP-II possessed the ability to inhibit HIV infection. Further, the unique ability of this chemokine analog to tightly bind both of the main HIV co-receptors (CCR5 and CXCR4) gives it the potential to be more broadly acting than any of the current chemokine-based inhibitors, which are limited by their ability to bind receptors from only one family (i.e. either CCR5 or CXCR4). This is particularly significant given that initial HIV infection occurs with viruses using CCR5 (so-called R5 strains), while progression to AIDS is often correlated with the switch to X4 virus in a patient [40].

Structural studies have been reported on full length vMIP-II [14, 73, 211-213] and on peptide fragments of vMIP-II [213]. Other work has focused on peptides derived from vMIP-II in order to generate smaller molecules that retain anti-HIV properties, including the use of D-peptides [214-217]. Interestingly, in studies investigating the binding of vMIP-II to human chemokine receptors, data indicated that vMIP-II does not utilize the F13/Y13 residue that is known for human chemokines to be essential for tight binding to CCR5 [10, 218, 219]. Studies with mutated chemokine receptors also indicated differences in receptor binding between vMIP-II and human chemokines, again indicating that vMIP-II may bind chemokine receptors differently than host chemokines [207]. While these experiments show differences between vMIP-II and chemokines, they also provide evidence for one of the most important facets of vMIP-II action, namely the manner in which it is uniquely able to bind multiple, diverse chemokine receptors, a function not shared with human chemokines, despite these proteins sharing as much as 40% sequence identity and an essentially identical tertiary structure.

The chemokine RANTES has been improved as an HIV inhibitor by a variety of changes to the N-terminus, the most promising of which is the “5P12” mutation used in the present work. Previous research by others also included chemical modifications at the amino terminus [59, 198]. These have been shown in at least some cases to be transferrable to other chemokines [202]. 5P12-RANTES has been found to retain the ability to tightly bind the receptor CCR5, while having a greatly increased potency against R5 HIV with EC_{50}s usually in the picomolar range. The inhibitor is also very robust to HIV mutation with “virus escape” being rare and requiring a switch to CXCR4 coreceptor use [203]. 5P12-RANTES does not inhibit X4 HIV *in vitro*, since this chemokine does not significantly interact with the CXCR4 receptor [68]. Previously, in order to

overcome this limitation we expressed 5P12-RANTES covalently linked with a peptide that is derived from the C-terminus of HIV gp41 (a C-peptide) that is known to bind to the N-terminal helices of gp41 and inhibit viral entry. This bifunctional chimera strategy was very successful, resulting in potent inhibition of both R5 and X4 viral strains [70]. Here, we sought to clarify two major issues regarding vMIP-II. First, could its anti-HIV properties against R5 virus be improved by substituting the N-terminus with the "5P12" sequence, while retaining inhibition against X4 virus; and the related second question, namely whether vMIP-II binds CCR5 using the same mechanism as that used by the human chemokine RANTES.

Our results show that 5P12-vMIP-II is a folded protein that is stable over a range of pH values and that likely retains structural similarity to wild type vMIP-II. Unlike 5P12-RANTES, 5P12-vMIP-II is able to inhibit X4 strains of HIV. However, 5P12-vMIP-II is much less potent than 5P12-RANTES against R5 HIV, and shows similar effectiveness as wild type vMIP-II. Therefore, while the "5P12" N-terminus did not significantly reduce the effectiveness of vMIP-II, it also clearly does not enable interaction with the receptor in the same way as it does when placed onto RANTES, where it usually engenders subnanomolar inhibition against R5 HIV. This provides evidence that vMIP-II does not bind CCR5 in the same was as RANTES (nor, by extension, the other human chemokines MIP-1β and MIP-1α). Therefore, it appears that vMIP-II's ability to bind multiple chemokine receptors from multiple families relies on shared structural features among chemokines, and likely on the highly basic surface on vMIP-II [10], but that this comes at the price of not binding these receptors identically to their natural chemokine ligands.

4.6 Conclusion

vMIP-II is a virally expressed chemokine analog that has the unique ability to bind both HIV co-receptors, CCR5 and CXCR4. We have modified vMIP-II at its N-terminus to make 5P12-vMIP-II, based on the N-terminal modification in 5P12-RANTES, which had made RANTES one of the most potent known R5 HIV entry inhibitors. While 5P12-vMIP-II retained anti-HIV activity against both R5 and X4 HIV strains, the 5P12 N-terminus did not improve the inhibitor. This provides evidence that despite high sequence identity and essentially identical structure to human chemokines, vMIP-II does not interact with chemokine receptors in an analogous manner to their natural chemokine ligands.

Chapter 5

Conclusion and Future direction

5.1 Conclusion

Griffithsin (Grft) is a protein lectin extracted from red algae [47]. It is among the most potent HIV entry inhibitors reported so far, and also a promising microbicide candidate [52, 53, 139, 220]. However, important biochemical details on the antiviral mechanism of Grft function remain unexplored. Crystallization of Grft in complex with mannose showed that Grft forms a domain swapped dimer, with three carbohydrate binding sites on each subunit [1]. In order to understand the role of the three individual carbohydrate-binding sites (CBS) in Grft, mutations were made at each site (D30A, D70A, and D112A), and the resulting mutants were investigated. As shown in Chapter 2, while the mutants retain a very similar structure as the wild type, mutations of any of the three sites result in a loss of at least 26-fold in ability to inhibit HIV, even though these single mutations only moderately affect the ability of Grft to bind gp120 or gp41. The disparity between HIV-1 gp120 binding ability and HIV inhibitory potency for these Grft variants indicated that Grft does not inhibit HIV through simple "binding and blocking" mechanism, leading the question to the role of Grft dimerization in its activity.

In chapter 3, we continue the work and investigate the role of Grft dimerization in Grft's anti-HIV function. Structural work and analytical ultracentrifugation confirmed that the protein is a tight dimer [1, 55], and that individual carbohydrate binding sites are critical for function [55]. An obligate dimer of Grft was designed by expressing the protein with a peptide linker between the two subunits. This "Grft-linker-Grft" is a folded protein dimer, apparently nearly identical in structural properties to the wild-type protein (as shown by our NMR experiments). A "one-armed" obligate dimer was also designed (Grft-linker-Grft OneArm), with each of the three carbohydrate binding sites of one subunit mutated while the other subunit remained intact. Both constructed dimers retained the ability to bind gp120 and the viral surface. However, Grft-linker-Grft OneArm was 84- to 1,010-fold less able to inhibit HIV than wild-type Grft, while Grft-linker-Grft had near-wild-type antiviral potency. Furthermore, while the wild-type protein demonstrated the ability to alter the structure of gp120 by exposing the CD4 binding site, Grft-linker-Grft OneArm largely lost this ability. This work elucidates an important component of the mechanism of Grft, namely that its mode of inhibition of HIV is not simply based on its ability to bind gp120, but that it also requires two functional dimer subunits.

5.1.1 Possible mechanisms for Grft function

There are several possible mechanisms for Grft function. Lectins are able to bind carbohydrates on the gp120 surface, and this "binding and blocking" mechanism has been shown to be part of Grft inhibition [1, 47, 49].

In Chapter 2, we studied the individual carbohydrate binding sites on Grft. Our results showed that the three nearly-equivalent mannose binding sites are each critical for full potency of the anti-HIV activity of the protein. However, there is a lack of correlation between Grft binding and inhibition, such that removal of one carbohydrate binding site leads to about 2- to 3- fold loss of binding but 26- to 1900- fold loss of inhibitory potency. This indicates that Grft does not inhibit HIV entry by a simple "binding and blocking" mechanism.

In Chapter 3, we studied the role of Grft dimerization in its antiviral function and investigated the possible conformational change on gp120 induced only by Grft with two functional arms. We confirmed that Grft induces gp120 conformational change by exposing a CD4 binding site, and this conformational change is correlated with Grft inhibition. This "conformational change" is also involved in Grft function, and this might be true for other similar protein lectins such as cyanovirin, which also needs two carbohydrate binding sites to maintain its potency [86]. In addition, twisting the gp120 conformation by exposing the CD4 binding site may only be part of Grft's function on gp120, in that there may be a more global conformational change that we were not able to observe due to the limitations of the assay. New assays need to be developed in order to detect other aspects of this conformational change on gp120, not only induced by Grft, but also other similar lectins or broadly neutralizing antibodies such as cyanovirin and 2G12, as discussed later on.

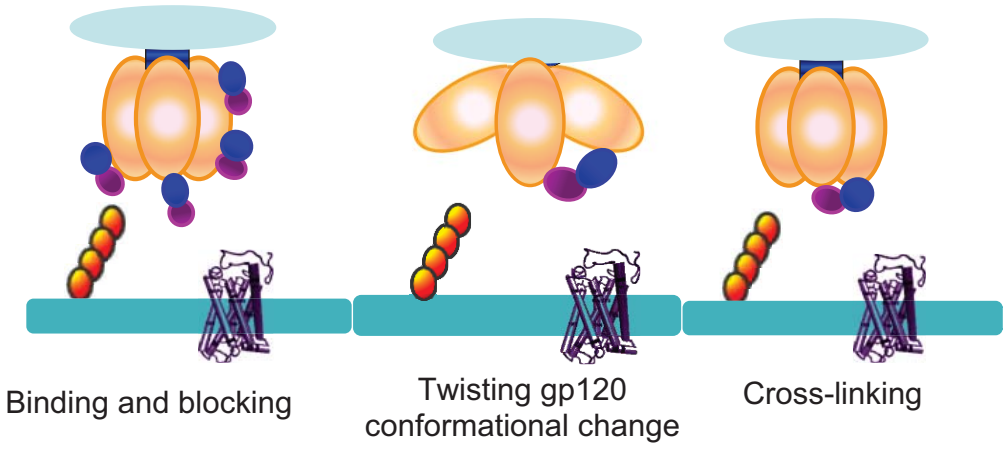

Figure 5-1: Possible mechanisms involved in Grft function.

Left: Grft is able to bind glycans on gp120, sterically blocking gp120 interaction with receptor and coreceptor.

Middle: Grft might use both carbohydrate binding arms twisting gp120 conformational change. This possible conformational change can be partially detected by using CD4 binding site antibody.

Right: Grft might use both carbohydrate binding arms to cross-link two separate gp120 subunits, impairing the functional trimeric spike.

The third mechanism involved in Grft function (in addition to bind-and-block and inducing conformational change in gp120) might be cross-linking gp120, as proposed for other lectins and carbohydrate-binding antibodies. Here, we showed that Grft wild type and the obligate dimer are able to cross-link two separate gp120 subunits, while the One-Armed Grft dimer is not able to cross-link gp120 (Figure 3-12). Considering One-Armed Grft exhibits a ~84 to 1010 fold reduction in activity but only a moderate loss of binding to gp120 mentioned in Chapter 3 [147], cross-linking may be an important mechanism involved in Grft function. On the HIV viral surface, Grft might cross-link two gp120 subunits on the same env spike, and interfere with key steps during entry (for example, CD4 binding site). Lectins or antibodies with multiple binding sites may possibly cross-link two gp120 subunits, in the same env spike or two env spikes (intra- or inter-spike) depending on the distances between the carbohydrate binding sites or epitopes. This “cross-linking” may impair the functional env trimer, making the spike less efficient for infection.

In addition to Grft, some protein lectins are shown to require at least 2 carbohydrate binding sites to perform potent inhibition [86, 87, 181, 182, 221]. Increasing the number of carbohydrate binding sites is also shown to have higher potency [85, 87]. One example of these protein lectins is cyanovirin, a protein

lectin produced by cyanobacterium [102]. This lectin has two carbohydrate binding sites per monomer, and exhibits a monomeric structure in solution and a domain swapped dimer structure in X-ray crystallography [177, 222]. The dimer Kd of cyanovirin is higher than the EC_{50} value (2.5 mM vs nM), indicating that cyanovirin functions as a monomer [223]. In addition, designed oligomers of cyanovirin monomers also leads to increased activity [85]; Linking two defective monomer mutants of lectin cyanovirin leads to restored function, with only a slight change in activity [86]. Enhanced inhibition due to multiple binding sites can often be explained by the avidity effect of the inhibitor, as mentioned in Chapter 1 [84, 85]. These data suggest that some lectins may need multiple binding sites for potent activity, and this is possibly due reduction of dissociation of the second binding site (avidity), or potentially to cross-link gp120 subunits (intra-spike or inter-spike cross-linking) [84].

5.1.2 Possible glycan sites critical for Grft function

If some glycan sites on gp120/gp41 are more important than others on the HIV surface for Grft inhibition, what is the role of these glycans? It is possible that while Grft is able to bind all the high mannose sites, there are a few specific sites that are important for Grft in carrying out functions such as structural change in gp120 or cross-linking gp120. Previous publications and our data showed that there are several glycosylation sites important for Grft function, including N234, N295, and N448 [37-39, 147].

Figure 5-2 shows a map of these glycosylation sites on the structure of unglycosylated monomeric and trimeric gp120. An analysis of these sites shows that the distance between N234 and N295 on the same gp120 subunit is ~33 Å (Figure 5-2). The distance between N234 and N295 is ~90 Å if they are from neighboring gp120 subunits on a deglycosylated env trimer (most structures of gp120 utilities the deglycosylated form due to difficulty in obtaining crystals with saccharides present). Therefore it is highly likely that Grft fits into the spacing formed by these two glycans N234 and N295 from neighboring gp120 subunit, cross-linking or manipulate gp120 conformation. This conformational change on gp120 possibly impairs the functional env trimer (possibly CD4 binding site) and interferes with viral entry. Another possibility would be that Grft binds N234 and N295 on the same subunit, and induces this conformational change. But this hypothesis is less likely because of the incompatible distance. Recent studies showed that HIV does not need three functional env subunits for entry, and only needs 2 functional gp120 subunits for infection [83, 224]. If Grft is able to bind these glycans on the same gp120 subunit, HIV still has two other functional subunits for full infection, so Grft would still allow infection if it only bound to one subunit.

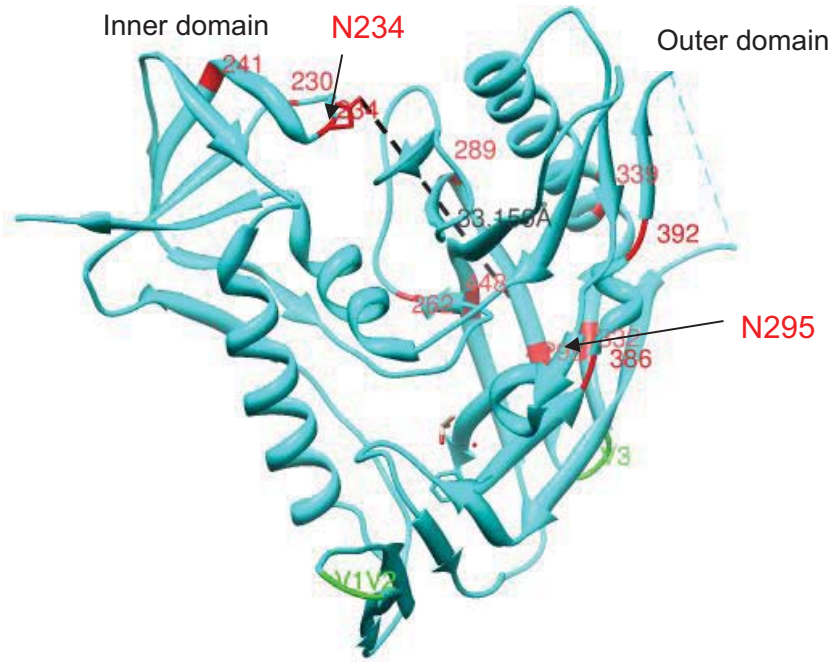

Figure 5-2: Structure of unglycosylated monomeric gp120 with glycosylation sites labeled in red.

Momomeric gp120 was crystallized in complex with CD4 and antibody 17b (CCR5 binding site antibody, not shown here) [3]. V1/V2 loop, V3 loop are partially missing and labeled in green. Red arrows indicate glycosylation sites at N234 and N295, locating at opposite site on gp120. The distance between N234 and N295 on the same gp120 subunit is ~33 Å, as shown in the dashed line. Structure was made with the program Chimera [5] using PDB structure 1g9m [3].

5.1.3 Distance between carbohydrate binding sites and lectin activity

Investigations into lectins with multivalent binding sites and their antiviral activities have been carried. The prokaryotic lectin cyanovirin-N has two carbohydrate binding sites per monomer and has been observed as either a dimer and a monomer form, both of which are apparently very potent [176, 177]. At least two carbohydrate binding sites are necessary for potent antiviral activity; mutated monomeric forms with only one CBS are not functional, but these defective monomers could restore their activities through covalent linking [86]. This may be due not just to multiple binding sites (avidity) [84], but also due to potential inter or intra spike cross-linking [85].

Even though linking two defective monomeric cyanovirin leads to regained activity of cyanovirin, this cyanovirin mutant showed slightly reduced activity with the same number of carbohydrate binding sites [86]. This means avidity (multiple

binding sites) is not the only mechanism for lectin potency since potency is not just correlated to numbers of carbohydrate binding sites. The antiviral activities seem to correlate to the distances between the two carbohydrate binding sites (Figure 5-3). Interestingly, the optimal distance between two carbohydrate binding sites for cyanovirin is 43 to 48 Å, very similar to the distance for Grft 48 Å. Notice that domain-swapped dimer of cyanovirin, even though the two of carbohydrate binding sites have lower affinity, still have higher potency than the disulfide-linked dimer. This strongly suggests that in addition to the number of CBS, other factors, such as the distance or orientation between carbohydrate binding sites also play important role in lectin function.

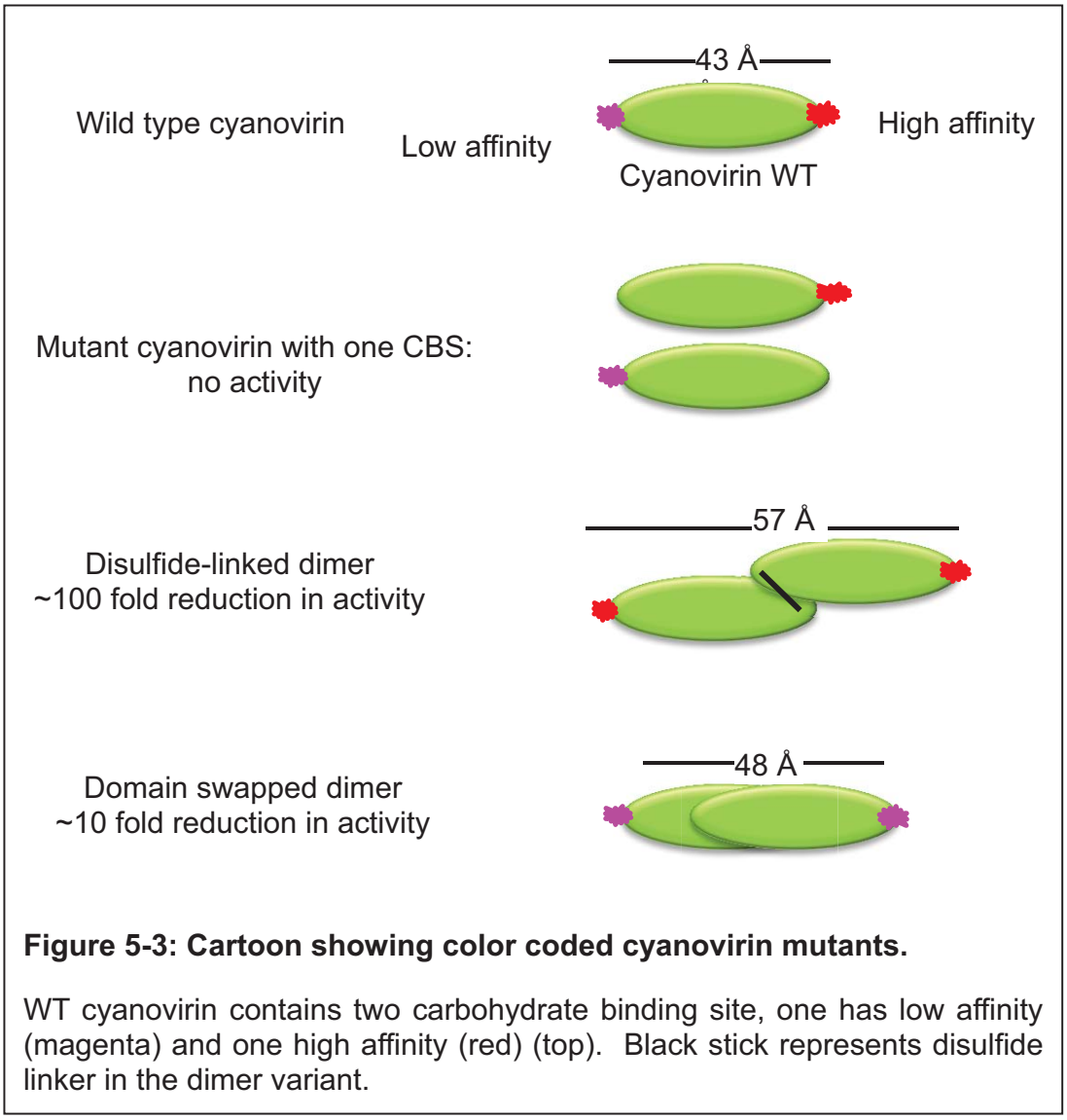

Figure 5-3: Cartoon showing color coded cyanovirin mutants.

WT cyanovirin contains two carbohydrate binding site, one has low affinity (magenta) and one high affinity (red) (top). Black stick represents disulfide linker in the dimer variant.

Another example we can use to elucidate the mechanisms of carbohydrate binding lectins or antibodies is 2G12. This broadly neutralizing antibody binds high-mannose carbohydrates on gp120, possibly through the V3 loop which is critical in forming interactions with chemokine receptors [160, 161, 178, 179]. Different from other antibodies, 2G12 has an unusual domain swapped structure that has a shorter distance between the two primary binding sites (35 Å versus a typical IgG 150 Å), and this leads to 2 additional potential CBS [84, 180] (Figure 5-4). The distance between CBS may be important in optimal HIV inhibition because the apparent ideal distance between 2 CBS involved in cyanovirin appears to be around 40 Å [86], the 2G12 primary binding sites are 35 Å apart, and the X-ray structure of Grft shows about a 47 Å distance between the two carbohydrate binding arms [1]. Therefore, effective HIV inhibition appears in these cases to arise from multisite carbohydrate binding of defined (around 40 Å) distance, though these various proteins (which do tend to effectively compete with each other [39, 93, 160, 183]) may not always bind at the same high-mannose glycan sites.

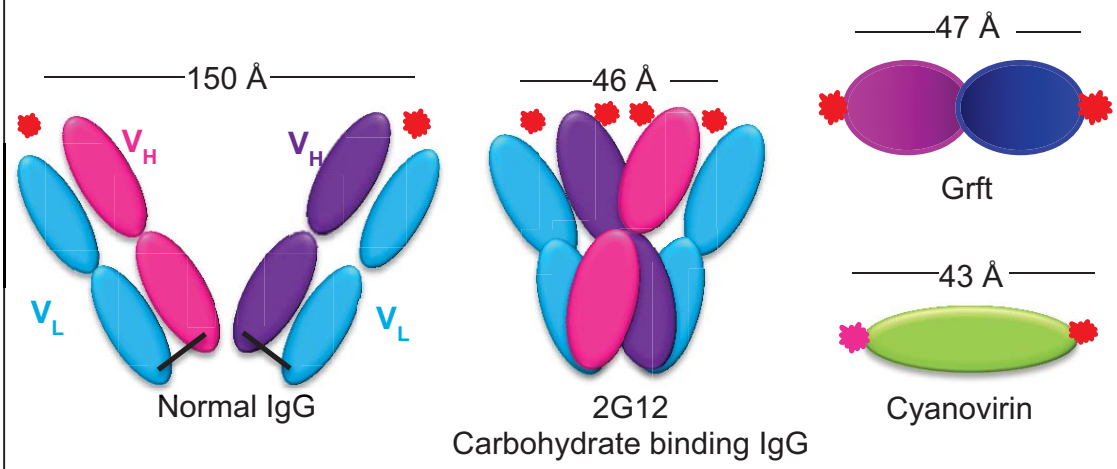

Figure 5-4: Models showing carbohydrate binding antibody or lectin structures and distance between carbohydrate binding sites.

Cyan represent antibody light chain, while purple and pink represent antibody heavy chain. Red dots represent carbohydrate binding sites. Magenta dot in cyanovirin represents the carbohydrate binding site with lower affinity.

Left: A typical distance between two ligand binding sites from the two Fabs is 150 Å.

Middle: 2G12 forms an unusual domain swapped structure, creating two more carbohydrate binding sites. The distance between these CBS is 46 Å. This unusual domain swapped structure of 2G12 creates four carbohydrate binding sites: two conventional binding sites between antibody heavy chain and light chains, and two unusual binding sites between antibody heavy chains.

Right: Grft forms domain swapped dimer with the distance between the two carbohydrate binding sites being 47 Å. Cyanovirin, which is a monomer in solution, have two carbohydrate binding sites with the distance 43 Å.

In summary, here we investigated the mechanisms of a potent anti-HIV lectin GRFT, and we uncovered that there are several mechanisms involved in GRFT function, including “bind and block”, gp120 conformational change, and possibly the cross-linking of gp120 subunits. We also discussed the factors important for other anti-HIV lectins or carbohydrate binding antibodies. Our work not only gave insight to the Grft or lectin mechanism, but also may be used in structure-based drug discovery for the prevention and treatment of HIV-1 infection.

5.2 Future directions

5.2.1 Continue current work to investigate the mechanism of antiviral lectins

Here, we showed that several mechanisms are involved in Grft function, including binding carbohydrates on the HIV surface, manipulating the gp120 conformation and possibly cross-linking different gp120 subunits. However, due to limitations of assays and constructs we currently have, other experiments need to be done to further study and confirm these mechanisms. In particular, we would like to obtain more solid proof of Grft manipulation of gp120 conformation, and cross-linking two env spikes on a real virus surface. To further investigate the mechanism of Grft activity, several new experiments could be done:

1. Test Grft cross-linking and manipulation of gp120 conformational change using complementation of HIV viruses

Make HIV pseudo viruses with diverse defective env [224]. We can make these functional complementary spikes by co-expressing inactive gp120 variants harboring different functional deficiencies. It has been reported that HIV viruses only need two wild type subunits within an envelope glycoprotein trimer to support virus entry [83]. The first thing we can do is to make pseudo viruses with only 2 functional env subunits, or making three gp120 subunits having different glycosylation sites. For example, we know that N234 and N295 are important for Grft function, so it is possible that Grft binds these two glycans to manipulate the gp120 conformation. We can make deletion mutations on N234 and N295 on one of the three gp120 subunits while leaving the other high mannose sites intact. If Grft does induce gp120 conformational change using these two glycans, then the CD4 binding site exposure would be very low and Grft may have reduced activity on these strains. Similar experiments could be done by making pseudo viruses with N234 deletion on one gp120 subunit while N295 deletion on the neighboring subunits.

2. Varying the distance of the two carbohydrate binding arms in Grft

In chapter 3 we used a flexible Gly-Ser linker to covalently link two Grft subunits and make an obligate dimer. Crystallization of Grft in complex with mannose showed that the distance between the two carbohydrate binding sites (CBS) is 47 Å, and in previous chapter we showed that some other lectins or carbohydrate binding antibodies also have similar distance between the two CBS. In order to determine whether the ~47 Å is the optimal distance of the two carbohydrate binding sites, we can use different linker to covalently link the two Grft subunits. A rigid linker $\{G(Q)_4\}_3$ [225] can be used to control the distance between the two carbohydrate binding sites, making it shorter and longer, and study the activity. Using different linker length, we can calculate and control the

distance between the two carbohydrate binding arms. However, since Grft is a domain swapped dimer, this rigid linker may disrupt the interaction between the swapped subunits, making the protein unfolded.

In addition, we can make an obligate Grft dimer with different defective mutations on each subunit to test the role of individual carbohydrate binding sites in specific functions such as cross-linking or conformational change on viruses. We can also use this defective Grft mutant to test the mechanism of Grft fusion proteins, Grft-linker-C37 for instance.

3. Test whether Grft binds the pre-fusion or post-fusion state of gp120, and if this Grft induced conformational change facilitate or hinders infection.

Since env undergoes conformational change during HIV entry, it is useful to detect whether Grft is able to hold gp120 in the pre-fusion state ("closed form", as mentioned in Chapter 1), or whether it induces gp120 conformational change and binds the post-fusion state ("open form", a receptor and co-receptor bound form). In chapter 3, we showed that Grft is able to manipulate gp120 conformational change, and this could be detected using an anti-gp120 antibody that recognizes the CD4 binding site. Grft is able to inhibit infection by exposing the CD4 binding site, and this effect is more significant for virus strains when Grft is more potent. However, it is still not known about the role of this CD4 binding site exposure, whether it is part of gp120 conformational change, and whether it facilitates or hinders entry.

We can test the hypothesis that Grft binds the pre-fusion and lock the gp120 in this conformation using HeLa-env cell lines or 293FT env transfected cell lines. We pre-incubate HeLa-env cells with Grft to bind Grft to gp120, and then remove Grft by PBS washing and centrifuge. Then we use some methods to test the binding of these pre-treated Hela cells to TZM-bl cells, which have receptor and coreceptor expressed. The control experiments would be HeLa-env cells no incubation with Grft. However, gp120 may go back to its original conformation when Grft is washed off.

If we used 293FT cell line, we can use gp140 plasmid (mimics gp120 plus extracellular domain of gp41) to transfect 293 cells and mimic the pre-fusion state. If we can use the 17b bound gp120 as post-fusion state to test post-fusion state gp120 binding to target cells.

4. Test whether entry inhibitors Grft, 5P12-RANTES, 5P12-linker-C37 decreases virus binding to target cells

Grft binds high mannose glycans on gp120 surface, and 5P12-RANTES binds CCR5 to inhibit HIV entry. 5P12-linker-C37, a chimeric protein, is able to binds both CCR5 and gp41. However, though 5P12-linker-C37 showed great potency against HIV infection, it may bring more viruses to its target sites since CCR5 is

on cell surface and gp41 is on viral surface. Therefore, it is useful to detect how these entry inhibitors affect virus binding to the cell surface.

We can plate single layers of TZM-bl cells in a 96 well plate, and then add different concentration of Grft, 5P12-RANTES or 5P12-linker-C37 into plate. Then we apply virus on to the plates, incubate. We would then centrifuge the plate, and wash cells with PBS to retain only virus that has bound to the cells in the presence of inhibitor. To detect the amount of virus, it is lysed and a subsequent p24 ELISA assay is carried out. This is a rough detection method since it involves transferring and the sensitivity is low. A more clear way is to use immunofluorescence to detect the binding.

If we did these experiment, I would expect Grft reduce virus binding to TZM-bl. However, 5P12 may not affect virus binding since virus can also bind CD4 which would still be possible if 5P12 were binding to CCR5. 5P12-linker-C37 might increase virus binding since 5P12-RANTES binds CCR5 while C37 binds gp41 on virus surface.

5.2.2 Test current HIV entry inhibitors in our lab for a microbicide study

1. Test stability and long-term release of HIV entry inhibitors

We are currently detecting whether silk fibroin would stabilize Grft, Grft-linker-C37, 5P12-RANTES, 5P12-RANTES-linker-C37 in 25 °C, 37 °C and 50 °C for 6 months. Here, we use simulated vaginal fluid (SVF, pH 4.5) [95] to hydrate silk fibroin samples after incubation, followed by testing for antiviral potency. Preliminary results show that inhibitors behave well in SVF-dissolved silk samples. We are also studying the long-term release of these inhibitors. By using different formulation of silk fibrion formulated inhibitors, we use SVF to soak these samples and change media every day for at least 30 days, and test if the inhibitor-infused silk matrix allows sustained release. The ultimate goal is to put these entry inhibitors to clinical use as microbicides, and for sustained and effective release.

2. Test combination of HIV entry inhibitors in silk

Previous publications showed that Grft has a synergistic effect when combined with other anti-HIV drugs, lectins or antibodies [54, 93]. Also, Grft is less potent for viruses from the clade C strain which are usually lacking N234 and N295 [37, 39]. However, clade C viruses tend to exclusively use CCR5 as coreceptor irrespective of disease stage [226, 227]. 5P12-RANTES is very potent to R5 strain viruses, but has no effect on X4 strain viruses. These data suggest a possibility to use a combination of Grft with other inhibitors, such as 5P12-RANTES for instance, and it would be useful to test the combination for stability in silk fibroin and time-released experiments.

References

1. Ziolkowska NE, O'Keefe BR, Mori T, Zhu C, Giomarelli B, Vojdani F, Palmer KE, McMahon JB, Wlodawer A: **Domain-swapped structure of the potent antiviral protein griffithsin and its mode of carbohydrate binding.** *Structure* 2006, **14:**1127-1135.
2. Ziolkowska NE, Wlodawer A: **Structural studies of algal lectins with anti-HIV activity.** *Acta Biochim Pol* 2006, **53:**617-626.
3. Kwong PD, Wyatt R, Robinson J, Sweet RW, Sodroski J, Hendrickson WA: **Structure of an HIV gp120 envelope glycoprotein in complex with the CD4 receptor and a neutralizing human antibody. [see comments].** *Nature* 1998, **393:**648-659.
4. Zhu P, Liu J, Bess J, Jr., Chertova E, Lifson JD, Grise H, Ofek GA, Taylor KA, Roux KH: **Distribution and three-dimensional structure of AIDS virus envelope spikes.** *Nature* 2006, **441:**847-852.
5. Pettersen EF, Goddard TD, Huang CC, Couch GS, Greenblatt DM, Meng EC, Ferrin TE: **UCSF Chimera--a visualization system for exploratory research and analysis.** *Journal of Computational Chemistry* 2004, **25:**1605-1612.
6. Bartesaghi A, Merk A, Borgnia MJ, Milne JL, Subramaniam S: **Prefusion structure of trimeric HIV-1 envelope glycoprotein determined by cryo-electron microscopy.** *Nat Struct Mol Biol* 2013, **20:**1352-1357.
7. Lyumkis D, Julien JP, de Val N, Cupo A, Potter CS, Klasse PJ, Burton DR, Sanders RW, Moore JP, Carragher B, et al: **Cryo-EM Structure of a Fully Glycosylated Soluble Cleaved HIV-1 Envelope Trimer.** *Science* 2013.
8. Wainberg MA: **HIV-1 subtype distribution and the problem of drug resistance.** *AIDS* 2004, **18 Suppl 3:**S63-68.
9. Schneider CA, Rasband WS, Eliceiri KW: **NIH Image to ImageJ: 25 years of image analysis.** *Nat Methods* 2012, **9:**671-675.
10. Zhao B, Liwang PJ: **Characterization of the interactions of vMIP-II, and a dimeric variant of vMIP-II, with glycosaminoglycans.** *Biochemistry* 2010, **49:**7012-7022.
11. Shenoy SR, Barrientos LG, Ratner DM, O'Keefe BR, Seeberger PH, Gronenborn AM, Boyd MR: **Multisite and multivalent binding between cyanovirin-N and branched oligomannosides: calorimetric and NMR characterization.** *Chem Biol* 2002, **9:**1109-1118.
12. Chung C, Cooke, R.M., Proudfoot, A.E.I. and Wells, T.N.C.: **The three-dimensional solution structure of RANTES.** *Biochemistry* 1995, **34:**3907-9314.
13. Balzarini J: **Targeting the glycans of glycoproteins: a novel paradigm for antiviral therapy.** *Nat Rev Microbiol* 2007, **5:**583-597.
14. LiWang AC, Wang ZX, Sun Y, Peiper SC, LiWang PJ: **The solution structure of the anti-HIV chemokine vMIP-II.** *Protein Science* 1999, **8:**2270-2279.

15. Tan Q, Zhu Y, Li J, Chen Z, Han GW, Kufareva I, Li T, Ma L, Fenalti G, Zhang W, et al: **Structure of the CCR5 chemokine receptor-HIV entry inhibitor maraviroc complex.** *Science* 2013, **341:**1387-1390.
16. Johnson LM, Horne WS, Gellman SH: **Broad distribution of energetically important contacts across an extended protein interface.** *J Am Chem Soc* 2011, **133:**10038-10041.
17. Beyrer C, Abdool Karim Q: **The changing epidemiology of HIV in 2013.** *Curr Opin HIV AIDS* 2013, **8:**306-310.
18. Hladik F, McElrath MJ: **Setting the stage: host invasion by HIV.** *Nat Rev Immunol* 2008, **8:**447-457.
19. Taylor BS, Sobieszczyk ME, McCutchan FE, Hammer SM: **The challenge of HIV-1 subtype diversity.** *N Engl J Med* 2008, **358:**1590-1602.
20. Hemelaar J, Gouws E, Ghys PD, Osmanov S: **Global and regional distribution of HIV-1 genetic subtypes and recombinants in 2004.** *AIDS* 2006, **20:**W13-23.
21. Kantor R, Katzenstein DA, Efron B, Carvalho AP, Wynhoven B, Cane P, Clarke J, Sirivichayakul S, Soares MA, Snoeck J, et al: **Impact of HIV-1 subtype and antiretroviral therapy on protease and reverse transcriptase genotype: results of a global collaboration.** *PLoS Med* 2005, **2:**e112.
22. Colman PM, Lawrence MC: **The structural biology of type I viral membrane fusion.** *Nat Rev Mol Cell Biol* 2003, **4:**309-319.
23. Yamaguchi M, Danev R, Nishiyama K, Sugawara K, Nagayama K: **Zernike phase contrast electron microscopy of ice-embedded influenza A virus.** *J Struct Biol* 2008, **162:**271-276.
24. Mao Y, Wang L, Gu C, Herschhorn A, Desormeaux A, Finzi A, Xiang SH, Sodroski JG: **Molecular architecture of the uncleaved HIV-1 envelope glycoprotein trimer.** *Proc Natl Acad Sci U S A* 2013, **110:**12438-12443.
25. Speck RF, Wehrly K, Platt EJ, Atchison RE, Charo IF, Kabat D, Chesebro B, Goldsmith MA: **Selective employment of chemokine receptors as human immunodeficiency virus type 1 coreceptors determined by individual amino acids within the envelope V3 loop.** *J Virol* 1997, **71:**7136-7139.
26. Tran EE, Borgnia MJ, Kuybeda O, Schauder DM, Bartesaghi A, Frank GA, Sapiro G, Milne JL, Subramaniam S: **Structural mechanism of trimeric HIV-1 envelope glycoprotein activation.** *PLoS Pathog* 2012, **8:**e1002797.
27. Myers G, MacInnes K, Korber B: **The emergence of simian/human immunodeficiency viruses.** *AIDS Res Hum Retroviruses* 1992, **8:**373-386.
28. Polonoff E, Machida CA, Kabat D: **Glycosylation and intracellular transport of membrane glycoproteins encoded by murine leukemia viruses. Inhibition by amino acid analogues and by tunicamycin.** *J Biol Chem* 1982, **257:**14023-14028.

29. Zhu X, Borchers C, Bienstock RJ, Tomer KB: **Mass spectrometric characterization of the glycosylation pattern of HIV-gp120 expressed in CHO cells.** *Biochemistry* 2000, **39:**11194-11204.
30. Raska M, Takahashi K, Czernekova L, Zachova K, Hall S, Moldoveanu Z, Elliott MC, Wilson L, Brown R, Jancova D, et al: **Glycosylation patterns of HIV-1 gp120 depend on the type of expressing cells and affect antibody recognition.** *J Biol Chem* 2010, **285:**20860-20869.
31. Go EP, Liao HX, Alam SM, Hua D, Haynes BF, Desaire H: **Characterization of host-cell line specific glycosylation profiles of early transmitted/founder HIV-1 gp120 envelope proteins.** *J Proteome Res* 2013, **12:**1223-1234.
32. Pollakis G, Kang S, Kliphuis A, Chalaby MI, Goudsmit J, Paxton WA: **N-linked glycosylation of the HIV type-1 gp120 envelope glycoprotein as a major determinant of CCR5 and CXCR4 coreceptor utilization.** *J Biol Chem* 2001, **276:**13433-13441.
33. Doores KJ, Bonomelli C, Harvey DJ, Vasiljevic S, Dwek RA, Burton DR, Crispin M, Scanlan CN: **Envelope glycans of immunodeficiency virions are almost entirely oligomannose antigens.** *Proc Natl Acad Sci U S A* 2010, **107:**13800-13805.
34. Cho MW, Lee MK, Carney MC, Berson JF, Doms RW, Martin MA: **Identification of determinants on a dualtropic human immunodeficiency virus type 1 envelope glycoprotein that confer usage of CXCR4.** *J Virol* 1998, **72:**2509-2515.
35. Zhang M, Gaschen B, Blay W, Foley B, Haigwood N, Kuiken C, Korber B: **Tracking global patterns of N-linked glycosylation site variation in highly variable viral glycoproteins: HIV, SIV, and HCV envelopes and influenza hemagglutinin.** *Glycobiology* 2004, **14:**1229-1246.
36. Ogert RA, Lee MK, Ross W, Buckler-White A, Martin MA, Cho MW: **N-linked glycosylation sites adjacent to and within the V1/V2 and the V3 loops of dualtropic human immunodeficiency virus type 1 isolate DH12 gp120 affect coreceptor usage and cellular tropism.** *J Virol* 2001, **75:**5998-6006.
37. Alexandre KB, Moore PL, Nonyane M, Gray ES, Ranchobe N, Chakauya E, McMahon JB, O'Keefe BR, Chikwamba R, Morris L: **Mechanisms of HIV-1 subtype C resistance to GRFT, CV-N and SVN.** *Virology* 2013, **446:**66-76.
38. Huang X, Jin W, Griffin GE, Shattock RJ, Hu Q: **Removal of two high-mannose N-linked glycans on gp120 renders human immunodeficiency virus 1 largely resistant to the carbohydrate-binding agent griffithsin.** *J Gen Virol* 2011, **92:**2367-2373.
39. Alexandre KB, Gray ES, Lambson BE, Moore PL, Choge IA, Mlisana K, Karim SS, McMahon J, O'Keefe B, Chikwamba R, Morris L: **Mannose-rich glycosylation patterns on HIV-1 subtype C gp120 and sensitivity to the lectins, Griffithsin, Cyanovirin-N and Scytovirin.** *Virology* 2010, **402:**187-196.

40. Connor RI, Sheridan KE, Ceradini D, Choe S, Landau NR: **Change in coreceptor use correlates with disease progression in HIV-1--infected individuals.** *J Exp Med* 1997, **185:**621-628.
41. Williamson C, Morris L, Maughan MF, Ping LH, Dryga SA, Thomas R, Reap EA, Cilliers T, van Harmelen J, Pascual A, et al: **Characterization and selection of HIV-1 subtype C isolates for use in vaccine development.** *AIDS Res Hum Retroviruses* 2003, **19:**133-144.
42. Wu B, Chien EY, Mol CD, Fenalti G, Liu W, Katritch V, Abagyan R, Brooun A, Wells P, Bi FC, et al: **Structures of the CXCR4 chemokine GPCR with small-molecule and cyclic peptide antagonists.** *Science* 2010, **330:**1066-1071.
43. Huang CC, Lam SN, Acharya P, Tang M, Xiang SH, Hussan SS, Stanfield RL, Robinson J, Sodroski J, Wilson IA, et al: **Structures of the CCR5 N terminus and of a tyrosine-sulfated antibody with HIV-1 gp120 and CD4.** *Science* 2007, **317:**1930-1934.
44. Reeves JD, Miamidian JL, Biscone MJ, Lee FH, Ahmad N, Pierson TC, Doms RW: **Impact of mutations in the coreceptor binding site on human immunodeficiency virus type 1 fusion, infection, and entry inhibitor sensitivity.** *Journal of Virology* 2004, **78:**5476-5485.
45. Brelot A, Heveker N, Montes M, Alizon M: **Identification of residues of CXCR4 critical for human immunodeficiency virus coreceptor and chemokine receptor activities.** *J Biol Chem* 2000, **275:**23736-23744.
46. Garcia-Perez J, Rueda P, Alcami J, Rognan D, Arenzana-Seisdedos F, Lagane B, Kellenberger E: **Allosteric model of maraviroc binding to CC chemokine receptor 5 (CCR5).** *J Biol Chem* 2011, **286:**33409-33421.
47. Mori T, O'Keefe BR, Sowder RC, 2nd, Bringans S, Gardella R, Berg S, Cochran P, Turpin JA, Buckheit RW, Jr., McMahon JB, Boyd MR: **Isolation and characterization of griffithsin, a novel HIV-inactivating protein, from the red alga Griffithsia sp.** *J Biol Chem* 2005, **280:**9345-9353.
48. Nixon B, Stefanidou M, Mesquita PM, Fakioglu E, Segarra T, Rohan L, Halford W, Palmer KE, Herold BC: **Griffithsin Protects Mice from Genital Herpes by Preventing Cell-to-Cell Spread.** *J Virol* 2013.
49. Ishag HZ, Li C, Huang L, Sun MX, Wang F, Ni B, Malik T, Chen PY, Mao X: **Griffithsin inhibits Japanese encephalitis virus infection in vitro and in vivo.** *Arch Virol* 2012.
50. Meuleman P, Albecka A, Belouzard S, Vercauteren K, Verhoye L, Wychowski C, Leroux-Roels G, Palmer KE, Dubuisson J: **Griffithsin has antiviral activity against hepatitis C virus.** *Antimicrob Agents Chemother* 2011, **55:**5159-5167.
51. O'Keefe BR, Vojdani F, Buffa V, Shattock RJ, Montefiori DC, Bakke J, Mirsalis J, d'Andrea AL, Hume SD, Bratcher B, et al: **Scaleable manufacture of HIV-1 entry inhibitor griffithsin and validation of its safety and efficacy as a topical microbicide component.** *Proc Natl Acad Sci U S A* 2009, **106:**6099-6104.

52. Kouokam JC, Huskens D, Schols D, Johannemann A, Riedell SK, Walter W, Walker JM, Matoba N, O'Keefe BR, Palmer KE: **Investigation of griffithsin's interactions with human cells confirms its outstanding safety and efficacy profile as a microbicide candidate.** *PLoS One* 2011, **6:**e22635.
53. Emau P, Tian B, O'Keefe B R, Mori T, McMahon JB, Palmer KE, Jiang Y, Bekele G, Tsai CC: **Griffithsin, a potent HIV entry inhibitor, is an excellent candidate for anti-HIV microbicide.** *J Med Primatol* 2007, **36:**244-253.
54. Ferir G, Palmer KE, Schols D: **Synergistic activity profile of griffithsin in combination with tenofovir, maraviroc and enfuvirtide against HIV-1 clade C.** *Virology* 2011, **417:**253-258.
55. Xue J, Gao Y, Hoorelbeke B, Kagiampakis I, Zhao B, Demeler B, Balzarini J, Liwang PJ: **The role of individual carbohydrate-binding sites in the function of the potent anti-HIV lectin griffithsin.** *Mol Pharm* 2012, **9:**2613-2625.
56. Cocchi F, DeVico AL, Garzino-Demo A, Arya SK, Gallo RC, Lusso P: **Identification of RANTES, MIP-1 alpha, and MIP-1 beta as the major HIV-suppressive factors produced by CD8+ T cells.** *Science* 1995, **270:**1811-1815.
57. Alkhatib G, Combadiere C, Broder CC, Feng Y, Kennedy PE, Murphy PM, Berger EA: **CC CKR5: a RANTES, MIP-1alpha, MIP-1beta receptor as a fusion cofactor for macrophage-tropic HIV-1.** *Science* 1996, **272:**1955-1958.
58. Dragic T, Litwin V, Allaway GP, Martin SR, Huang Y, Nagashima KA, Cayanan C, Maddon PJ, Koup RA, Moore JP, Paxton WA: **HIV-1 entry into CD4+ cells is mediated by the chemokine receptor CC-CKR-5.** *Nature* 1996, **381:**667-673.
59. Simmons G, Clapham PR, Picard L, Offord RE, Rosenkilde MM, Schwartz TW, Buser R, Wells TNC, Proudfoot AEI: **Potent inhibition of HIV-1 infectivity in macrophages and lyphocytes by a novel CCR5 antagonist.** *Science* 1997, **276:**276-279.
60. Signoret N, Oldridge, J., Pelchen-Matthews, A., Klasse, P.J., Tran, T., Brass, L.F., Rosenkilde, M.M., Schwartz, J.W., Holmes, W., Dallas, W., Luther, M.A., Wells, T.N.C., Hoxie, J.A., and Marsh, M.: **Phorbol esters and SDF-1 induce rapid endocytosis and down modulation of the chemokine receptor CXCR4.** *J Cell Biol* 1997, **139:**651-664.
61. Schmidtmayerova H, Sherry B, Bukrinsky M: **Chemokines and HIV replication.** *Nature* 1996, **382:**767.
62. Dolei A, Biolchini A, Serra C, Curreli S, Gomes E, Dianzani F: **Increased replication of T-cell-tropic HIV strains and CXC-chemokine receptor-4 induction in T cells treated with macrophage inflammatory protein (MIP)-1alpha, MIP-1beta and RANTES beta-chemokines.** *AIDS* 1998, **12:**183-190.

63. Galvin SR, Cohen MS: **The role of sexually transmitted diseases in HIV transmission.** *Nat Rev Microbiol* 2004, **2:**33-42.
64. Trkola A, Gordon C, Matthews J, Maxwell E, Ketas T, Czaplewski L, Proudfoot AE, Moore JP: **The CC-chemokine RANTES increases the attachment of human immunodeficiency virus type 1 to target cells via glycosaminoglycans and also activates a signal transduction pathway that enhances viral infectivity.** *Journal of Virology* 1999, **73:**6370-6379.
65. Proudfoot AEI, Fritchley S, Borlat F, Shaw JP, Vilbois F, Zwahlen C, Trkola A, Marchant D, Clapham PR, Wells TNC: **THe BBXB motif of RANTES is the principal site for heparin binding and controls receptor selectivity.** *J Biol Chem* 2001, **276:**10620-10626.
66. Pastore C, Picchio GR, Galimi F, Fish R, Hartley O, Offord RE, Mosier DE: **Two mechanisms for human immunodeficiency virus type 1 inhibition by N-terminal modifications of RANTES.** *Antimicrobial Agents & Chemotherapy* 2003, **47:**509-517.
67. Polo S, Nardese V, De Santis C, Arcelloni C, Paroni R, Sironi F, Verani A, Rizzi M, Bolognesi M, Lusso P: **Enhancement of the HIV-1 inhibitory activity of RANTES by modification of the N-terminal region: dissociation from CCR5 activation.** *European Journal of Immunology* 2000, **30:**3190-3198.
68. Gaertner H, Cerini F, Escola JM, Kuenzi G, Melotti A, Offord R, Rossitto-Borlat I, Nedellec R, Salkowitz J, Gorochov G, et al: **Highly potent, fully recombinant anti-HIV chemokines: reengineering a low-cost microbicide.** *Proc Natl Acad Sci U S A* 2008, **105:**17706-17711.
69. Hartley O, Dorgham K, Perez-Bercoff D, Cerini F, Heimann A, Gaertner H, Offord RE, Pancino G, Debre P, Gorochov G: **Human immunodeficiency virus type 1 entry inhibitors selected on living cells from a library of phage chemokines.** *Journal of Virology* 2003, **77:**6637-6644.
70. Zhao B, Mankowski MK, Snyder BA, Ptak RG, Liwang PJ: **Highly potent chimeric inhibitors targeting two steps of HIV cell entry.** *J Biol Chem* 2011, **286:**28370-28381.
71. Vangelista L, Secchi M, Liu X, Bachi A, Jia L, Xu Q, Lusso P: **Engineering of Lactobacillus jensenii to secrete RANTES and a CCR5 antagonist analogue as live HIV-1 blockers.** *Antimicrob Agents Chemother* 2010, **54:**2994-3001.
72. Li Y, Liu D, Cao R, Kumar S, Dong C, An J, Wilson SR, Gao YG, Huang Z: **Crystal structure of chemically synthesized vMIP-II.** *Proteins* 2007, **67:**243-246.
73. Fernandez EJ, Wilken J, Thompson DA, Peiper SC, Lolis E: **Comparison of the structure of vMIP-II with eotaxin-1, RANTES, and MCP-3 suggests a unique mechanism for CCR3 activation.** *Biochemistry* 2000, **39:**12837-12844.
74. Kledal TN, Rosenkilde MM, Coulin F, Simmons G, Johnsen AH, Alouani S, Power CA, Luttichau HR, Gerstoft J, Clapham PR, et al: **A broad-**

spectrum chemokine antagonist encoded by Kaposi's sarcoma-associated herpesvirus. *Science* 1997, **277:**1656-1659.

75. Boshoff C, Endo Y, Collins PD, Takeuchi Y, Reeves JD, Schweickart VL, Siani MA, Sasaki T, Williams TJ, Gray PW, et al: **Angiogenic and HIV-inhibitory functions of KSHV-encoded chemokines.** *Science* 1997, **278:**290-294.
76. Weber KS, Grone HJ, Rocken M, Klier C, Gu S, Wank R, Proudfoot AE, Nelson PJ, Weber C: **Selective recruitment of Th2-type cells and evasion from a cytotoxic immune response mediated by viral macrophage inhibitory protein-II.** *European Journal of Immunology* 2001, **31:**2458-2466.
77. Sozzani S, Luini W, Bianchi G, Allavena P, Wells TNC, Napolitano M, Bernardini G, Vecchi A, D'Ambrosio D, Mazzeo D, et al: **The viral chemokine macrophage inflammatory protein-II is a selective Th2 chemoattractant.** *Blood* 1998, **92:**4035-4039.
78. Eckert DM, Kim PS: **Mechanisms of viral membrane fusion and its inhibition.** *Annu Rev Biochem* 2001, **70:**777-810.
79. Eggink D, Bontjer I, Langedijk JP, Berkhout B, Sanders RW: **Resistance of human immunodeficiency virus type 1 to a third-generation fusion inhibitor requires multiple mutations in gp41 and is accompanied by a dramatic loss of gp41 function.** *Journal of virology* 2011, **85:**10785-10797.
80. Pan C, Cai L, Lu H, Lu L, Jiang S: **A novel chimeric protein-based HIV-1 fusion inhibitor targeting gp41 glycoprotein with high potency and stability.** *The Journal of biological chemistry* 2011, **286:**28425-28434.
81. Liu J, Bartesaghi A, Borgnia MJ, Sapiro G, Subramaniam S: **Molecular architecture of native HIV-1 gp120 trimers.** *Nature* 2008, **455:**109-113.
82. Sougrat R, Bartesaghi A, Lifson JD, Bennett AE, Bess JW, Zabransky DJ, Subramaniam S: **Electron tomography of the contact between T cells and SIV/HIV-1: implications for viral entry.** *PLoS Pathog* 2007, **3:**e63.
83. Yang X, Kurteva S, Ren X, Lee S, Sodroski J: **Subunit stoichiometry of human immunodeficiency virus type 1 envelope glycoprotein trimers during virus entry into host cells.** *J Virol* 2006, **80:**4388-4395.
84. Klein JS, Bjorkman PJ: **Few and far between: how HIV may be evading antibody avidity.** *PLoS Pathog* 2010, **6:**e1000908.
85. Keeffe JR, Gnanapragasam PN, Gillespie SK, Yong J, Bjorkman PJ, Mayo SL: **Designed oligomers of cyanovirin-N show enhanced HIV neutralization.** *Proc Natl Acad Sci U S A* 2011, **108:**14079-14084.
86. Matei E, Zheng A, Furey W, Rose J, Aiken C, Gronenborn AM: **Anti-HIV activity of defective cyanovirin-N mutants is restored by dimerization.** *J Biol Chem* 2010, **285:**13057-13065.
87. Wolbank S, Kunert R, Stiegler G, Katinger H: **Characterization of human class-switched polymeric (immunoglobulin M [IgM] and IgA) anti-human immunodeficiency virus type 1 antibodies 2F5 and 2G12.** *J Virol* 2003, **77:**4095-4103.

88. Klein JS, Webster A, Gnanapragasam PN, Galimidi RP, Bjorkman PJ: **A dimeric form of the HIV-1 antibody 2G12 elicits potent antibody-dependent cellular cytotoxicity.** *AIDS* 2010, **24:**1633-1640.
89. Harris A, Borgnia MJ, Shi D, Bartesaghi A, He H, Pejchal R, Kang YK, Depetris R, Marozsan AJ, Sanders RW, et al: **Trimeric HIV-1 glycoprotein gp140 immunogens and native HIV-1 envelope glycoproteins display the same closed and open quaternary molecular architectures.** *Proceedings of the National Academy of Sciences of the United States of America* 2011, **108:**11440-11445.
90. Bewley CA, Otero-Quintero S: **The potent anti-HIV protein cyanovirin-N contains two novel carbohydrate binding sites that selectively bind to Man(8) D1D3 and Man(9) with nanomolar affinity: implications for binding to the HIV envelope protein gp120.** *J Am Chem Soc* 2001, **123:**3892-3902.
91. Plosker GL: **Emtricitabine/tenofovir disoproxil fumarate: a review of its use in HIV-1 pre-exposure prophylaxis.** *Drugs* 2013, **73:**279-291.
92. Abdool Karim Q, Abdool Karim SS, Frohlich JA, Grobler AC, Baxter C, Mansoor LE, Kharsany AB, Sibeko S, Mlisana KP, Omar Z, et al: **Effectiveness and safety of tenofovir gel, an antiretroviral microbicide, for the prevention of HIV infection in women.** *Science* 2010, **329:**1168-1174.
93. Ferir G, Huskens D, Palmer KE, Boudreaux DM, Swanson MD, Markovitz DM, Balzarini J, Schols D: **Combinations of Griffithsin with Other Carbohydrate-Binding Agents Demonstrate Superior Activity Against HIV Type 1, HIV Type 2, and Selected Carbohydrate-Binding Agent-Resistant HIV Type 1 Strains.** *AIDS Res Hum Retroviruses* 2012, **28:**1513-1523.
94. Smith JM, Rastogi R, Teller RS, Srinivasan P, Mesquita PM, Nagaraja U, McNicholl JM, Hendry RM, Dinh CT, Martin A, et al: **Intravaginal ring eluting tenofovir disoproxil fumarate completely protects macaques from multiple vaginal simian-HIV challenges.** *Proc Natl Acad Sci U S A* 2013, **110:**16145-16150.
95. Wang NX, Sieg SF, Lederman MM, Offord RE, Hartley O, von Recum HA: **Using Glycosaminoglycan/Chemokine Interactions for the Long-Term Delivery of 5P12-RANTES in HIV Prevention.** *Mol Pharm* 2013, **10:**3564-3573.
96. Root MJ, Steger HK: **HIV-1 gp41 as a target for viral entry inhibition.** 2004**:**1805-1825.
97. Moulaei T, Shenoy SR, Giomarelli B, Thomas C, McMahon JB, Dauter Z, O'Keefe BR, Wlodawer A: **Monomerization of viral entry inhibitor griffithsin elucidates the relationship between multivalent binding to carbohydrates and anti-HIV activity.** *Structure* 2010, **18:**1104-1115.
98. Ziolkowska NE, Shenoy SR, O'Keefe BR, Wlodawer A: **Crystallographic studies of the complexes of antiviral protein griffithsin with glucose and N-acetylglucosamine.** *Protein Sci* 2007, **16:**1485-1489.

99. Botos I, Mori T, Cartner LK, Boyd MR, Wlodawer A: **Domain-swapped structure of a mutant of cyanovirin-N.** *Biochem Biophys Res Commun* 2002, **294:**184-190.
100. Alexandre KB, Gray ES, Mufhandu H, McMahon JB, Chakauya E, O'Keefe BR, Chikwamba R, Morris L: **The lectins griffithsin, cyanovirin-N and scytovirin inhibit HIV-1 binding to the DC-SIGN receptor and transfer to CD4(+) cells.** *Virology* 2012, **423:**175-186.
101. Ziolkowska NE, Shenoy SR, O'Keefe BR, McMahon JB, Palmer KE, Dwek RA, Wormald MR, Wlodawer A: **Crystallographic, thermodynamic, and molecular modeling studies of the mode of binding of oligosaccharides to the potent antiviral protein griffithsin.** *Proteins* 2007, **67:**661-670.
102. Boyd MR, Gustafson KR, McMahon JB, Shoemaker RH, O'Keefe BR, Mori T, Gulakowski RJ, Wu L, Rivera MI, Laurencot CM, et al: **Discovery of cyanovirin-N, a novel human immunodeficiency virus-inactivating protein that binds viral surface envelope glycoprotein gp120: potential applications to microbicide development.** *Antimicrob Agents Chemother* 1997, **41:**1521-1530.
103. Gendelman HE, Baca LM, Kubrak CA, Genis P, Burrous S, Friedman RM, Jacobs D, Meltzer MS: **Induction of IFN-alpha in peripheral blood mononuclear cells by HIV-infected monocytes. Restricted antiviral activity of the HIV-induced IFN.** *J Immunol* 1992, **148:**422-429.
104. Gendelman HE, Orenstein JM, Baca LM, Weiser B, Burger H, Kalter DC, Meltzer MS: **The macrophage in the persistence and pathogenesis of HIV infection.** *AIDS* 1989, **3:**475-495.
105. Gendelman HE, Orenstein JM, Martin MA, Ferrua C, Mitra R, Phipps T, Wahl LA, Lane HC, Fauci AS, Burke DS, et al.: **Efficient isolation and propagation of human immunodeficiency virus on recombinant colony-stimulating factor 1-treated monocytes.** *J Exp Med* 1988, **167:**1428-1441.
106. Westervelt P, Gendelman HE, Ratner L: **Identification of a determinant within the human immunodeficiency virus 1 surface envelope glycoprotein critical for productive infection of primary monocytes.** *Proc Natl Acad Sci U S A* 1991, **88:**3097-3101.
107. Connor RI, Chen BK, Choe S, Landau NR: **Vpr is required for efficient replication of human immunodeficiency virus type-1 in mononuclear phagocytes.** *Virology* 1995, **206:**935-944.
108. Cheng-Mayer C, Liu R, Landau NR, Stamatatos L: **Macrophage tropism of human immunodeficiency virus type 1 and utilization of the CC-CKR5 coreceptor.** *J Virol* 1997, **71:**1657-1661.
109. Stamatatos L, Lim M, Cheng-Mayer C: **Generation and structural analysis of soluble oligomeric gp140 envelope proteins derived from neutralization-resistant and neutralization-susceptible primary HIV type 1 isolates.** *AIDS Res Hum Retroviruses* 2000, **16:**981-994.

110. Stamatatos L, Wiskerchen M, Cheng-Mayer C: **Effect of major deletions in the V1 and V2 loops of a macrophage-tropic HIV type 1 isolate on viral envelope structure, cell entry, and replication.** *AIDS Res Hum Retroviruses* 1998, **14:**1129-1139.
111. Bax A: **Triple resonance three-dimensional protein NMR: before it became a black box.** *Journal of magnetic resonance* 2011, **213:**442-445.
112. Bax A, Grzesiek S: **Methodological advances in protein NMR.** *Acct Chem Res* 1993, **26:**131-138.
113. Grzesiek S, Bax A: **Correlating backbone amide and side chain resonances in larger proteins by multiple relayed triple resonance NMR.** *J Am Chem Soc* 1992, **114:**6291-6293.
114. Grzesiek S, Bax A: **An efficient experiment for sequential backbone assignment of medium-sized isotopically enriched proteins.** *J Magn Reson* 1992, **99:**201-207.
115. Delaglio F, Grzesiek S, Vuister GW, Hu G, Pfeifer J, Bax A: **NMRPipe: A multidimensional spectral processing system based on UNIX pipes.** *J Biomol NMR* 1995, **6:**277-293.
116. Garrett DS, Powers R, Gronenborn AM, Clore GM: **A common sense approach to peak picking in two-, three-, and four-dimensional spectra using automatic computer analysis of contour diagrams.** *J Magn Reson* 1991, **95:**214-220.
117. **Sparky 3** [http://www.cgl.ucsf.edu/home/sparky/]
118. Johnson BA: **Using NMRView to visualize and analyze the NMR spectra of macromolecules.** In *Methods in molecular biology.* 2nd edition. Totowa, N.J.: Humana Press; 2004: 313-352
119. Garrett DS, Seok YJ, Peterkofsky A, Clore GM, Gronenborn AM: **Identification by NMR of the binding surface for the histidine-containing phosphocarrier protein HPr on the N-terminal domain of enzyme I of the Escherichia coli phosphotransferase system.** *Biochemistry* 1997, **36:**4393-4398.
120. Zhang L, Liwang PJ: **Resonance assignments of the 34 kD rabbitpox vCCI:human MIP-1beta complex.** *J Biomol NMR* 2006, **36 Suppl 1:**49.
121. Eggink D, Melchers M, Wuhrer M, van Montfort T, Dey AK, Naaijkens BA, David KB, Le Douce V, Deelder AM, Kang K, et al: **Lack of complex N-glycans on HIV-1 envelope glycoproteins preserves protein conformation and entry function.** *Virology* 2010, **401:**236-247.
122. **UltraScan version 9.9: A comprehensive data analysis software package for analytical ultracentrifugation experiments** [http://www.ultrascan.uthscsa.edu/]
123. Demeler B: **UltraScan: A Comprehensive Data Analysis Software Package for Analytical Ultracentrifugation Experiments** In *Modern Analytical Ultracentrifugation: Techniques and Methods* Edited by Scott D, Harding S, Rowe A. Cambridge, UK: Royal Society of Chemistry; 2005: 210-229

124. Brookes E, Demeler B: **Parallel computational techniques for the analysis of sedimentation velocity experiments in UltraScan.** *Colloid and Polymer Science* 2008, **286:**139-148.
125. Brookes E, Demeler B, Rosano C, Rocco M: **The implementation of SOMO (SOlution MOdeller) in the UltraScan analytical ultracentrifugation data analysis suite: enhanced capabilities allow the reliable hydrodynamic modeling of virtually any kind of biomacromolecule.** *Eur Biophys J* 2010, **39:**423-435.
126. Brookes E, Demeler B: **Genetic algorithm optimization for obtaining accurate molecular weight distributions from sedimentation velocity experiments.** *Analytical Ultracentrifugation VIII* 2006, **131:**33-40.
127. Demeler B, van Holde KE: **Sedimentation velocity analysis of highly heterogeneous systems.** *Analytical Biochemistry* 2004, **335:**279-288.
128. Brookes EH, Demeler B: **Parsimonious Regularization using Genetic Algorithms Applied to the Analysis of Analytical Ultracentrifugation Experiments.** *Gecco 2007: Genetic and Evolutionary Computation Conference, Vol 1 and 2* 2007**:**361-368.
129. Demeler B, Brookes E: **Monte Carlo analysis of sedimentation experiments.** *Colloid and Polymer Science* 2008, **286:**129-137.
130. Kagiampakis I, Gharibi A, Mankowski MK, Snyder BA, Ptak RG, Alatas K, LiWang PJ: **Potent strategy to inhibit HIV-1 by binding both gp120 and gp41.** *Antimicrob Agents Chemother* 2011, **55:**264-275.
131. Demeler B, Saber H, Hansen JC: **Identification and interpretation of complexity in sedimentation velocity boundaries.** *Biophysical Journal* 1997, **72:**397-407.
132. Brookes E, Boppana RV, Demeler B: **Computing Large Sparse Multivariate Optimization Problems with an Application in Biophysics.** *Supercomputing '06 ACM 0-7695-2700-0/06* 2006.
133. Brookes E, Cao W, Demeler B: **A two-dimensional spectrum analysis for sedimentation velocity experiments of mixtures with heterogeneity in molecular weight and shape.** *Eur Biophys J* 2010, **39:**405-414.
134. Hoorelbeke B, Huskens D, Ferir G, Francois KO, Takahashi A, Van Laethem K, Schols D, Tanaka H, Balzarini J: **Actinohivin, a broadly neutralizing prokaryotic lectin, inhibits HIV-1 infection by specifically targeting high-mannose-type glycans on the gp120 envelope.** *Antimicrob Agents Chemother* 2010, **54:**3287-3301.
135. Hoorelbeke B, Van Damme EJ, Rouge P, Schols D, Van Laethem K, Fouquaert E, Balzarini J: **Differences in the mannose oligomer specificities of the closely related lectins from Galanthus nivalis and Zea mays strongly determine their eventual anti-HIV activity.** *Retrovirology* 2011, **8:**10.
136. Furuta RA, Wild CT, Weng Y, Weiss CD: **Capture of an early fusion-active conformation of HIV-1 gp41.[erratum appears in Nat Struct Biol 1998 Jul;5(7):612].** *Nature Structural Biology* 1998, **5:**276-279.

137. Reeves JD, Gallo SA, Ahmad N, Miamidian JL, Harvey PE, Sharron M, Pohlmann S, Sfakianos JN, Derdeyn CA, Blumenthal R, et al: **Sensitivity of HIV-1 to entry inhibitors correlates with envelope/coreceptor affinity, receptor density, and fusion kinetics.** *Proceedings of the National Academy of Sciences of the United States of America* 2002, **99:**16249-16254.
138. Balzarini J, Van Laethem K, Hatse S, Vermeire K, De Clercq E, Peumans W, Van Damme E, Vandamme AM, Bolmstedt A, Schols D: **Profile of resistance of human immunodeficiency virus to mannose-specific plant lectins.** *Journal of virology* 2004, **78:**10617-10627.
139. Zeitlin L, Pauly M, Whaley KJ: **Second-generation HIV microbicides: continued development of griffithsin.** *Proc Natl Acad Sci U S A* 2009, **106:**6029-6030.
140. Leonard CK, Spellman MW, Riddle L, Harris RJ, Thomas JN, Gregory TJ: **Assignment of intrachain disulfide bonds and characterization of potential glycosylation sites of the type 1 recombinant human immunodeficiency virus envelope glycoprotein (gp120) expressed in Chinese hamster ovary cells.** *J Biol Chem* 1990, **265:**10373-10382.
141. Balzarini J: **Carbohydrate-binding agents: a potential future cornerstone for the chemotherapy of enveloped viruses?** *Antivir Chem Chemother* 2007, **18:**1-11.
142. O'Keefe BR, Giomarelli B, Barnard DL, Shenoy SR, Chan PK, McMahon JB, Palmer KE, Barnett BW, Meyerholz DK, Wohlford-Lenane CL, McCray PB, Jr.: **Broad-spectrum in vitro activity and in vivo efficacy of the antiviral protein griffithsin against emerging viruses of the family Coronaviridae.** *J Virol* 2010, **84:**2511-2521.
143. Alexandre KB, Gray ES, Pantophlet R, Moore PL, McMahon JB, Chakauya E, O'Keefe BR, Chikwamba R, Morris L: **Binding of the mannose-specific lectin, griffithsin, to HIV-1 gp120 exposes the CD4-binding site.** *J Virol* 2011, **85:**9039-9050.
144. Pejchal R, Doores KJ, Walker LM, Khayat R, Huang PS, Wang SK, Stanfield RL, Julien JP, Ramos A, Crispin M, et al: **A potent and broad neutralizing antibody recognizes and penetrates the HIV glycan shield.** *Science* 2011, **334:**1097-1103.
145. Walker LM, Huber M, Doores KJ, Falkowska E, Pejchal R, Julien JP, Wang SK, Ramos A, Chan-Hui PY, Moyle M, et al: **Broad neutralization coverage of HIV by multiple highly potent antibodies.** *Nature* 2011, **477:**466-470.
146. Moscoso CG, Sun Y, Poon S, Xing L, Kan E, Martin L, Green D, Lin F, Vahlne AG, Barnett S, et al: **Quaternary structures of HIV Env immunogen exhibit conformational vicissitudes and interface diminution elicited by ligand binding.** *Proceedings of the National Academy of Sciences of the United States of America* 2011, **108:**6091-6096.

147. Xue J, Hoorelbeke B, Kagiampakis I, Demeler B, Balzarini J, Liwang PJ: **The griffithsin dimer is required for high-potency inhibition of HIV-1: evidence for manipulation of the structure of gp120 as part of the griffithsin dimer mechanism.** *Antimicrob Agents Chemother* 2013, **57:**3976-3989.
148. Quinones-Mateu ME, Vanham G: **HIV microbicides: where are we now?** *Current HIV research* 2012, **10:**1-2.
149. Selhorst P, Vazquez AC, Terrazas-Aranda K, Michiels J, Vereecken K, Heyndrickx L, Weber J, Quinones-Mateu ME, Arien KK, Vanham G: **Human immunodeficiency virus type 1 resistance or cross-resistance to nonnucleoside reverse transcriptase inhibitors currently under development as microbicides.** *Antimicrobial agents and chemotherapy* 2011, **55:**1403-1413.
150. Barrientos LG, Gronenborn AM: **The highly specific carbohydrate-binding protein cyanovirin-N: structure, anti-HIV/Ebola activity and possibilities for therapy.** *Mini Rev Med Chem* 2005, **5:**21-31.
151. Tanaka H, Chiba H, Inokoshi J, Kuno A, Sugai T, Takahashi A, Ito Y, Tsunoda M, Suzuki K, Takenaka A, et al: **Mechanism by which the lectin actinohivin blocks HIV infection of target cells.** *Proc Natl Acad Sci U S A* 2009, **106:**15633-15638.
152. Hu Q, Mahmood N, Shattock RJ: **High-mannose-specific deglycosylation of HIV-1 gp120 induced by resistance to cyanovirin-N and the impact on antibody neutralization.** *Virology* 2007, **368:**145-154.
153. Moncla BJ, Pryke K, Rohan LC, Graebing PW: **Degradation of naturally occurring and engineered antimicrobial peptides by proteases.** *Adv Biosci Biotechnol* 2011, **2:**404-408.
154. Demeler B: **Methods for the design and analysis of sedimentation velocity and sedimentation equilibrium experiments with proteins.** *Curr Protoc Protein Sci* 2010, **Chapter 7:**Unit 7 13.
155. Li M, Gao F, Mascola JR, Stamatatos L, Polonis VR, Koutsoukos M, Voss G, Goepfert P, Gilbert P, Greene KM, et al: **Human immunodeficiency virus type 1 env clones from acute and early subtype B infections for standardized assessments of vaccine-elicited neutralizing antibodies.** *J Virol* 2005, **79:**10108-10125.
156. Li M, Salazar-Gonzalez JF, Derdeyn CA, Morris L, Williamson C, Robinson JE, Decker JM, Li Y, Salazar MG, Polonis VR, et al: **Genetic and neutralization properties of subtype C human immunodeficiency virus type 1 molecular env clones from acute and early heterosexually acquired infections in Southern Africa.** *J Virol* 2006, **80:**11776-11790.
157. Derdeyn CA, Decker JM, Bibollet-Ruche F, Mokili JL, Muldoon M, Denham SA, Heil ML, Kasolo F, Musonda R, Hahn BH, et al: **Envelope-constrained neutralization-sensitive HIV-1 after heterosexual transmission.** *Science* 2004, **303:**2019-2022.

158. Wei X, Decker JM, Liu H, Zhang Z, Arani RB, Kilby JM, Saag MS, Wu X, Shaw GM, Kappes JC: **Emergence of resistant human immunodeficiency virus type 1 in patients receiving fusion inhibitor (T-20) monotherapy.** *Antimicrob Agents Chemother* 2002, **46:**1896-1905.
159. Wei X, Decker JM, Wang S, Hui H, Kappes JC, Wu X, Salazar-Gonzalez JF, Salazar MG, Kilby JM, Saag MS, et al: **Antibody neutralization and escape by HIV-1.** *Nature* 2003, **422:**307-312.
160. Scanlan CN, Pantophlet R, Wormald MR, Ollmann Saphire E, Stanfield R, Wilson IA, Katinger H, Dwek RA, Rudd PM, Burton DR: **The broadly neutralizing anti-human immunodeficiency virus type 1 antibody 2G12 recognizes a cluster of alpha1-->2 mannose residues on the outer face of gp120.** *J Virol* 2002, **76:**7306-7321.
161. Trkola A, Purtscher M, Muster T, Ballaun C, Buchacher A, Sullivan N, Srinivasan K, Sodroski J, Moore JP, Katinger H: **Human monoclonal antibody 2G12 defines a distinctive neutralization epitope on the gp120 glycoprotein of human immunodeficiency virus type 1.** *J Virol* 1996, **70:**1100-1108.
162. Li Y, O'Dell S, Walker LM, Wu X, Guenaga J, Feng Y, Schmidt SD, McKee K, Louder MK, Ledgerwood JE, et al: **Mechanism of neutralization by the broadly neutralizing HIV-1 monoclonal antibody VRC01.** *J Virol* 2011, **85:**8954-8967.
163. Wu SR, Loving R, Lindqvist B, Hebert H, Koeck PJ, Sjoberg M, Garoff H: **Single-particle cryoelectron microscopy analysis reveals the HIV-1 spike as a tripod structure.** *Proc Natl Acad Sci U S A* 2010, **107:**18844-18849.
164. Mao Y, Wang L, Gu C, Herschhorn A, Xiang SH, Haim H, Yang X, Sodroski J: **Subunit organization of the membrane-bound HIV-1 envelope glycoprotein trimer.** *Nat Struct Mol Biol* 2012, **19:**893-899.
165. Hoorelbeke B, van Montfort T, Xue J, LiWang PJ, Tanaka H, Igarashi Y, Van Damme EJ, Sanders RW, Balzarini J: **HIV-1 envelope trimer has similar binding characteristics for carbohydrate-binding agents as monomeric gp120.** *FEBS Lett* 2013, **587:**860-866.
166. Mouquet H, Nussenzweig MC: **Polyreactive antibodies in adaptive immune responses to viruses.** *Cell Mol Life Sci* 2012, **69:**1435-1445.
167. Binley JM, Sanders RW, Clas B, Schuelke N, Master A, Guo Y, Kajumo F, Anselma DJ, Maddon PJ, Olson WC, Moore JP: **A recombinant human immunodeficiency virus type 1 envelope glycoprotein complex stabilized by an intermolecular disulfide bond between the gp120 and gp41 subunits is an antigenic mimic of the trimeric virion-associated structure.** *J Virol* 2000, **74:**627-643.
168. McCaffrey RA, Saunders C, Hensel M, Stamatatos L: **N-linked glycosylation of the V3 loop and the immunologically silent face of gp120 protects human immunodeficiency virus type 1 SF162 from neutralization by anti-gp120 and anti-gp41 antibodies.** *J Virol* 2004, **78:**3279-3295.

169. Moore JP, McKeating JA, Weiss RA, Sattentau QJ: **Dissociation of gp120 from HIV-1 virions induced by soluble CD4.** *Science* 1990, **250:**1139-1142.
170. Thali M, Furman C, Helseth E, Repke H, Sodroski J: **Lack of correlation between soluble CD4-induced shedding of the human immunodeficiency virus type 1 exterior envelope glycoprotein and subsequent membrane fusion events.** *Journal of virology* 1992, **66:**5516-5524.
171. Fischer PB, Karlsson GB, Dwek RA, Platt FM: **N-butyldeoxynojirimycin-mediated inhibition of human immunodeficiency virus entry correlates with impaired gp120 shedding and gp41 exposure.** *J Virol* 1996, **70:**7153-7160.
172. Ringe R, Bhattacharya J: **Association of enhanced HIV-1 neutralization by a single Y681H substitution in gp41 with increased gp120-CD4 interaction and macrophage infectivity.** *PLoS One* 2012, **7:**e37157.
173. Zhang MY, Yuan T, Li J, Rosa Borges A, Watkins JD, Guenaga J, Yang Z, Wang Y, Wilson R, Li Y, et al: **Identification and characterization of a broadly cross-reactive HIV-1 human monoclonal antibody that binds to both gp120 and gp41.** *PLoS One* 2012, **7:**e44241.
174. Balzarini J, Schols D, Neyts J, Van Damme E, Peumans W, De Clercq E: **Alpha-(1-3)- and alpha-(1-6)-D-mannose-specific plant lectins are markedly inhibitory to human immunodeficiency virus and cytomegalovirus infections in vitro.** *Antimicrob Agents Chemother* 1991, **35:**410-416.
175. Balzarini J, Hatse S, Vermeire K, Princen K, Aquaro S, Perno CF, De Clercq E, Egberink H, Vanden Mooter G, Peumans W, et al: **Mannose-specific plant lectins from the Amaryllidaceae family qualify as efficient microbicides for prevention of human immunodeficiency virus infection.** *Antimicrobial agents and chemotherapy* 2004, **48:**3858-3870.
176. Barrientos LG, Lasala F, Delgado R, Sanchez A, Gronenborn AM: **Flipping the switch from monomeric to dimeric CV-N has little effect on antiviral activity.** *Structure* 2004, **12:**1799-1807.
177. Bewley CA, Gustafson KR, Boyd MR, Covell DG, Bax A, Clore MG, Gronenborn AM: **Solution structure of cyanovirin-N, a potent HIV-inactivating protein.** *Nat Struct Biol* 1998, **5:**571-578.
178. Banerjee K, Michael E, Eggink D, van Montfort T, Lasnik AB, Palmer KE, Sanders RW, Moore JP, Klasse PJ: **Occluding the mannose moieties on human immunodeficiency virus type 1 gp120 with griffithsin improves the antibody responses to both proteins in mice.** *AIDS Res Hum Retroviruses* 2012, **28:**206-214.
179. Moore JP, Sodroski J: **Antibody cross-competition analysis of the human immunodeficiency virus type 1 gp120 exterior envelope glycoprotein.** *J Virol* 1996, **70:**1863-1872.

180. Calarese DA, Scanlan CN, Zwick MB, Deechongkit S, Mimura Y, Kunert R, Zhu P, Wormald MR, Stanfield RL, Roux KH, et al: **Antibody domain exchange is an immunological solution to carbohydrate cluster recognition.** *Science* 2003, **300:**2065-2071.
181. West AP, Jr., Galimidi RP, Foglesong CP, Gnanapragasam PN, Huey-Tubman KE, Klein JS, Suzuki MD, Tiangco NE, Vielmetter J, Bjorkman PJ: **Design and expression of a dimeric form of human immunodeficiency virus type 1 antibody 2G12 with increased neutralization potency.** *J Virol* 2009, **83:**98-104.
182. Luo XM, Lei MY, Feidi RA, West AP, Jr., Balazs AB, Bjorkman PJ, Yang L, Baltimore D: **Dimeric 2G12 as a potent protection against HIV-1.** *PLoS Pathog* 2010, **6:**e1001225.
183. Sanders RW, Venturi M, Schiffner L, Kalyanaraman R, Katinger H, Lloyd KO, Kwong PD, Moore JP: **The mannose-dependent epitope for neutralizing antibody 2G12 on human immunodeficiency virus type 1 glycoprotein gp120.** *J Virol* 2002, **76:**7293-7305.
184. Cernak I, Noble-Haeusslein LJ: **Traumatic brain injury: an overview of pathobiology with emphasis on military populations.** *J Cereb Blood Flow Metab* 2010, **30:**255-266.
185. Bellamy-McIntyre AK, Lay CS, Baar S, Maerz AL, Talbo GH, Drummer HE, Poumbourios P: **Functional links between the fusion peptide-proximal polar segment and membrane-proximal region of human immunodeficiency virus gp41 in distinct phases of membrane fusion.** *The Journal of biological chemistry* 2007, **282:**23104-23116.
186. Fontenot D, Jones JK, Hossain MM, Nehete PN, Vela EM, Dwyer VA, Jagannadha Sastry K: **Critical role of Arg59 in the high-affinity gp120-binding region of CD4 for human immunodeficiency virus type 1 infection.** *Virology* 2007, **363:**69-78.
187. Li M, Patton DL, Cosgrove-Sweeney Y, Ratner D, Rohan LC, Cole AM, Tarwater PM, Gupta P, Ramratnam B: **Incorporation of the HIV-1 microbicide cyanovirin-N in a food product.** *J Acquir Immune Defic Syndr* 2011, **58:**379-384.
188. DeBruyne LA, Li K, Bishop DK, Bromberg JS: **Gene transfer of virally encoded chemokine antagonists vMIP-II and MC148 prolongs cardiac allograft survival and inhibits donor-specific immunity.** *Gene Therapy* 2000, **7:**575-582.
189. Pillai RG, Beutelspacher SC, Larkin DF, George AJ: **Expression of the chemokine antagonist vMIP II using a non-viral vector can prolong corneal allograft survival.** *Transplantation* 2008, **85:**1640-1647.
190. Eng LF, Lee YL: **Response of chemokine antagonists to inflammation in injured spinal cord.** *Neurochem Res* 2003, **28:**95-100.
191. Ghirnikar RS, Lee YL, Eng LF: **Chemokine antagonist infusion attenuates cellular infiltration following spinal cord contusion injury in rat.** *Journal of Neuroscience Research* 2000, **59:**63-73.

192. Ghirnikar RS, Lee YL, Eng LF: **Chemokine antagonist infusion promotes axonal sparing after spinal cord contusion injury in rat.** *Journal of Neuroscience Research* 2001, **64:**582-589.
193. Takami S, Minami M, Nagata I, Namura S, Satoh M: **Chemokine receptor antagonist peptide, viral MIP-II, protects the brain against focal cerebral ischemia in mice.** *Journal of Cerebral Blood Flow & Metabolism* 2001, **21:**1430-1435.
194. Deng H, Liu R, Ellmeier W, Choe S, Unutmaz D, Burkhart M, Di Marzio P, Marmon S, Sutton RE, Hill CM, Davis, C.B., et al: **Identification of a major co-receptor for primary isolates of HIV-1.** *Nature* 1996, **381:**661-666.
195. Alkhatib G, Combadiere C, Broder CC, Feng Y, Kennedy PE, Murphy PM, Berger EA: **CC CKR5: A RANTES, MIP-1a, MIP-1b receptor as a fusion cofactor for macrophage-tropic HIV-1.** *Science* 1996, **272:**1955-1958.
196. Bleul CC, Farzan M, Choe H, Parolin C, Clark-Lewis I, Sodroski J, Springer TA: **The lymphocyte chemoattractant SDF-1 is a ligand for LESTR/fusin and blocks HIV-1 entry.** *Nature* 1996, **382:**829-833.
197. Oberlin E, Amara A, Bachelerie F, Bessia C, Virelizier JL, Arenzana-Seisdedos F, Schwartz O, Heard JM, Clark-Lewis I, Legler DF, et al: **The CXC chemokine SDF-1 is the ligand for LESTR/fusin and prevents infection by T-cell-line-adapted HIV-1.** *Nature* 1996, **382:**833-835.
198. Hartley O, Gaertner H, Wilken J, Thompson D, Fish R, Ramos A, Pastore C, Dufour B, Cerini F, Melotti A, et al: **Medicinal chemistry applied to a synthetic protein: development of highly potent HIV entry inhibitors.** *Proceedings of the National Academy of Sciences of the United States of America* 2004, **101:**16460-16465.
199. Veazey RS, Ling B, Green LC, Ribka EP, Lifson JD, Piatak M, Jr., Lederman MM, Mosier D, Offord R, Hartley O: **Topically applied recombinant chemokine analogues fully protect macaques from vaginal simian-human immunodeficiency virus challenge.** *J Infect Dis* 2009, **199:**1525-1527.
200. Dudley DM, Wentzel JL, Lalonde MS, Veazey RS, Arts EJ: **Selection of a simian-human immunodeficiency virus strain resistant to a vaginal microbicide in macaques.** *J Virol* 2009, **83:**5067-5076.
201. Lederman MM, Veazey RS, Offord R, Mosier DE, Dufour J, Mefford M, Piatak M, Jr., Lifson JD, Salkowitz JR, Rodriguez B, et al: **Prevention of vaginal SHIV transmission in rhesus macaques through inhibition of CCR5.[see comment].** *Science* 2004, **306:**485-487.
202. Townson JR, Graham GJ, Landau NR, Rasala B, Nibbs RJ: **Aminooxypentane addition to the chemokine macrophage inflammatory protein-1alpha P increases receptor affinities and HIV inhibition.** *J Biol Chem* 2000, **275:**39254-39261.
203. Nedellec R, Coetzer M, Lederman MM, Offord RE, Hartley O, Mosier DE: **Resistance to the CCR5 inhibitor 5P12-RANTES requires a difficult**

evolution from CCR5 to CXCR4 coreceptor use. *PloS one* 2011, **6:**e22020.

204. Skelton NJ, Aspiras F, Ogez J, Schall TJ: **Proton NMR assignments and solution conformation of RANTES, a chemokine of the C-C type.** *Biochemistry* 1995, **34:**5329-5342.
205. Lodi PJ, Garrett DS, Kuszewski J, Tsang ML-S, Weatherbee JA, Leonard WJ, Gronenborn AM, Clore GM: **High-resolution solution structure of the beta chemokine hMIP-1b by multidimensional NMR.** *Science* 1994, **263:**1762-1767.
206. Czaplewski LG, McKeating J, Craven CJ, Higgins LD, Appay V, Brown A, Dudgeon T, Howard LA, Meyers T, Owen J, et al: **Identification of amino acid residues critical for aggregation of human CC chemokines Macrophage Inflammatory Protein (MIP)-1α, MIP-1β, and RANTES.** *J Biol Chem* 1999, **274:**16077-16084.
207. Navenot JM, Wang ZX, Trent JO, Murray JL, Hu QX, DeLeeuw L, Moore PS, Chang Y, Peiper SC: **Molecular anatomy of CCR5 engagement by physiologic and viral chemokines and HIV-1 envelope glycoproteins: differences in primary structural requirements for RANTES, MIP-1 alpha, and vMIP-II Binding.** *Journal of Molecular Biology* 2001, **313:**1181-1193.
208. Page KA, Landau NR, Littman DR: **Construction and use of a human immunodeficiency virus vector for analysis of virus infectivity.** *J Virol* 1990, **64:**5270-5276.
209. Seaman MS, Janes H, Hawkins N, Grandpre LE, Devoy C, Giri A, Coffey RT, Harris L, Wood B, Daniels MG, et al: **Tiered categorization of a diverse panel of HIV-1 Env pseudoviruses for assessment of neutralizing antibodies.** *J Virol* 2010, **84:**1439-1452.
210. Moore PS, Boshoff C, Weiss RA, Chang Y: **Molecular mimicry of human cytokine and cytokine response pathway genes by KSHV.** *Science* 1996, **274:**1739-1744.
211. LiWang AC, Cao JJ, Zheng H, Lu Z, Peiper SC, LiWang PJ: **Dynamics Study on the anti-human immunodieficiency virus chemokine viral macrophage inflammatory protein-II (vMIP-II) reveals a fully monomeric protein.** *Biochemistry* 1999, **38:**442-453.
212. Shao W, Fernandez E, Wilken J, Thompson DA, Siani MA, West J, Lolis E, Schweitzer BI: **Accessibility of selenomethionine proteins by total chemical synthesis: structural studies of human herpesvirus-8 MIP-II.** *FEBS Letters* 1998, **441:**77-82.
213. Crump MP, Elisseeva E, Gong J, Clark-Lewis I, Sykes BD: **Structure/function of human herpesvirus-8 MIP-II (1-71) and the antagonist N-terminal segment (1-10).** *FEBS Letters* 2001, **489:**171-175.
214. Luo Z, Fan X, Zhou N, Hiraoka M, Luo J, Kaji H, Huang Z: **Structure-function study and anti-HIV activity of synthetic peptide analogues derived from viral chemokine vMIP-II.** *Biochemistry* 2000, **39:**13545-13550.

215. Zhou N, Luo Z, Luo J, Fan X, Cayabyab M, Hiraoka M, Liu D, Han X, Pesavento J, Dong CZ, et al: **Exploring the stereochemistry of CXCR4-peptide recognition and inhibiting HIV-1 entry with D-peptides derived from chemokines.** *J Biol Chem* 2002, **277:**17476-17485.
216. Choi WT, Kumar S, Madani N, Han X, Tian S, Dong CZ, Liu D, Duggineni S, Yuan J, Sodroski JG, et al: **A novel synthetic bivalent ligand to probe chemokine receptor CXCR4 dimerization and inhibit HIV-1 entry.** *Biochemistry* 2012, **51:**7078-7086.
217. Wang J, Kumar S, Choi WT, Dong C, Huang Z: **Design and synthesis of novel chemokine analogs derived from vMIP-II.** *Protein Pept Lett* 2006, **13:**499-501.
218. Laurence JS, Blanpain C, Parmentier M, Burgner JW, LiWang PJ: **The CC chemokine MIP-1β can function as a monomer and depends on Phe13 for receptor binding.** *Biochemistry* 2000, **39:**3401-3409.
219. Pakianathan DR, Kuta EG, Artis DR, Skelton NJ, Hebert CA: **Distinct but overlapping epitopes for the interaction of a CC-chemokine with CCR1, CCR3 and CCR5.** *Biochemistry* 1997, **36:**9642-9648.
220. Giomarelli B, Schumacher KM, Taylor TE, Sowder RC, 2nd, Hartley JL, McMahon JB, Mori T: **Recombinant production of anti-HIV protein, griffithsin, by auto-induction in a fermentor culture.** *Protein Expr Purif* 2006, **47:**194-202.
221. Liu Y, Carroll JR, Holt LA, McMahon J, Giomarelli B, Ghirlanda G: **Multivalent interactions with gp120 are required for the anti-HIV activity of Cyanovirin.** *Biopolymers* 2009, **92:**194-200.
222. Yang F, Bewley CA, Louis JM, Gustafson KR, Boyd MR, Gronenborn AM, Clore GM, Wlodawer A: **Crystal structure of cyanovirin-N, a potent HIV-inactivating protein, shows unexpected domain swapping.** *J Mol Biol* 1999, **288:**403-412.
223. Matei E, Furey W, Gronenborn AM: **Solution and crystal structures of a sugar binding site mutant of cyanovirin-N: no evidence of domain swapping.** *Structure* 2008, **16:**1183-1194.
224. Salzwedel K, Berger EA: **Complementation of diverse HIV-1 Env defects through cooperative subunit interactions: a general property of the functional trimer.** *Retrovirology* 2009, **6:**75.
225. Kopetzki E, Jekle A, Ji C, Rao E, Zhang J, Fischer S, Cammack N, Sankuratri S, Heilek G: **Closing two doors of viral entry: intramolecular combination of a coreceptor- and fusion inhibitor of HIV-1.** *Virol J* 2008, **5:**56.
226. Ndung'u T, Sepako E, McLane MF, Chand F, Bedi K, Gaseitsiwe S, Doualla-Bell F, Peter T, Thior I, Moyo SM, et al: **HIV-1 subtype C in vitro growth and coreceptor utilization.** *Virology* 2006, **347:**247-260.
227. Cecilia D, Kulkarni SS, Tripathy SP, Gangakhedkar RR, Paranjape RS, Gadkari DA: **Absence of coreceptor switch with disease progression in human immunodeficiency virus infections in India.** *Virology* 2000, **271:**253-258.

Appendix A

Supporting information for Chapter 2

Supporting Information available: chemical shift changes of GRFT upon addition of mannose or changes upon mutation of three carbohydrate binding sites; NMR spectra of GRFT single point mutation D70A, D112A and Triple mutation D30A/D70A/D112A; van Holde-Weischet G(s) sedimentation coefficient distributions of GRFT Triple mutation; surface plasmon resonance sensorgrams of GRFT variants binding to gp120 III_B and gp41 H_XB2 strains; NMR spectrum of GRFT D30A/D70A/D112A in the presence of mannose.

Table A-1. Chemical shift changes of GRFT upon mutation of one of the 3 mannose binding sites or upon addition of mannose, as determined by NMR spectroscopy.

Mutants/ mannose titration	Chemical shift changes: Average + 1 SD	Chemical shift changes: Average + 2 SDs	Residues impossible to follow
D30A	A22, S25, A31, I32, I72, G83, G86, D109	S47, N71, G89， L111	G26, L29, N45
D70A	G8, G9, Y28, Y85, S91, L111	G26, L29, G66, G87	D67, Y68, I69, S88
D112A	F7, G26, L29, A31, I69, N71, N93, Y110, L111, Y117	G8, G66	S10, G12, D30, G41, S106, A107, G108, D109,
Mannose titration	G41, S42, Y68, S73, G86, A107	G8, A31, N45, I69, S91, Y110, D112, S113	G9, G12, G26, L29, S54, G66, N71, G90, G108,

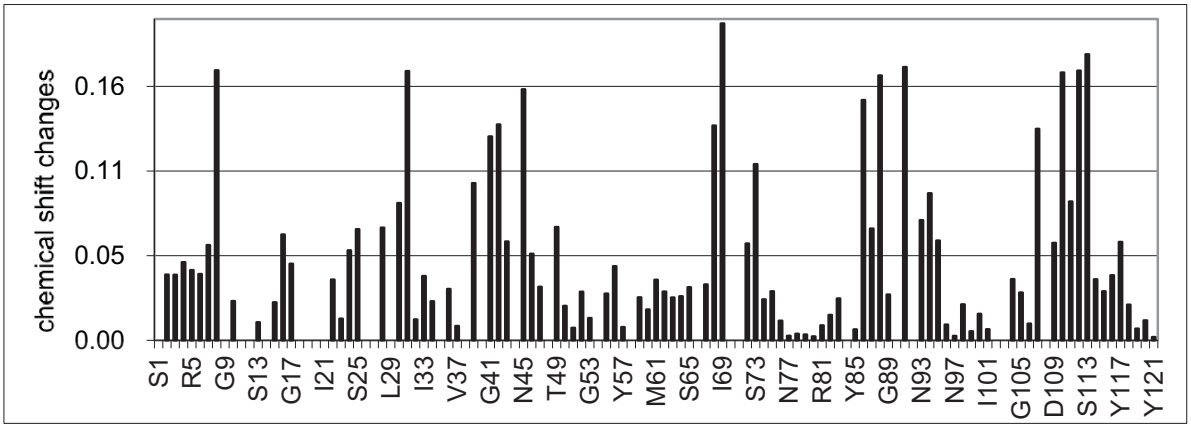

Figure A-1. Bar graph showing changes in chemical shift by titration of mannose in wild-type GRFT, as determined by NMR spectroscopy.

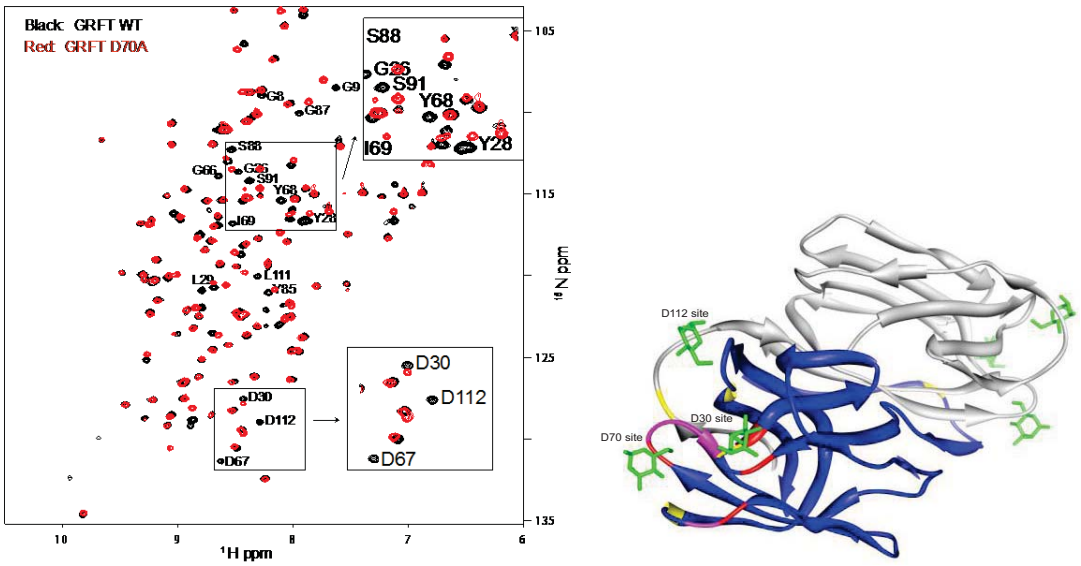

Figure A-2: Structure of GRFT single point mutant D70A.

Left: ^{15}N HSQC spectrum of GRFT D70A (red) overlaid with the spectrum of wild-type GRFT. Some peaks with significant movement upon mutation are labeled. Labeled peaks are those that have chemical shift changed by 2 standard deviations from the average.

Right: Structure of GRFT showing regions that have chemical shift change upon mutation of the mannose site at D70. Yellow indicates chemical shift change that is 1 standard deviation greater than average, red indicates chemical shift change that is 2 standard deviations greater than average, and magenta indicates peaks that disappear or that have moved too much to assign upon mutation. Mannose residues are shown in green. Residue G9 is from the domain-swapped other subunit. Structure is 2gud from (Ziolkowska, 2006).

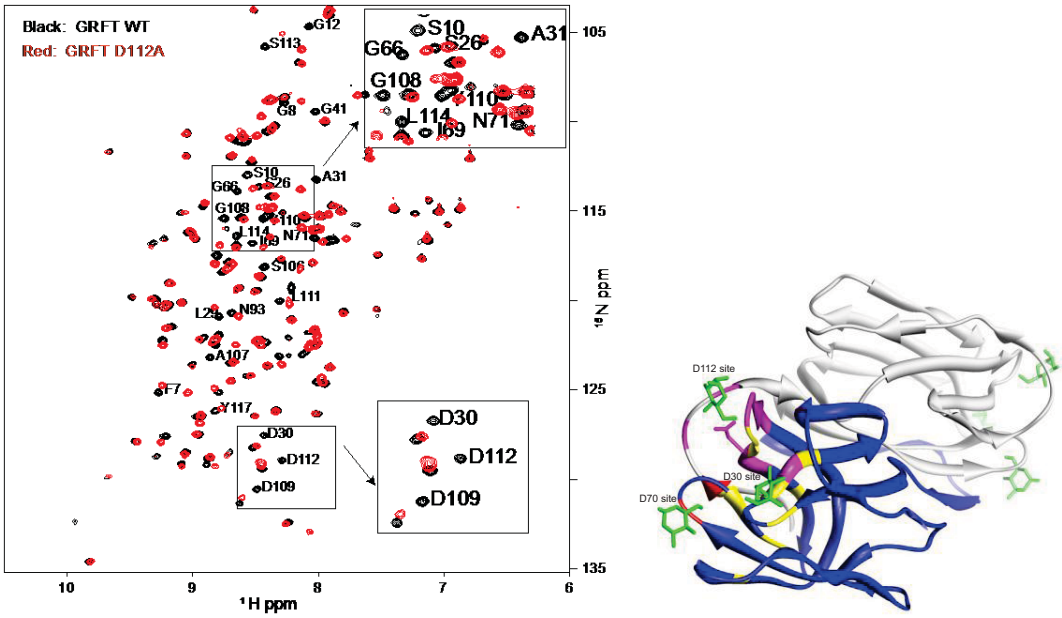

Figure A-3: Structure of GRFT single point mutant D112A.

Left. ^{15}N HSQC spectrum of GRFT D112A (red) overlaid with the spectrum of wild-type GRFT. Some peaks with significant movement upon mutation are labeled. Labeled peaks are those that have chemical shift changed by 2 standard deviations from the average.

Right. Structure of GRFT showing regions that have chemical shift changes upon mutation of the mannose site at D112. Yellow indicates chemical shift change that is 1 standard deviation greater than average, red indicates chemical shift change that is 2 standard deviations greater than average, and magenta indicates peaks that disappear or that have moved too much to assign upon mutation. Mannose residues are shown in green. Residues F7, G8, S10, S12 are from the domain-swapped other subunit. Structure is 2gud from (Ziolkowska, 2006)

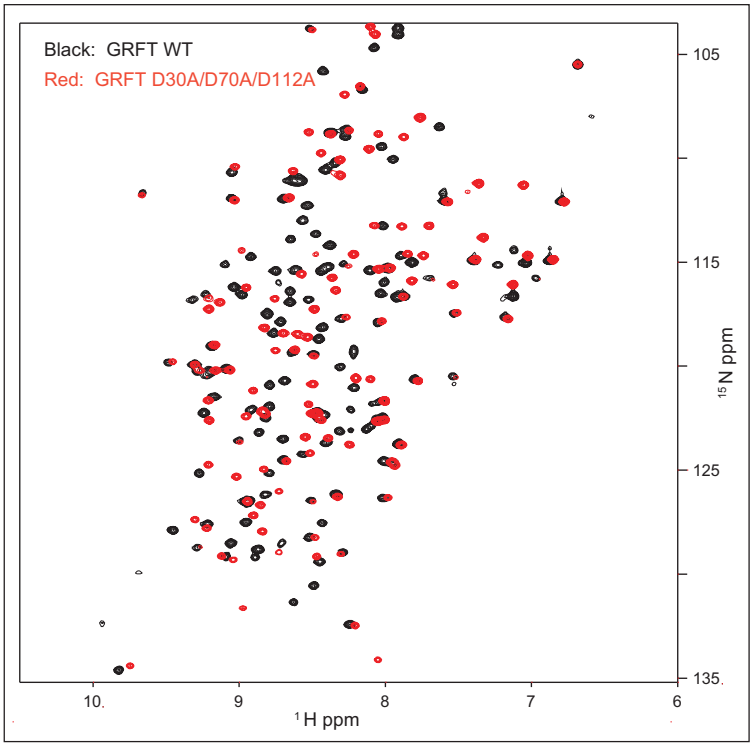

Figure A-4. ^{15}N HSQC spectrum of GRFT D30A/D70A/D112A (Triple) mutation (red) overlaid with the spectrum of wild type GRFT.

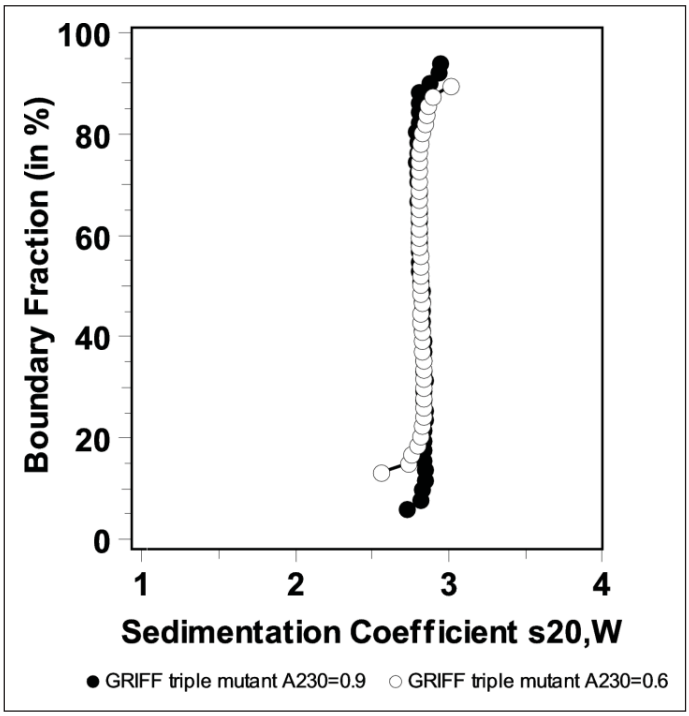

Figure A-5. Van Holde - Weischet G(s) sedimentation coefficient distributions of GRFT Triple mutant D30A/D70A/D112A at 2 concentrations.

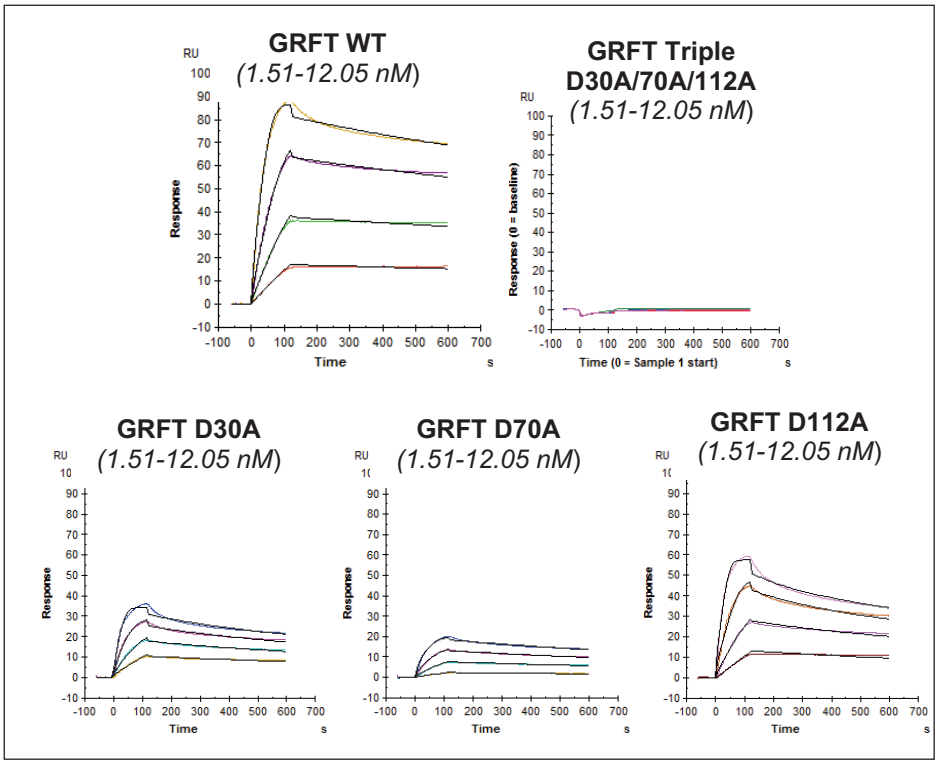

Figure A-6. Kinetic analysis of the interactions of GRFT and mutants with immobilized HIV-1 III_B gp120.

Serial two-fold analyte dilutions (covering a concentration range from 1.51 to 12.05 nM) were injected over the surface of the immobilized gp120. The experimental data (coloured curves) were fit using the 1:1 binding model (black lines) to determine the kinetic parameters. The biosensor chip density was 140 RU.

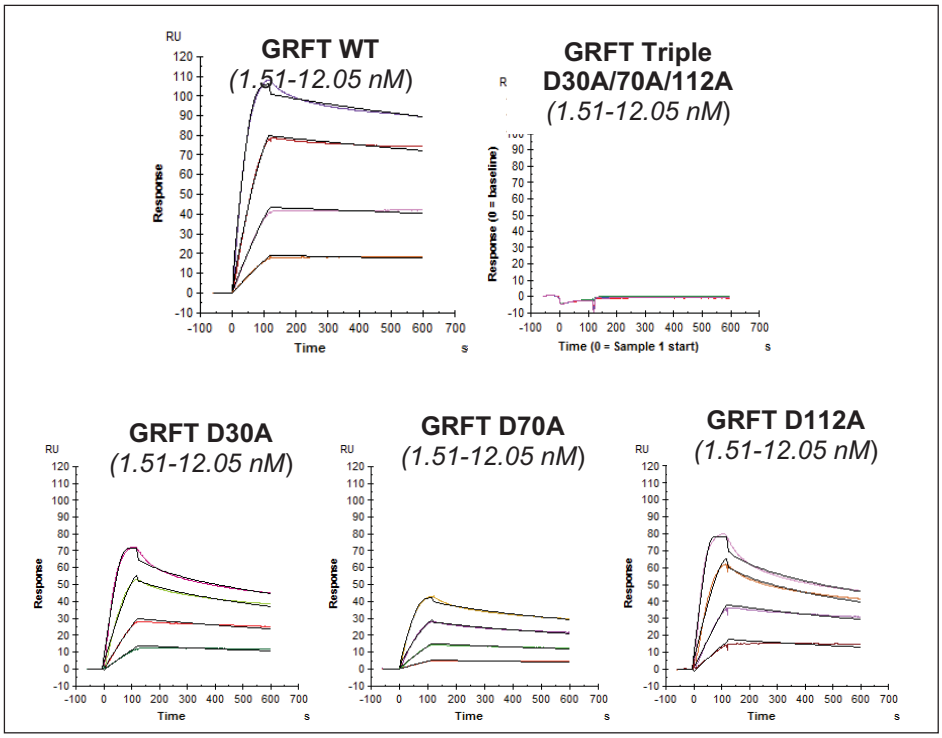

Figure A-7. Kinetic analysis of the interactions of GRFT and mutants with immobilized HIV-1 HxB2 gp41.

Serial two-fold sample dilutions (covering a concentration range from 1.51 to 12.05 nM) were injected over the surface of the immobilized gp120. The experimental data (colored curves) were fit using the 1:1 binding model (black lines) to determine the kinetic parameters. The biosensor chip density was 240 RU.

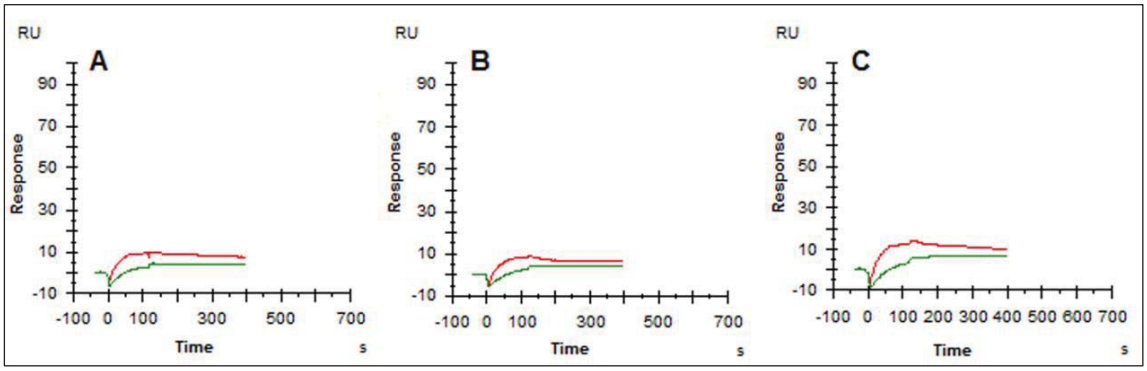

Figure A-8. Surface plasmon resonance analysis of GRFT D30A/D70A/D112A with immobilized HIV-1 ADA gp120 (Panel A), HIV-1 III_B gp120 (Panel B) and HIV-1 HxB2 gp41 (Panel C).

48.2 and 24.1 nM of GRFT mutants were injected over the surface of the immobilized envelope proteins.

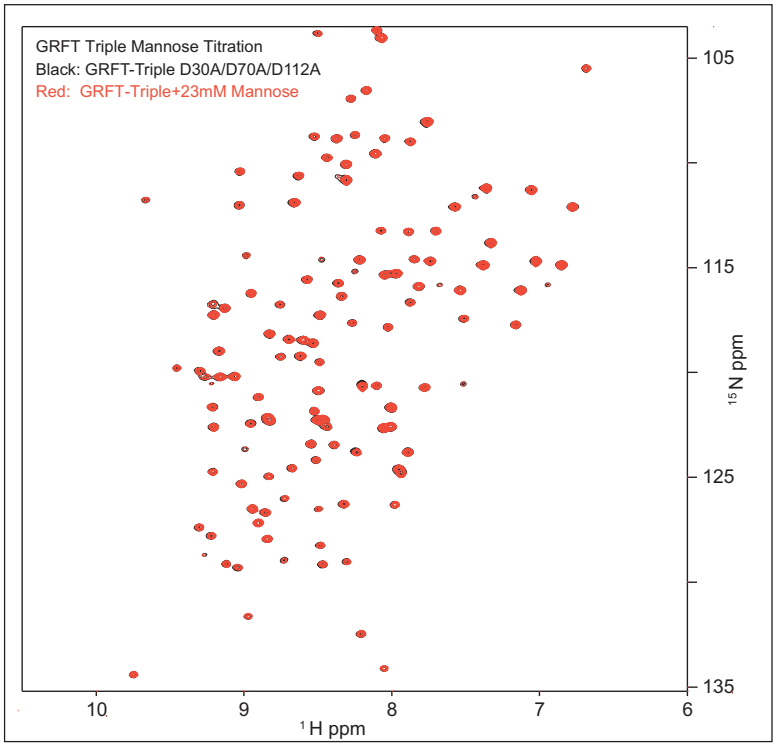

Figure A-9. ^{15}N HSQC of mannose titration of GRFT-Triple D30A/D70A/D112A.

Resonances for unliganded GRFT D30A/D70A/D112A are shown in black; resonances for the triple mutant in the presence of 23 mM mannose are shown in red. Lack of peak movement indicates no binding by mannose.

Appendix B

Supporting information for chapter 3

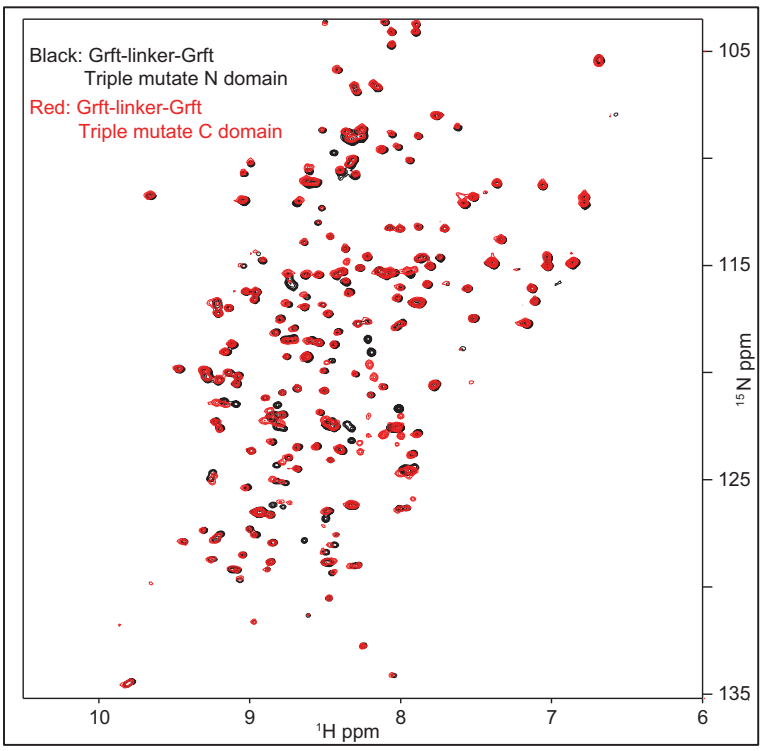

Figure B-1. ^{15}N HSQC spectrum of Grft-linker-Grft with the triple mutation D30A/D70A/D112A in the N-terminal domain (black) overlaid with the spectrum of Grft-linker-Grft with the triple mutation D30A/D70A/D112A in the C terminal domain (red).

The protein (red) with the mutation in the C-terminal domain was chosen as the one-armed variant to be tested in this work, and is called Grft-linker-GrftOneArm.

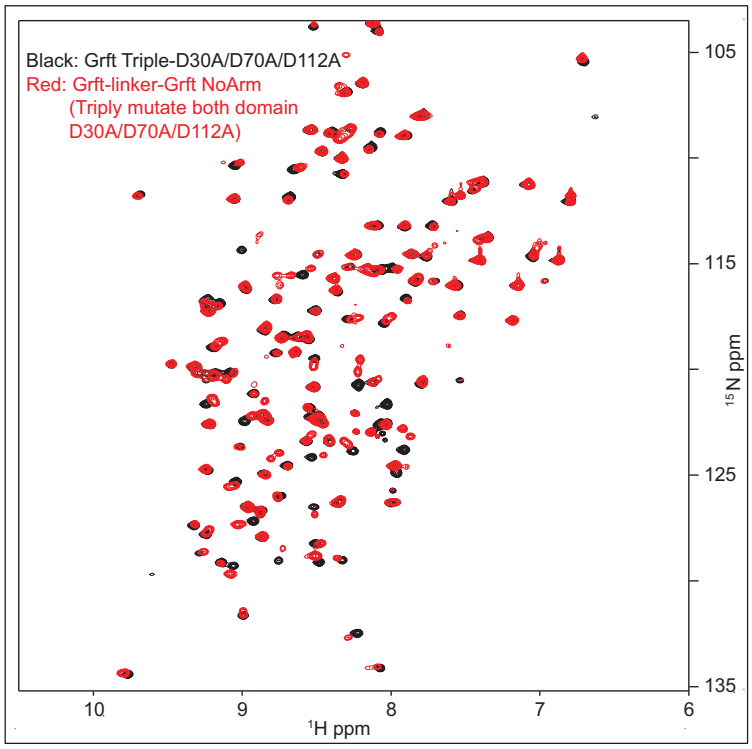

Figure B-2. ^{15}N HSQC spectrum of Grft D30A/D70A/D112A overlaid with spectrum of Grft-linker-Grft Triple D30A/70A/112A on both subunits.

Black spots represent the unlinked dimer, and both subunits bear the triple mutation. Red represents the Grft-linker-Grft-Triple NoArm. This variant is a linked dimer with D30A/D70A/D112A in both subunits of the obligate dimer. The spectra are quite similar, indicating similar structural properties for the linked and unlinked dimer with the triple mutation.

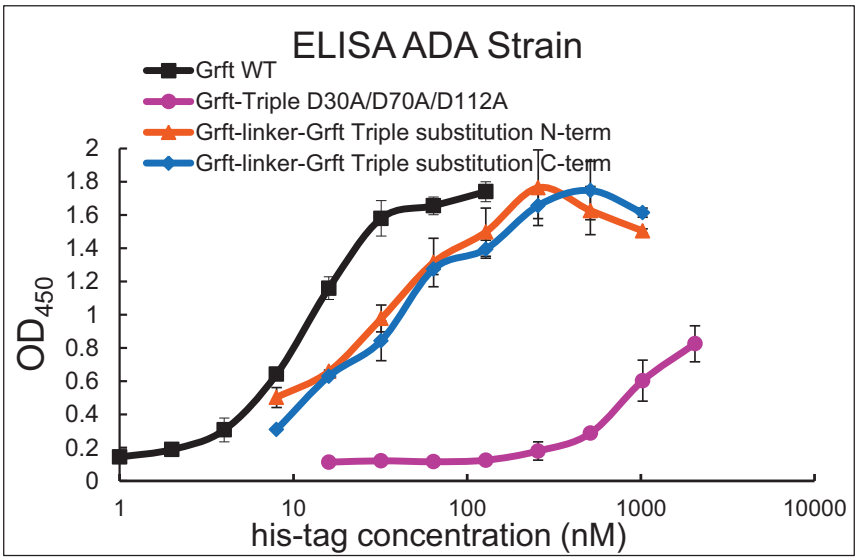

Figure B-3. ELISA assay indicating the ability of Grft and its dimer variants to bind to immobilized commercial HIV-1 gp120 ADA.

Wild-type Grft (black) binds well to $gp120_{ADA}$. The One-Armed obligate dimer, Grft-linker-Grft Triple-substitution N-terminus (D30A/D70A/D112A in N-term subunit; orange) and Grft-linker-Grft Triple-substitution C-terminus (D30A/D70A/D112A in C-term subunit; blue) bind similarly to $gp120_{ADA}$. The triple substitution D30A/D70A/D112A (magenta) binds poorly to $gp120_{ADA}$. Typical results are shown from an experiment in triplicate. Each experiment was repeated at least 3 times. Error bars indicate standard deviation from a typical triplicate experiment. Binding was detected using an HRP-conjugated anti-His-tag antibody.

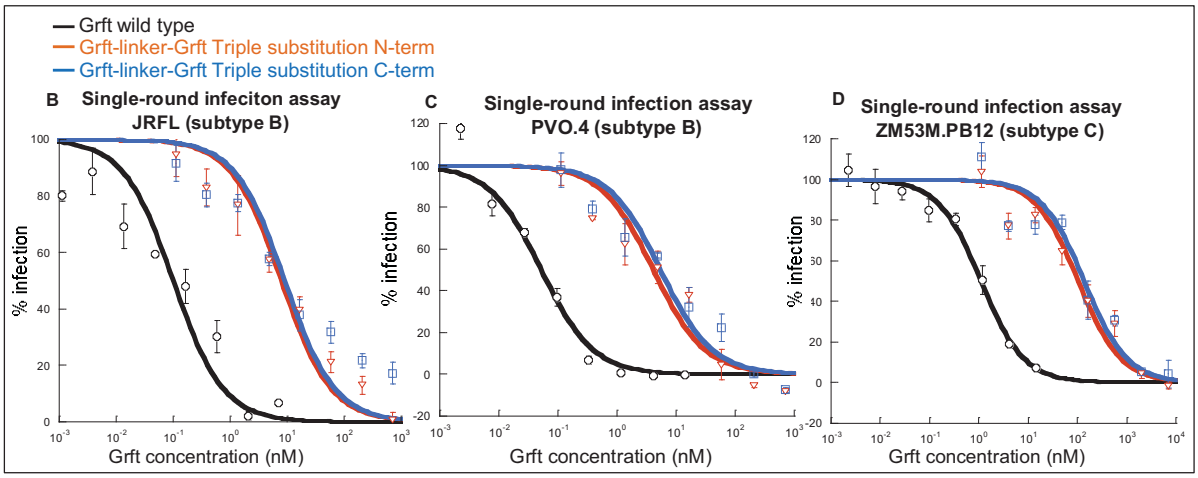

Figure B-4: Inhibition of HIV-1 infection by Grft variants in single-round virus assays.

Results are shown from experiments in triplicate using R5 strains JRFL (subtype B), PVO.4 (subtype B), and ZM53M.PB12 (subtype C). Wild-type Grft is shown in black; Grft-linker-Grft OneArm Triple substitution N-terminal domain in orange; Grft-linker-Grft Triple substitution C-terminal domain in blue. Each experiment was repeated at least 3 times. Error bars indicate the standard deviation from a triplicate experiment.

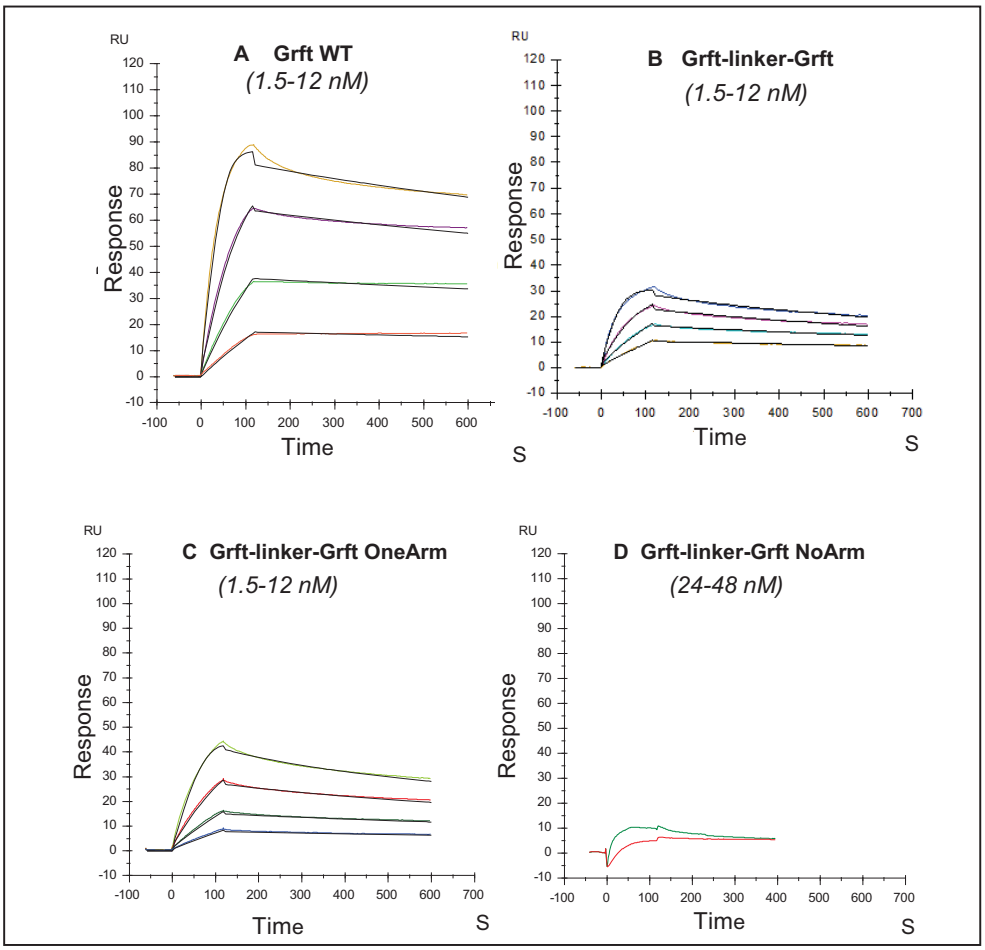

Figure B-5: Surface plasmon resonance sensorgrams of Grft binding to $gp120_{IIIB}$ immobilized on the surface of a CM5 chip.

The kinetic analysis of the interactions of Grft (Panel A), obligate dimer Grft-linker-Grft (Panel B), Grft-linker-Grft-OneArm (Panel C) and negative control obligate dimer with no functional arms (Panel D) with immobilized HIV-1 $gp120_{IIIB}$ are shown. Serial two-fold analyte dilutions (covering a concentration range from 1.5 to 12 nM in panels A-C and 24 and 48 nM in panel D) were injected over the surface of the immobilized gp120. The experimental data (colored curves) were fit using the 1:1 binding model (black lines) to determine the kinetic parameters. The biosensor chip density was 140 RU.

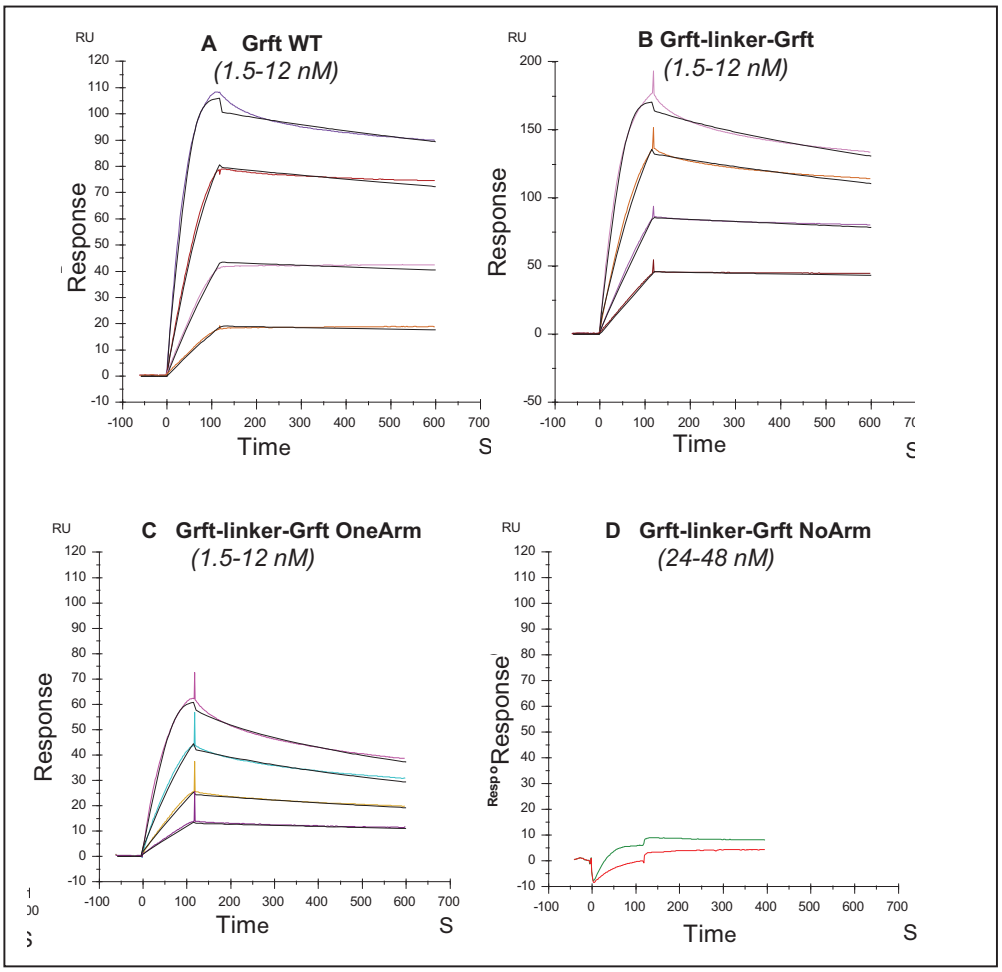

Figure B-6: Kinetic analysis of the interactions of Grft and mutants with immobilized HIV-1 HxB2 gp41.

Kinetics of the interactions of Grft (Panel A), obligate dimer Grft-linker-Grft (Panel B), Grft-linker-Grft-OneArm (Panel C) and negative control obligate dimer with no functional arms (Panel D) with immobilized HIV-1 HxB2 gp41 are shown. Serial two-fold analyte dilutions (covering a concentration range from 1.51 to 12.05 nM in panels A to C, and 24 and 48 nM in panel D) were injected over the surface of the immobilized gp41. The experimental data (colored curves) were fit using the 1:1 binding model (black lines) to determine the kinetic parameters. The biosensor chip density was 240 RU.

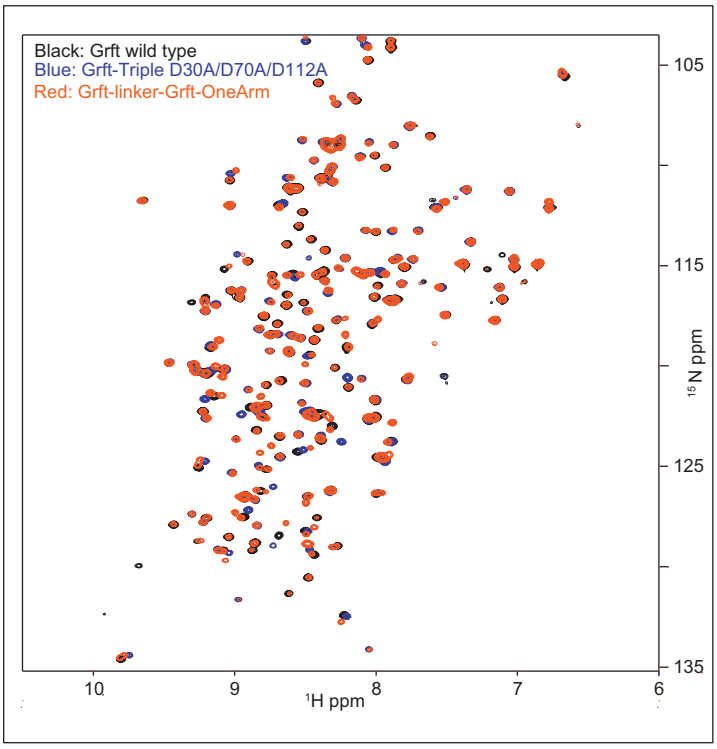

Figure B-7: ^{15}N HSQC spectra of wild-type Grft (black), Grft-Triple D30A/D70A/D112A (blue) and one-armed obligate dimer Grft-linker-Grft-OneArm (red).

Grft-linker-Grft OneArm has two sets of peaks: one set generally overlaps the wild-type Grft peaks, while the other site generally overlaps Grft-Triple D30A/D70A/D112A peaks.

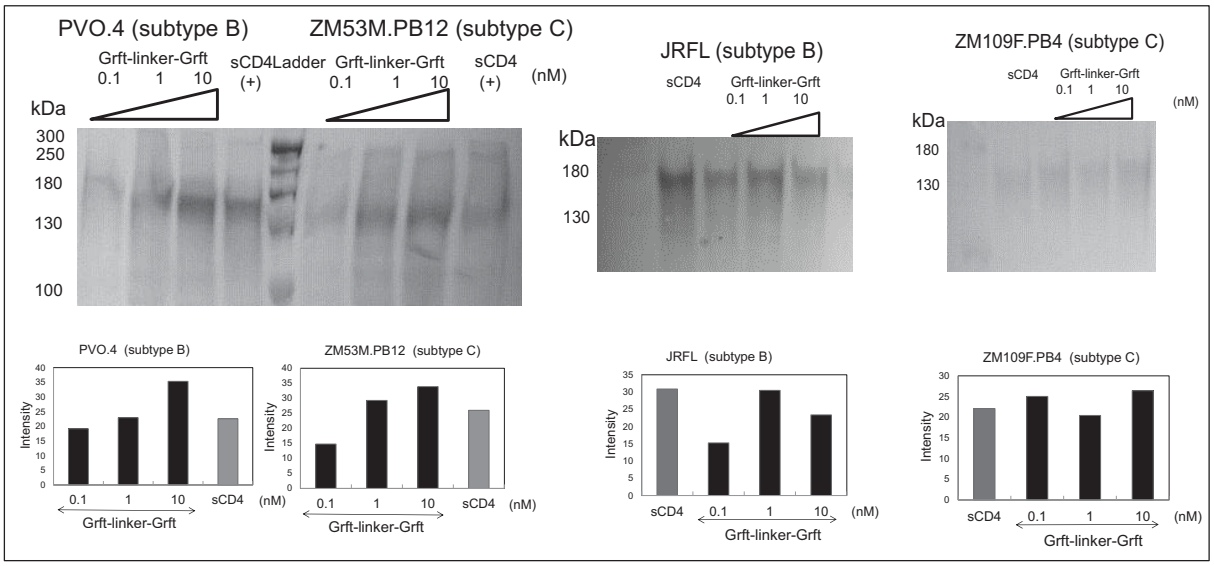

Figure B-8: Shedding of env from HIV transfected cells for PVO.4 (subtype B), ZM53M.PB12 (subtype C), JRFL (subtype B) and ZM109F.PB4 (subtype C).

Different concentrations of Grft-linker-Grft (0.1nM, 1nM, 10nM) were incubated with env-transfected 293FT cells. Ladder (middle lane) is the molecular weight ladder. sCD4 (25 ug/ml) was incubated with transfected 293FT cells and used as a positive control. Bottom: Intensity of bands as shown by densitometry.

Vita

EDUCATION

2008- 2014: Ph.D. University of California Merced, USA (Molecular Cell Biology)

- Study the mechanism of a potent HIV entry inhibitor griffithsin (GRFT). This protein lectin binds high mannose saccharides on the HIV gp120 and inhibits HIV entry.

2003-2008: MD equivalent. Sun Yat-Sen University,China (Clinical Medicine)

LIST OF PUBLICATIONS

Xue J, et al, "The role of individual carbohydrate-binding sites in the function of potent anti-HIV lectin Griffithsin", *Molecular Pharmaceutics*, 2012 Sep 4;9(9):2613-25.

Xue J, et al, "The griffithsin dimer is required for high potency inhibition of HIV-1: Evidence for manipulation of the structure of gp120 as part of the griffithsin dimer mechanism", *Antimicrobial Agents and Chemotherapy,* 2013 Aug;57(8):3976-89.

Xue J, et al, "A comparison of 5P12-vMIP-II and vMIP-II as HIV-1 entry inhibitors", *Journal of Biochemistry&Physiology,* 2013, S2-005: 2168-9652. *

Hoorelbeke B, **Xue J**, et al, "Role of the carbohydrate-binding sites of griffithsin in the prevention of DC-SIGN-mediated capture and transmission of HIV-1", *PLoS ONE, 2013 May 31;8(5):e64132 .*

Hoorelbeke B, Montfort TV, **Xue J**, et al, "HIV-1 envelope trimer has similar binding characteristics for carbohydrate-binding agents as monomeric gp120", *FEBS Lett.* 2013 Apr 2;587(7):860-6.

*Joint first-author

AWARDS AND FELLOWSHIPS

2013. QSB (Quantitative&System Biology) Research Award

2013. QSB Travel Award

2013. QSB Summer fellowship

2012. QSB Research Award

2012. QSB Travel Award

2012. Graduate Student Research summer fellowship

2012. Graduate Student General Award

2011-2012 National Institute of Health Center of Excellence on Health Disparity fellowship

2011. Graduate student research summer fellowship

2011. Keystone Symposia scholarship

2011. QSB Travel Award.